

การตั้งเอนไซม์ฮอร์สแรดิชเปอร์ออกซิเดสในวัสดุคอมโพสิตของมีโซพอร์ซิดิกา
อนุภาคนาโนของเงินและโคโตซานเพื่อประยุกต์ใช้ในงานไบโอเซนเซอร์



นายสกันธ์ พันธุ์วิทยาภูด

ศูนย์วิทยทรัพยากร

วิทยานิพนธ์นี้เป็นส่วนหนึ่งของการศึกษาตามหลักสูตรปริญญาวิทยาศาสตรมหาบัณฑิต

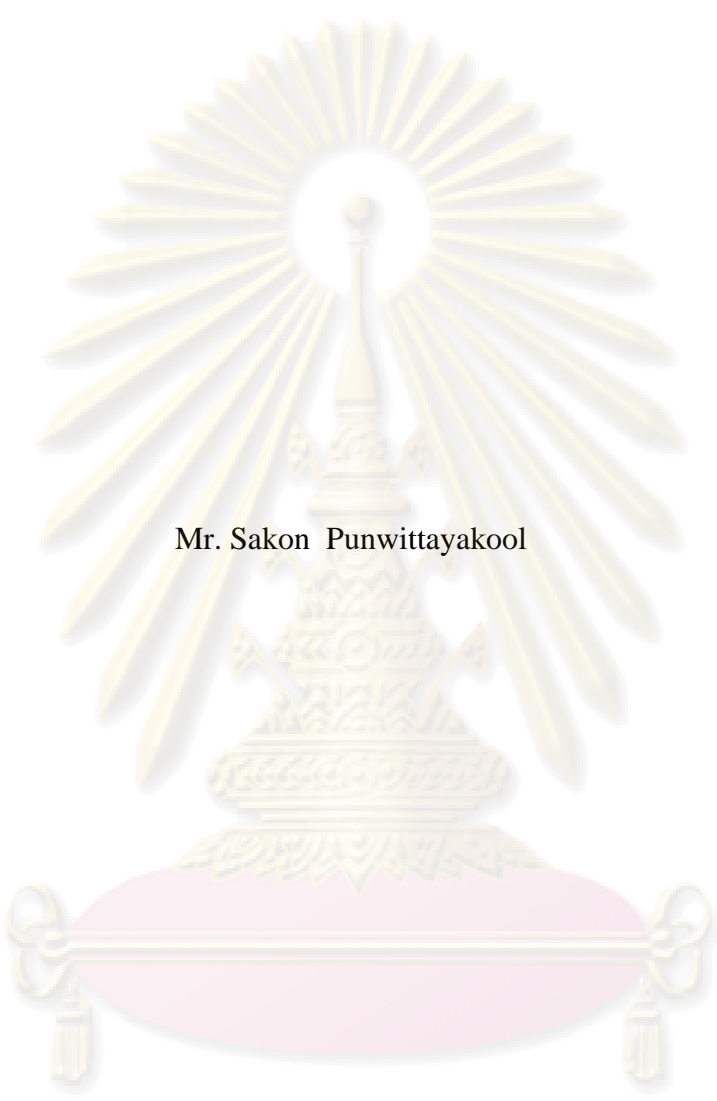
สาขาวิชาวิศวกรรมเคมี ภาควิชาวิศวกรรมเคมี

คณะวิศวกรรมศาสตร์ จุฬาลงกรณ์มหาวิทยาลัย

ปีการศึกษา 2551

ลิขสิทธิ์ของจุฬาลงกรณ์มหาวิทยาลัย

IMMOBILIZATION OF HORSERADISH PEROXIDASE IN MESOPOROUS SILICA/
SILVER NANOPARTICLE/CHITOSAN COMPOSITE MATERIAL
FOR BIOSENSOR APPLICATION



Mr. Sakon Punwittayakool

A Thesis Submitted in Partial Fulfillment of the Requirements
for the Degree of Master of Engineering Program in Chemical Engineering

Department of Chemical Engineering

Faculty of Engineering

Chulalongkorn University

Academic Year 2008

Copyright of Chulalongkorn University

สภานิสิต พันธุ์วิทยาเขต : การตรึงเอนไซม์ฮอร์สเรดิชเปอร์ออกซิเดสในวัสดุคอมโพสิตของ
มีโซพอร์ซิลิกาอนุภาคนาโนของเงินและโคโคซานเพื่อประยุกต์ใช้งานไบโอเซนเซอร์

(IMMOBILIZATION OF HORSERADISH PEROXIDASE IN
MESOPOROUS SILICA/SILVER NANOPARTICLE/CHITOSAN
COMPOSITE MATERIAL FOR BIOSENSOR APPLICATION)

อ.ที่ปรึกษาหลัก : รศ. ดร. สิริรุ่ง ปริษานนท์ , อ.ที่ปรึกษาร่วม : รศ. ดร. มานะ ศรียุทธศักดิ์,
110 หน้า

งานวิจัยนี้ศึกษาการตรึงเอนไซม์ฮอร์สเรดิชเปอร์ออกซิเดสในวัสดุที่มีมีโซพอร์ซิลิกา
อนุภาคนาโนเงินและโคโคซานเป็นองค์ประกอบด้วยวิธีทางไฟฟ้าเคมี โดยทำการตรึงอยู่บน
อิเล็กโทรดชนิดกาสีคาร์บอน งานวิจัยส่วนแรกศึกษาการสังเคราะห์มีโซพอร์ซิลิกาชนิดเอ็มซี
เอฟและสังเคราะห์อนุภาคนาโนของเงินบนเอ็มซีเอฟ โดยเอ็มซีเอฟที่สังเคราะห์ได้มีรูพรุนขนาด
23.7 นาโนเมตรและมีพื้นที่ผิวทั้งหมด 629.97 ตารางเมตรต่อกรัม ส่วนที่สองทำการศึกษาอิทธิพล
ของปริมาณของมีโซพอร์ซิลิกาในสารละลายโคโคซาน (0.1 – 1 % น้ำหนัก/ปริมาตร) ความเข้มข้น
โคโคซาน (0.1 – 1 % น้ำหนัก/ปริมาตร) และปริมาณของอนุภาคนาโนเงิน (20 – 1000 ส่วนในล้าน
ส่วน) พบว่า สารเติมแต่งที่เพิ่มเข้าไป เช่น เอ็มซีเอฟและอนุภาคของเงินช่วยในการกระจายตัวของ
เอนไซม์ อย่างไรก็ตามความเข้มข้นของสารเติมแต่งที่มากเกินไปทำให้อัตราการถ่ายเทมวลสารของ
สารตั้งต้นและผลิตภัณฑ์ถูกจำกัด อนุภาคของเงินยังช่วยเพิ่มการตอบสนองสัญญาณทางไฟฟ้าอีก
ด้วย สภาวะที่เหมาะสมในการตรึงเอนไซม์ คือ ปริมาณของมีโซพอร์ซิลิกาเท่ากับ 0.7 % น้ำหนัก/
ปริมาตร ความเข้มข้นโคโคซาน 0.5 % น้ำหนัก/ปริมาตร และปริมาณของอนุภาคนาโนเงิน 20
ส่วนในล้านส่วน ส่วนสุดท้ายศึกษาเสถียรภาพในการนำกลับมาใช้ใหม่ของเอนไซม์ตรึงรูปที่
สภาวะที่เหมาะสม พบว่า เอนไซม์ตรึงรูปในวัสดุประกอบที่สภาวะเหมาะสมนี้ไม่สามารถนำ
กลับมาใช้ใหม่ได้ อันเนื่องมาจากการหลุดออกของเอนไซม์จากการห่อหุ้มด้วยโคโคซาน

จุฬาลงกรณ์มหาวิทยาลัย

ภาควิชา วิศวกรรมเคมี
สาขาวิชา วิศวกรรมเคมี
ปีการศึกษา 2551

ลายมือชื่อนิสิต.....
ลายมือชื่ออาจารย์ที่ปรึกษาหลัก.....
ลายมือชื่ออาจารย์ที่ปรึกษาร่วม.....

4970614821 : MAJOR CHEMICAL ENGINEERING

KEY WORD: MESOPOROUS SILICA / HORSERADISH PEROXIDASE / SILVER NANOPARTICLE / BIOSENSOR

SAKON PUNWITTAYAKOOL: (IMMOBILIZATION OF HORSERADISH PEROXIDASE IN MESOPOROUS SILICA/SILVER NANOPARTICLE/ CHITOSAN COMPOSITE MATERIAL FOR BIOSENSOR APPLICATION)

THESIS PRINCIPAL ADVISOR : ASSOC. PROF. SEEROONG

PRICHANONT, Ph.D., THESIS CO-ADVISOR : ASSOC. PROF. MANA SRIYUDTHSAK, D.Eng., 110 pp.

The ultimate aim of this research was to investigate the immobilization of Horseradish peroxidase in mesoporous silica/silver nanoparticle/chitosan composite material using electrochemical method with glassy carbon electrode. In this study, the experiments were divided into three parts. Firstly, mesoporous silica type MCF was synthesized and silver nanoparticles were attached on MCF. The synthesized MCF has average pore size of 23.7 nm and total surface area of 629.97 m²/g. Secondly, the effects of amount of mesoporous silica (0.1 – 1 % w/v), chitosan concentration (0.1 – 1 % w/v), and silver nanoparticle concentration (20 – 100 ppm) on electrochemical response were studied. It was revealed that additives such as MCF and Ag particles helped enzyme dispersion to a certain concentration, however, higher concentration of additives resulted in higher substrate/product mass transfer limitation. In addition, Ag particles were found to help enhancing electrical response. Optimal compositions of modified electrode were 20 ppm Ag solution, 0.5 %w/v chitosan, 0.7%w/v modified MCF and 10 mg/ml HRP. Finally, the optimal composition of enzyme immobilization was further applied to investigate the reusability of immobilized enzyme. The use of modified electrode was limited to only once. The main cause was probably enzyme leakage from chitosan matrix.

Department : Chemical Engineering

Field of study : Chemical Engineering

Academic year : 2008

Student's signature :

Thesis Principal Advisor's signature :

Thesis Co-advisor's signature :

ACKNOWLEDGEMENTS

The author would like to express his sincere gratitude and appreciation to his advisor, Associate Professor Seeroong Prichanont, for her supervision, encouraging guidance, advice, discussion and helpful suggestions throughout the course of this Master Degree study. Also, he is very grateful to his co-advisor, Associate Professor Mana Sriyudthsak, who gave him very kind and useful suggestions in bioelectrochemical knowledge. In addition, the author would also be grateful to Associate Professor Muenduen Phisalaphong, as the chairman, Assistant Professor Jarun Chutmanop, Assistant Professor Artiwan Shotipruk as the members of the thesis committee. The financial supports of the Thailand Research Fund (TRF) and the Graduate School of Chulalongkorn University are gratefully acknowledged.

Special thanks to Miss Wilaiwan Chouyyok, PhD student in Biochemical Engineering laboratory, for many useful suggestions and helps.

Most of all, the author would like to express his highest gratitude to his parents who always pay attention to his all the times for suggestions and listen his complain. The most success of graduation is devoted to my parents.

Finally, the author wishes to thank all members of the Biochemical Engineering Research Laboratory and all my friends in the Department of Chemical Engineering for their assistance and warm collaborations.

ศูนย์วิจัยทรัพยากร
จุฬาลงกรณ์มหาวิทยาลัย

CONTENTS

	Page
ABSTRACT (THAI)	iv
ABSTRACT (ENGLISH)	v
ACKNOWLEDGEMENTS	vi
CONTENTS	vii
LIST OF TABLES	x
LIST OF FIGURES	xi
CHAPTER I: INTRODUCTION	1
1.1 Motivation.....	1
1.2 Objectives.....	2
1.3 Working Scopes.....	2
1.4 Expected benefits.....	2
CHAPTER II: BACKGROUND & LITERATURE REVIEW	3
2.1 Horseradish Peroxidase.....	3
2.2 Immobilized enzyme.....	4
2.2.1 Covalent attachment to solid supports.....	4
2.2.2 Adsorption to solid supports.....	4
2.2.3 Entrapment in a here-dimensional polymer network	5
2.2.4 Microencapsulation.....	5
2.2.5 Cross-linking with bifunctional reagents.....	6
2.3 Chitosan.....	8
2.4 Silica.....	9
2.5 Mesoporous silica.....	10
2.6 Synthesis of mesoporous silica.....	11
2.7 Characterization of mesoporous silica.....	12
2.8 Silver nanoparticle (Ag).....	15
2.8.1 Chemical reduction method.....	15

2.8.2 In situ reduction method.....	16
2.9 Biosensor.....	16
2.10 Electrochemical method.....	17
2.10.1 Cyclic voltammetry.....	17
2.10.2 Amperometry.....	19
2.11 Performance Factors.....	19
2.12 Literature reviews.....	21
2.12.1 HRP for phenol detection.....	21
2.12.2 Mesoporous silica on biosensor.....	25
2.12.3 Chitosan on biosensor.....	26
2.12.4 Metal on biosensor.....	27
CHAPTER III: MATERIALS & METHODS.....	29
3.1 Chemicals.....	29
3.2 Apparatus.....	29
3.3 Synthesis of mesoporous silica.....	31
3.4 Synthesis of Ag/MCF and Ag/SiO ₂	31
3.5 Characterization of MCF, Ag/MCF and Ag/SiO ₂	32
3.6 Synthesis of Ag.....	32
3.7 Prepare chitosan solution.....	33
3.8 Preparation of Ag/chitosan solution	
3.9 Procedures for modified electrode.....	33
3.9.1 Working electrode cleaning.....	33
3.9.2 Preparation of the modified electrode.....	33
3.9.2.2 Chitosan/MCF composite film.....	34
3.9.2.3 Chitosan/(Ag/MCF) and Chitosan/(Ag/SiO ₂) composite film.....	34
3.9.2.4 (Ag/Chitosan solution)/MCF composite film.....	34
3.9.2.5 Cyclic voltammetric and Amperometric phenol sensor.....	34
3.9.3 Reusability of modified electrode.....	35

CHAPTER IV: RESULTS & DISCUSSION.....	36
4.1 Characterization of MCF and SiO ₂ nanopowder.....	36
4.2 Characterization of Ag/MCF and Ag/SiO ₂	40
4.3 The effect of amount of MCF, chitosan concentration, and amount of Ag in each composite film on cyclic voltammogram.....	44
4.3.1 The effect of base solutions on cyclic voltammogram.....	45
4.3.2 The effect of HRP on cyclic voltammogram	46
4.3.3 The effect of MCF on cyclic voltammogram.....	47
4.3.4 The effect of chitosan concentration on cyclic voltammogram.....	49
4.3.5 The effect of amount of Ag in MCF on cyclic voltammogram.....	50
4.3.6 The effect of amount of silver in SiO ₂ nanopowder on cyclic voltammogram.....	51
4.3.7 The effect of amount of silver in chitosan on cyclic voltammogram.....	52
4.3.8 The effect of various matrices on cyclic voltammogram.....	53
4.4 Reusability.....	54
CHAPTER V: CONCLUSION & RECOMMENDATIONS.....	61
5.1 Conclusion.....	61
5.2 Recommendations for the future studies.....	62
REFERENCES.....	63
APPENDICES.....	71
APPENDIX A Raw data.....	72
APPENDIX B Conference.....	105
VITA.....	110

LIST OF TABLES

	Page
Table 2.1 Methods used for enzyme immobilization.....	4
Table 2.2 Methods for entrapping enzymes.....	6
Table 2.3 IUPAC classification of pores as a function of their size	10
Table 2.4 Condition on phenol and H ₂ O ₂ biosensor by immobilized enzyme.....	23
Table 4.1 Physical properties of MCF and SiO ₂ nanopowder	38
Table 4.2 Physical properties of MCF, SiO ₂ nanopowder and Ag/MCF.....	43



ศูนย์วิทยทรัพยากร
จุฬาลงกรณ์มหาวิทยาลัย

LIST OF FIGURES

	Page
Figure 2.1 Entrapping Enzyme.....	5
Figure 2.2 Cross-linking enzyme.....	6
Figure 2.3 Covalent attachment to solid supports.....	7
Figure 2.4 structure of chitin.....	8
Figure 2.5 structure of chitosan.....	8
Figure 2.6 Possible mechanistic pathways for the formation of MCM-41.....	11
Figure 2.7 Progress of the morphological transition in P123 templated materials swollen by TMB.....	12
Figure 2.8 Type of physisorption isotherms.....	14
Figure 2.9 Types of hysteresis loops.....	14
Figure 2.10 Schematic illustration of in situ formation of Ag nanoparticle inside the pore channels of MCM-41.....	16
Figure 2.11 Schematic layout of a biosensor.....	17
Figure 2.12 potential-time plot for cyclic voltammetry.....	18
Figure 2.13 current-potential plot for cyclic voltammetry.....	18
Figure 2.14 Current-time for constant potential amperometry.....	19
Figure 2.15 Method of determining the detection limit.....	20
Figure 2.16 Mechanism of mediated electron transfer at HRP modified carbon paste electrode.....	21
Figure 2.17 Mechanism of the direct electron transfer between HRP and base electrode.....	22
Figure 3.1 Schematic diagram of experiments.....	30
Figure 3.2 working electrode, counter electrode and reference electrode.....	30
Figure 3.3 Glucosen potentiostat.....	31
Figure 4.1 N ₂ adsorption-desorption isotherm of MCF.....	36
Figure 4.2 Pore size distribution of MCF.....	37
Figure 4.3 XRD patterns of MCF.....	37
Figure 4.4 Schematic illustration of modified surface of silica with APTS.....	38
Figure 4.5 Schematic illustration of in situ formation of Ag nanoparticle on modified surface silica.....	39

Figure 4.6 FTIR of MCF, modified MCF, SiO ₂ nanopowder and modified SiO ₂ compare with modified MCM-41.....	40
Figure 4.7 UV-vis spectrums of Ag/SiO ₂ with various amount of Ag.....	41
Figure 4.8 UV-vis spectrums of Ag/MCF with various amount of Ag.....	41
Figure 4.9 TEM micrograph of synthesized MCF , Ag/MCF and Ag/SiO ₂	42
Figure 4.10 Proposed schematic diagrams for HRP were entrapped in chitosan , MCF and chitosan, Ag/MCF and chitosan and Ag/chitosan and MCF....	44
Figure 4.11 Proposed schematic diagram of mass transport processes in this study...	45
Figure 4.12 Cyclic voltammograms of bare electrode of base solutions: PBS (pH 7), H ₂ O ₂ and Phenol. Scan rate is 50 mV/s.....	46
Figure 4.13 Cyclic voltammograms of modified electrode with 0.5% w/v chitosan / HRP in presence of 0.1 mM of Phenol and 0.1 mM of H ₂ O ₂ compared with base solution . Scan rate is 50 mV/s.....	47
Figure 4.14 Cyclic voltammograms of modified electrode with 0.5% w/v chitosan /HRP and 0.5% w/v chitosan / HRP / 0.1% w/v MCF in presence of 0.1 mM of Phenol and 0.1 mM of H ₂ O ₂ . Scan rate is 50 mV/s.....	48
Figure 4.15 Cyclic voltammograms of modified electrode with 0.5% w/v chitosan / HRP / various amount of MCF compared with 0.5% w/v chitosan / HRP in presence of 0.1 mM of Phenol and 0.1 mM of H ₂ O ₂ . Scan rate is 50 mV/s.....	49
Figure 4.16 Cyclic voltammograms of modified electrode with various chitosan concentration / HRP / 0.7% w/v MCF in presence of 0.1 mM of Phenol and 0.1 mM of H ₂ O ₂ . Scan rate is 50 mV/s.....	50
Figure 4.17 Cyclic voltammograms of modified electrode with 0.5% w/v chitosan / HRP / various amount of Ag in 0.7% w/v MCF compared with 0.5 % w/v chitosan / HRP / 0.7% w/v MCF in presence of 0.1 mM of Phenol and 0.1 mM of H ₂ O ₂ . Scan rate is 50 mV/s.....	51
Figure 4.18 Cyclic voltammograms of modified electrode with 0.5% w/v chitosan / HRP / various amount of Ag in 0.7% w/v SiO ₂ nanopowder in presence of 0.1 mM of Phenol and 0.1 mM of H ₂ O ₂ . Scan rate is 50 mV/s.....	52
Figure 4.19 Cyclic voltammograms of modified electrode with 0.5% w/v chitosan / various amount of Ag solution / HRP / 0.7% w/v modified MCF in presence of 0.1 mM of Phenol and 0.1 mM of H ₂ O ₂ . Scan rate is 50 mV/s.....	53

Figure 4.20 Cyclic voltammograms of modified electrode with various matrices in presence of 0.1 mM of Phenol and 0.1 mM of H ₂ O ₂ . Scan rate is 50 mV/s.....	53
Figure 4.21 Amperometric of modified electrode with 0.5% w/v chitosan mixed with 20 ppm Ag solution, HRP and 0.7% w/v modified MCF in presence of 0.1 mM of Phenol and 0.1 mM of H ₂ O ₂ at 0 volt.....	54
Figure 4.22 Amperometric of modified electrode with 0.5% w/v chitosan, HRP and 0.7% w/v modified MCF in presence of 0.1 mM of Phenol and 0.1 mM of H ₂ O ₂ at 0 volt.....	55
Figure 4.23 Amperometric of modified electrode with 0.5% w/v chitosan, HRP and 20 ppm Ag solution in presence of 0.1 mM of Phenol and 0.1 mM of H ₂ O ₂ at 0 volt.....	56
Figure 4.24 Amperometric of modified electrode with 0.5% w/v chitosan and HRP in presence of 0.1 mM of Phenol and 0.1 mM of H ₂ O ₂ at 0 volt.....	56
Figure 4.25 Amperometric of modified electrode with various chitosan concentration and HRP in presence of 0.1 mM of Phenol and 0.1 mM of H ₂ O ₂ at 0 volt.....	58
Figure 4.26 Amperometric of modified electrode with 0.5% w/v chitosan and HRP in presence of 0.1 mM of Phenol and 0.1 mM of H ₂ O ₂ at various volt.....	59

CHAPTER I

INTRODUCTION

1.1 Motivation

Phenolic compounds can be found in industrial waste for example coal mining, oil refinery, paint, plastic, and pharmaceutical industry. It is highly toxic to man and to aquatic organisms (Lindgren et al., 1997). Many techniques have been used for determination of phenols from industrial wastes, such as colorimetry, gas chromatography, liquid chromatography, and capillary electrophoresis. However, these methods are very expensive, time-consuming, including complicated sample pretreatment and giving low sensitivity. Therefore, biosensor technique which is higher sensitivity, fast response, and lower cost, is an obviously advantageous alternative.

In order to detect phenolic compounds using enzyme biosensor. Enzyme immobilization is an important procedure for construction of biosensor. Horseradish peroxidase (HRP) has good performances in degrading the phenolic compounds and giving response to a large number of phenol derivatives in the presence of hydrogen peroxide by enzymatic catalytic reaction. However, there still exist some important problems such as the short lifetimes and enzyme instability. Thus, immobilization of HRP is able to improve these problems.

Enzyme immobilization is enzyme immobilized on transducer which is a part of a biosensor. Thus, enzyme support material is one of the important parameters in enzyme immobilization process. Many researchers have investigated enzyme immobilization on various porous materials such as alumina, polymeric resins, natural polymeric derivatives, organic gels, fibers, zeolite, and mesoporous molecular sieves (He et al., 2006). Among different support materials, mesoporous silica offer interesting properties, uniform and adjustable pore size, large surface area, pore volume and opened pore structures which make it more suitable for increase enzyme loading. However, the poor conductivity of mesoporous silica is an important drawback of this material, which might influence the performance of the biosensor.

To improve the conductivity, various metal nanoparticles such as silver (Ag), gold (Au), platinum (Pt) etc. are used in enzyme immobilization process. It is well known that Ag is the best conductor among metals and so Ag nanoparticles may facilitate more efficient electron transfer including can adsorb the protein by the interaction between the enzyme and Ag nanoparticle.

In this work, we are interested in immobilization of enzyme in mesoporous silica/silver nanoparticle/ chitosan composite. Chitosan was selected because it is a natural biopolymer, good film-forming ability, chemical inertness, high mechanical strength, biodegradable, biocompatible and inexpensive.

1.2 Objectives

To investigate the immobilization of Horseradish peroxidase in mesoporous silica/silver nanoparticle/chitosan composite material.

1.3 Working scopes

- 1.3.1 Synthesize and characterize mesoporous silica (MCF), Ag nanoparticle on mesoporous silica (MCF).
- 1.3.2 Immobilization of Horseradish peroxidase on mesoporous silica/silver nanoparticle/chitosan.
- 1.3.3 Investigate effects of the amount of silica in chitosan (0.1-1 %w/v), chitosan concentration (0.1-1%w/v) and amount of silver nanoparticle (100-1000 ppm) on HRP immobilization.
- 1.3.4 Determine the enzyme activity, reusability and stability.

1.4 Expected benefits

- 1.4.1 To increase efficiency of the enzyme immobilization in mesoporous silica support.
- 1.4.2 To acquire basic information for biosensor development.

CHAPTER II

BACKGROUND & LITERATURE REVIEWS

This chapter describes the properties and enzymatic reactions of HRP include method of enzyme immobilization. Supports for enzyme immobilization have described about synthesis, properties, and characterization. The basic data of biosensor such as measurement method and other parameters has described include literature reviews about material for enzyme immobilization on biosensor.

2.1 Horseradish peroxidase

Horseradish peroxidase is a monomeric glycoprotein with a molecular mass of 44 kDa, purified from horseradish roots (*Amoracia rusticana*), is a typical member of the plant peroxidases that catalyses the oxidation of a number of organic and inorganic compounds (the second substrate) with hydrogen peroxide or alkyl peroxide (the first substrate) (Sato et al., 1995). Horseradish peroxidase is of great importance for determination of phenolic compounds in environmental control, protection and health benefits due to their toxicity and persistency in the environment (Yang et al., 2006). Other applications of HRP include polymer synthesis especially for phenolic resin synthesis, diagnostic assays, nucleic acid analysis, biosensors, bioremediations, and other biotechnological processes (Liu et al. 2006).

Reactions of the enzyme can be shown as follows (Rosatto et al., 1999):



The first Eq. (a) represents a two-electron oxidation of the heme prosthetic group of the native peroxidase by H_2O_2 . This reaction results in the formation of an intermediate, $\text{HRP (Fe}^{5+})$ (oxidation state +5). In the next Eq. (b), $\text{HRP (Fe}^{5+})$ loses one oxidizing equivalent upon one-electron reduction by the electron donor AH_2 and forms $\text{HRP (Fe}^{4+})$ (oxidation state +4). In the third step (c), $\text{HRP (Fe}^{4+})$ accepts an

additional electron from the electron donor molecule AH_2 and the enzyme is returned to its native state (Ruzgas et al., 1996).

2.2 Immobilized enzyme

The immobilization method has significant influence to the properties of immobilized enzyme: such as, activity, stability, deactivation, and regeneration of immobilized enzyme. The methods used to immobilize enzymes are broadly of two types: attachment to insoluble supports; and entrapment (Table 2.1)

Table 2.1 Methods used for enzyme immobilization (Scragg,1998)

1. Attachment
Covalent attachment to supports
Adsorption
2. Entrapment
Within a polymer
Microencapsulation
Cross-linking
Semi-permeable membranes

2.2.1 Covalent attachment to solid supports

This technique is the formation of covalent bonds between the enzyme and the support matrix. Enzyme and support surface bind together with the chemical linker containing functional groups, such as amino, carboxyl and sulfhydryl. Generally, in this method, chemical reagents may block active site of enzyme. They cause inactivation of enzymes, shown in Figure 2.3

2.2.2 Adsorption to solid supports

Adsorption of an enzyme onto a solid is the simplest way of preparing immobilized enzymes. The method depends on physical interaction between the enzyme protein and the surface of the matrix, brought about by mixing a concentrated solution of enzyme with the solid. However, the leaching of enzyme is a common problem in this case.

2.2.3 Entrapment in a here-dimensional polymer network (Scragg,1998)

Enzymes can be immobilized within a polymer network by addition of the enzyme to the monomers before the gel is formed. The polymers used to form the gels can be either natural organic polymers or synthetic polymers, and these are listed in Table 2.2. The synthetic gels can be prepared in one of two ways:

- (1) The gel is made by polymerization of monomers with the cells present.
- (2) The gel is made by cross-linking preformed polymers in the presence of cells.

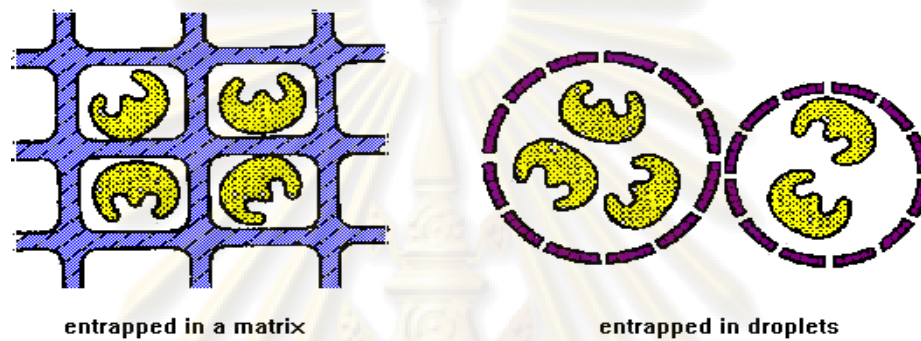


Figure 2.1 Entrapping Enzyme

From: www.rpi.edu/dept/chem-eng/Biotech-Environ/IMMOB/Immob

2.2.4 microencapsulation

This is a process by which teeny droplets or particles of liquid or solid material are surrounded or coated with a continuous film of polymeric material. This method has the advantage of high activity due to high surface-to-volume ratio.

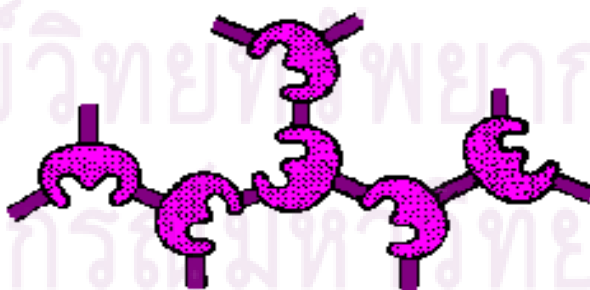
ศูนย์วิทยทรัพยากร
จุฬาลงกรณ์มหาวิทยาลัย

Table 2.2 Methods for entrapping enzymes (Scragg,1998)

Gel formation method	Polymer
Synthetic polymers polymerization	
Polymerization	Polyacrylamide
	Methacrylates
Cross-linking	Polyethylene glycol-based (photoreaction)
Polycondensation	Polyurethane
	Epoxy resin
Natural polymers	
Thermal gelation	Collagen
	Gelatin
	Agar- agarose
	k-carrageenan
Ionic gelation	Alginate (Ca ⁺⁺)
	Chitosan
Precipitation	Cellulose
	Cellulose triacetate

2.2.5 Cross-linking with bifunctional reagents

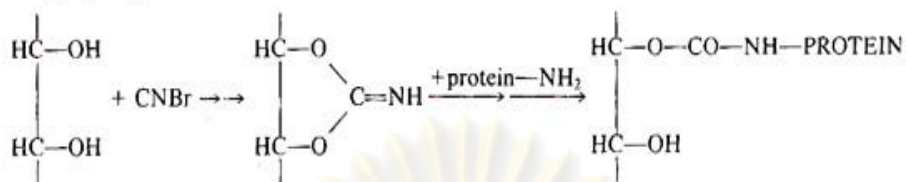
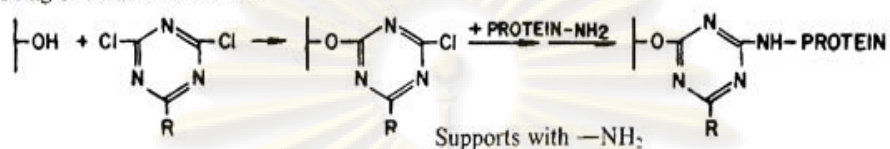
Enzymes can be immobilized by cross-linking with enzyme molecules together and so forming particles. The most popular cross-linking reagents are glutaraldehyde, dimethyladipimidate, dimethyl suberimidate, and aliphatic diamines.

**Figure 2.2** Cross-linking enzyme

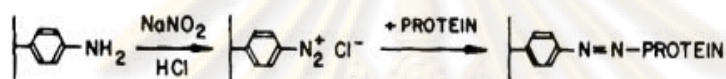
From: www.rpi.edu/dept/chem-eng/Biotech-Environ/IMMOB/Immob

Supports with —OH

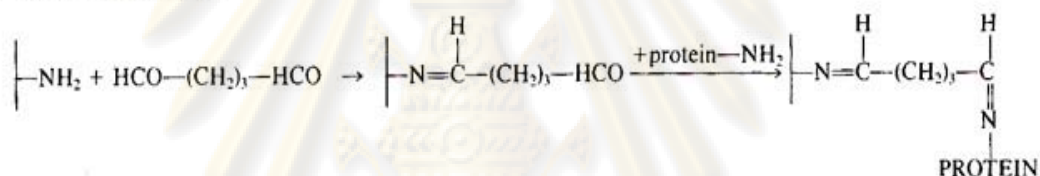
(f) Using cyanogen bromide

(g) Using *S*-triazine derivatives

(h) By diazotization

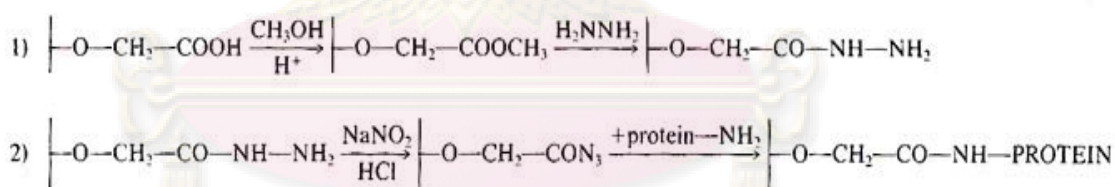


(i) Using glutaraldehyde

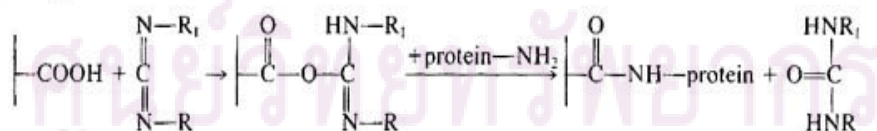


Supports with —COOH

(j) Via azide derivative



(k) Using a carbodiimide



Supports containing anhydrides

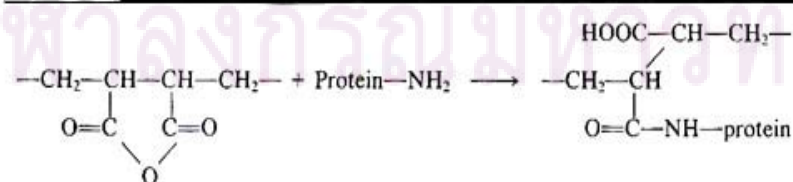


Figure 2.3 Covalent attachment to solid supports (Shuler and Kargi, 1992)

2.3 Chitosan

Chitin, the precursor of chitosan is natural polyaminosaccharides. Chitin is the most abundant natural fiber next to cellulose and is similar to cellulose in many aspects and formula is Poly [β -(1-4)-2-acetamido-2-deoxy-D-glucopyranose]

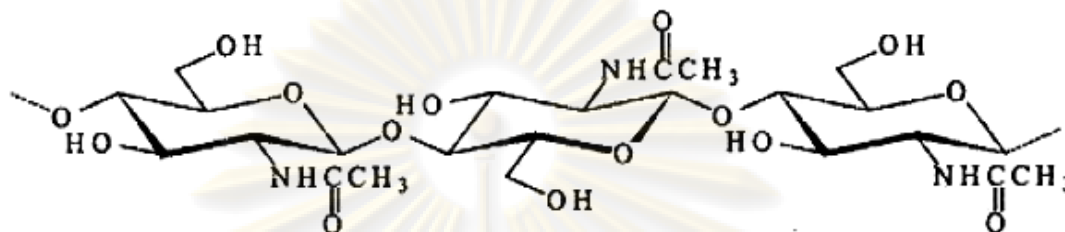


Figure 2.4 structure of chitin (Krajewska et al., 2004)

Chitin is found in the exoskeleton of arthropods or in the cell walls of fungi and yeast, up to now the main commercial sources of chitin have been crab and shrimp shells.

Chitosan, poly [β -(1-4)-linked-2-amino-2-deoxy-d-glucose], is the N-deacetylated product of chitin. Chitin with a degree of deacetylation of 75% or above is generally known as chitosan. In addition, the degree of deacetylation, which determines the content of free amino groups in the polysaccharides (Khan et al., 2002).

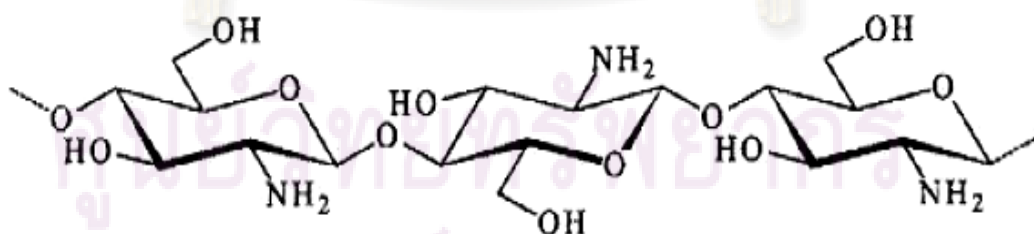


Figure 2.5 structure of chitosan (Krajewska, 2004)

Chitosan is insoluble in water, but is soluble in dilute organic acid solutions, such as acetic, propionic, formic and lactic acid and soluble in acidic solutions below pH about 6.5 (Krajewska, 2004). Chitosan is recommended as suitable functional

materials, because these natural polymers have excellent properties such as biocompatibility, biodegradability, non-toxicity, adsorption properties and low cost (Kumar et al., 2000). However, the determinants of chitosan properties have two most important which are degree of deacetylation and molecular weight (Ren et al., 2005). In study of Aiba S., (1991) found that the swelling of chitosan films depended on the degree of acetylation of original chitosan and Wiles et al., (2000) proved that the degree of deacetylation of chitosan and the viscosity of the casting solution did not have any effect on the water vapor transmission rate properties of chitosan films. In case of molecular weight, Nunthanid et al., (2001) reported that an increase in molecular weight of chitosan would increase the tensile strength and elongation as well as the moisture absorption capability of the resulting films. As enzyme immobilization supports, Alsarra et al., 2002 studied the effect of molecular weight and degree of deacetylation on lipase entrapment on chitosan bead. The results exhibit chitosan with high molecular weight and degree of deacetylation resulted in a higher loading. A lower activity was observed for beads produced with high degree of deacetylation chitosan. Molecular weight did not have a clearly effect on the activity. Some reason of the suitable of chitosan support for enzyme immobilization, chitosan can be formed by several methods, e.g. precipitation, emulsion cross-linking, spray drying, ionotropic gelation, emulsion-droplet coalescence and reverse micellar method. Its reactive amino and hydroxyl groups – after chemical modifications – make possible the coupling of enzymes. Therefore, chitosan is often used as support material for enzyme immobilization (Biró et al., 2008).

2.4 Silica

Silica or Silicon Dioxide (SiO_2) is one of the most common chemical compounds. SiO_2 crystals are found in nature in three polymorphic forms, the most common of which is quartz. Sand, agate, onyx, opal, amethyst and flint are silicon dioxide with traces of impurities. Pure silica is colorless to white. Silica has many important uses. It is used as filler for paint and rubber; in making ordinary glass; in ceramics; in construction; in the preparation of other substances and in the field of adsorption and catalyst supports because solids provide high surface areas and pore volume.

Nowadays, silica has been synthesized from self assembled aggregates of organic template and inorganic silica, due to their unique pore structures. In

particular, their remarkable textural properties such as high surface area and large pore volume make them well suitable for application as catalyst supports. Table 2.3 shown IUPAC classification of pores as a function of their size

Table 2.3 IUPAC classification of pores as a function of their size (Ayrál et al., 2006)

Micropores		Mesopores	Macropores
< 2 nm			
Ultra-micropores < 0.7 nm	Super-micropores > 0.7 nm	2-50 nm	> 50 nm

2.5 Mesoporous silica

Mesoporous silica has attracted much attention from scientists recently. These materials possess adjustable and uniformed pore sizes in the range of 2 to 50 nm, covering a new range of potential applications. The fundamental reasons for such rich morphological behaviors for mesoporous materials are:

- a. The silicate ions act as counterions to the cylindrical micelles to organize into soft hexagonal liquid crystalline phase.
- b. The rich organization of lyotropic surfactant system can be exploited to form many meso-structures.
- c. Control of higher hierarchical order of size above the nanometer scale can be achieved by finetuning the interface curvature, either by changing composition or reaction condition.
- d. Silica condensation reaction can be controlled as in the late stage of the reaction. The self-organization and siloxane bond formation processes can be separately controlled (Mou and Lin et al., 2000).

Silica-based mesoporous materials have been extensively studied in several catalytic reactions with high specific surface area, well-defined regular pore shape, narrow pore size distribution, large pore volume, and tunable pore size. For adsorption process with, mesoporous silica large pore volume and pore size flexibility are suited for selective adsorption of gases, liquids and solids.

2.6 Synthesis of mesoporous silica

Mesoporous materials were synthesized as first time by scientists of Mobil groups and then those matters have been continuously developed. The mesoporous silicas were synthesized as different template, silica source and reaction temperature to make its have different structure, pore size such as hexagonal phase (the MCM-41 has pore diameter range of 1.5-10 nm and SBA-15 has pore diameter range of 4-12 nm (Lettow et al., 2000), cubic phase (MCM-48) and lamellar phase (MCM-50). For example, synthesis of MCM-41 with surfactant templating (Figure 2.6).

The liquid crystal mechanism of MCM-41 formation suggests that the as-synthesized materials will have the micellar structures included intact. The occurrence of MCM-41 has two pathways (Beck et al., 1992). In pathway 1 of Figure 14, the surfactant micelles was dissolved in solvent and most likely arranged in a micellar array. When increase temperature during reaction, the micellar combine to rod and arrange for hexagonal MCM-41. Then, added inorganic silicate source to this micellar which rearranged to produce an inorganic structure after that calcination of this reaction mixtures for clear out the micellar to produce the hexagonal silica. While pathway 2 is another possible mechanistic pathway. This mechanism occurs due to gravity of silicate which add to micellar to make the hexagonal structure.

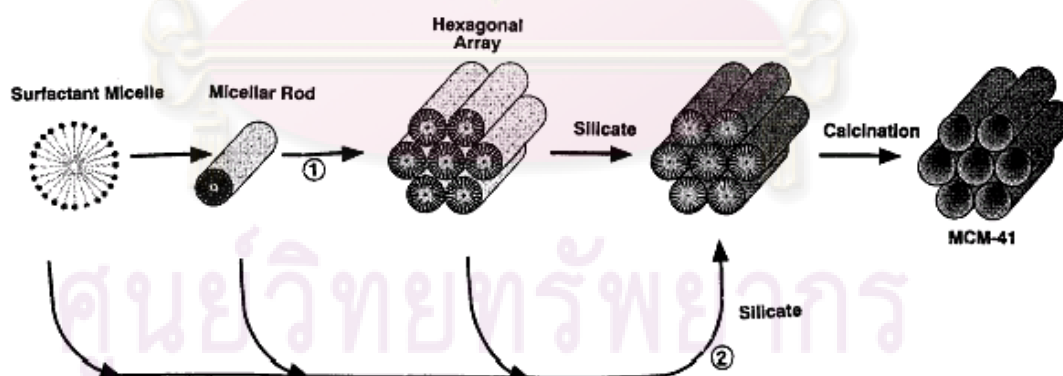


Figure 2.6 Possible mechanistic pathways for the formation of MCM-41:
(1) liquid crystal phase initiated and (2) silicate anion initiated.

In case of synthesis of mesocellular silica foams (MCF), the procedures have similar to MCM-41 but we added the swelling agents (oil) to surfactant micelles at

ratio 0.5 to form the mesocellular foam material (Figure 2.7). In this study, we choose MCF which is mesoporous silica possesses a system of interconnected pores with diameters of 22-42 nm because of HRP immobilized in MCF was high activity and stable under storage (Chouyyok et al., 2008).

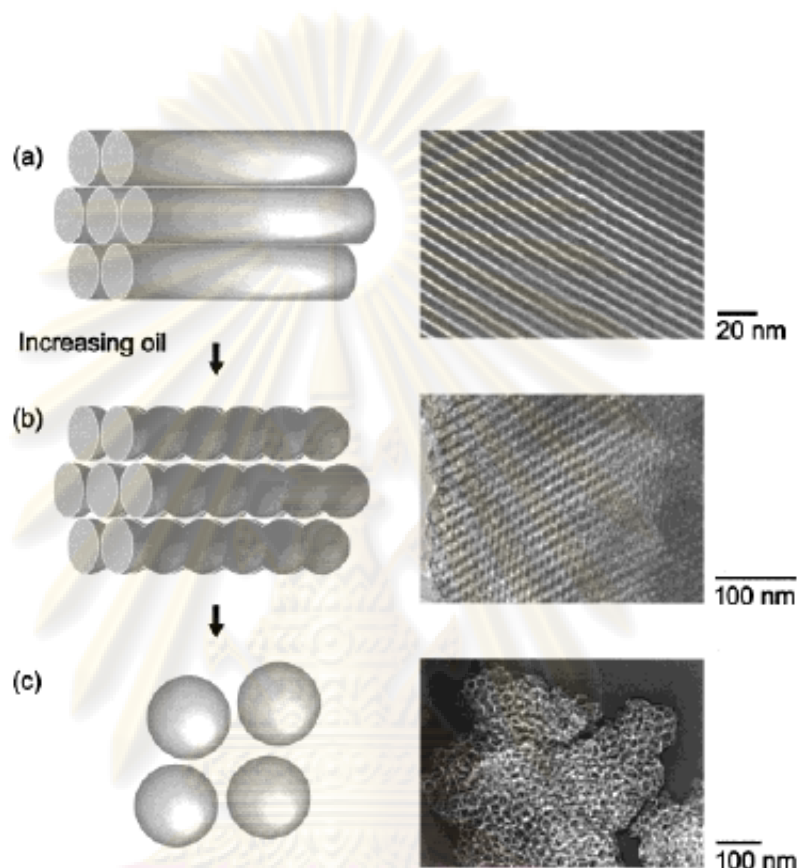


Figure 2.7 Progress of the morphological transition in P123 templated materials swollen by TMB. The proposed schemes show the formation and TEM micrographs of the mesoporous silicas synthesized at oil-polymer mass ratios of (a) 0 (b) 0.21 (c) 0.5 (Lettow et al., 2000).

2.7 Characterization of mesoporous silica (Sing K. S. W. et al., 1985)

Nitrogen adsorption represents the most widely used technique to determine catalyst surface area and characterize the porous texture. Starting point is the determination of the adsorption isotherm, which is the nitrogen adsorbed volume against its relative pressure. Isotherm shape depends on the solid porous texture. According to IUPAC classification six types can be differentiated (Figure 2.8).

The reversible Type I isotherm are given by microporous solids having relatively small external surfaces (e.g. activated carbons, molecular sieve zeolites and certain porous oxides).

The reversible Type II isotherm is the normal form of isotherm obtained with a non-porous or macroporous adsorbent. The Type II isotherm represents unrestricted monolayer-multilayer adsorption.

The reversible Type III isotherm is not common, but there are a number of systems (e.g. nitrogen on polyethylene). The adsorbate-adsorbate interactions play an important role to this isotherm.

Characteristic features of the Type IV isotherm are its hysteresis loop, which is associated with capillary condensation taking place in mesopores. The initial part of the Type IV isotherm is attributed to monolayer-multilayer adsorption since it follows the same path as the corresponding part of a Type II isotherm obtained with the given adsorbent on the same surface area of the adsorbent in a non-porous form. Type IV isotherms are given by many mesoporous industrial adsorbents.

The Type V isotherm is uncommon; it is related to the Type III isotherm in that the adsorbent-adsorbate interaction is weak, but is obtained with certain porous adsorbents.

The Type VI isotherm, in which the sharpness of the steps depends on the system and the temperature, represents stepwise multilayer adsorption on a uniform non-porous surface.

ศูนย์วิทยทรัพยากร
จุฬาลงกรณ์มหาวิทยาลัย

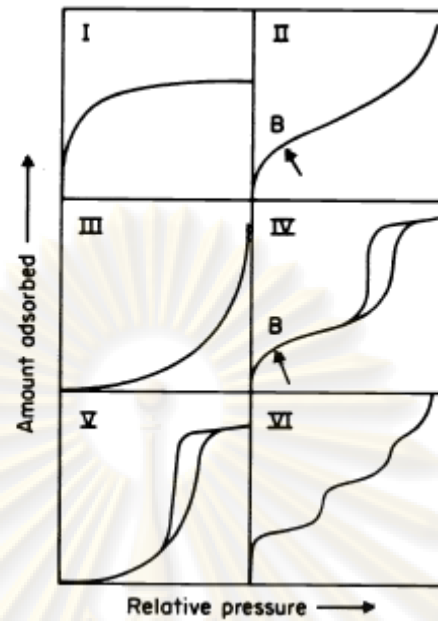


Figure 2.8 Type of physisorption isotherms

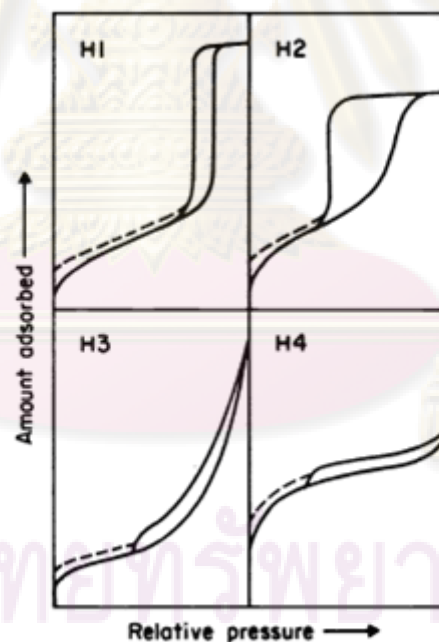


Figure 2.9 Types of hysteresis loops

Hysteresis (Figure 2.9) appearing in the multilayer range of physisorption isotherms is usually associated with capillary condensation in mesopore structures. Such hysteresis loops may exhibit a wide variety of shapes. Type H1 is often associated with porous materials known as compacts of approximately uniform spheres in a fairly regular array, and hence to have narrow distributions of pore size. Many

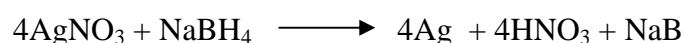
porous adsorbents (e.g. inorganic oxide gels and porous glasses) tend to give Type H2 loops, but in such systems the distribution of pore size and shape is not well-defined. Indeed, the H2 loop is especially difficult to interpret: in the past it was attributed to a difference in mechanism between condensation and evaporation processes occurring in pores with narrow necks and wide bodies (often referred to as ink bottle pores), but it is now recognised that this provides an over-simplified picture and the role of network effects must be taken into account. The Type H3 loop, which exhibit plate-like particles giving rise to slit-shaped pores. Similarly, the Type H4 loop is often associated with narrow slit-like pores.

2.8 Silver nanoparticle (Ag)

Silver nanoparticles have advantages to improve the character of the biosensor such as the metallic properties of the silver nanoparticle can enhance the electron conductivity, the other can adsorb the protein by the interaction between the enzyme and silver nanoparticle. Several methods currently have been applied to synthesize silver nano-particles, such as physical processes of atomization or milling, chemical methods of thermal decomposition, chemical reduction, sol-gel, water-in-oil (W/O) microemulsions, or electrochemical processes. However, the method of chemical reduction from aqueous solutions is most preferable for obtaining nano-sized particles of silver. The essential feature of this chemical reduction method is to give a desirable particle shape and size at high yield and low preparation costs (Kim et al., 2004).

2.8.1 chemical reduction method

Reducing agent such as NaBH₄, Na₃C₆H₅O₇ etc. is added to AgNO₃ aqueous solution for oxidation and reduction. In the formation of silver nano-particles by chemical reduction method, several factors are important for preparation of nano-sized powder of silver. Properties of silver nano-particles obtained by chemical reduction method are affected by various parameters such as the molar concentration ratio of R ([AgNO₃]/[reducing agent]) value (Kim et al., 2004). For example, synthesis of silver nanoparticle with NaBH₄ as reducing agent.



2.8.2 in situ reduction method

This method is directly synthesis of Au nanoparticles in the pore channels of mesoporous silica. As described below (Figure 2.10), the mesoporous silica was modified surface with the help of functional linker groups (APTS) to produce the nitridation of silica was a host for the incorporation of silver nanostructures. After nitridation, the surface Si–OH bonds of the host were at least partially replaced by Si–NH₂ and/or Si–NH–Si bonds. Silver nitrate was used as Ag⁺ source. The interaction between the surface NH_x species and the silver species is the key factor for incorporating silver into the channels of the nitrated host. The surface NH_x groups may act as anchors to help immobilizing silver ions in the channels. Finally, add the reductive reagent (DMF) reduced Ag⁺ to Ag. (Zhao et al., 2004).

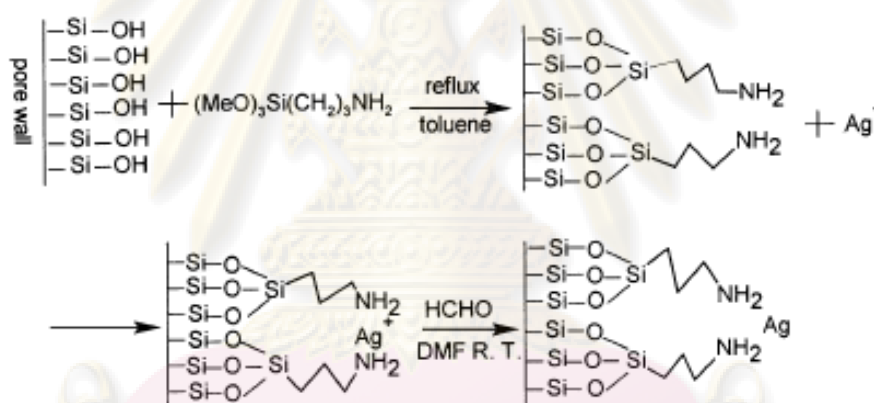


Figure 2.10 Schematic illustration of in situ formation of Ag nanoparticle inside the pore channels of MCM-41 (Zhao et al., 2004)

2.9 Biosensor

A biosensor is an analytical device which converts a biological response into an electrical signal. It is used to determine the concentration of substances and other parameters of biological. It consists of 3 parts (Figure 2.11).

- **The biological component** is an interaction of the biological component with the substrate is highly specific to that substrate alone; thus, avoiding interferences from other substances (such as enzymes, antibodies, nucleic acids, etc).

- **The transducer** or detector device converts an observed change (physical or chemical) into a measurable signal, generally an electronic signal whose magnitude is proportional to the concentration of a specific chemical or set of chemicals (Eggins, 1999).
- **The signal processors** usually converted to a digital signal and passed to a microprocessor stage where the data is processed, converted to concentration units and output to a display device or data store. The parameters in this part have many parameters such as potential range, applied potential and scan rate which these parameters are impact on the performance of biosensor. Therefore, we should select the value of these parameters proper with each experiment.

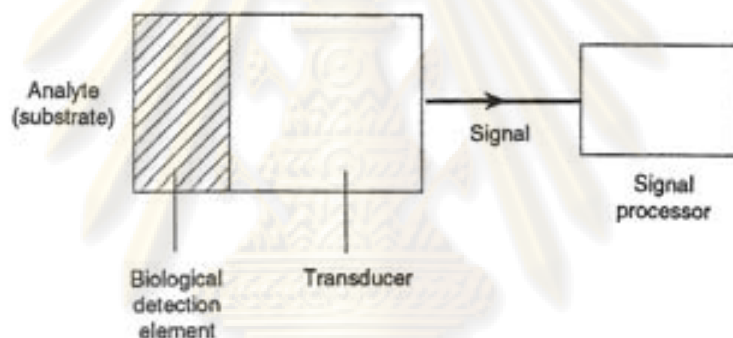


Figure 2.11 Schematic layout of a biosensor (Eggins, 1999).

2.10 Electrochemical method

2.10.1 Cyclic voltammetry (CV)

CV is an electroanalytical technique for studying electrochemical charge transfer reactions. The current at working electrode is monitored while the electrode voltage is changed to a higher or lower voltage, and finally, the voltage is changed back to the original value (Figure 2.12).

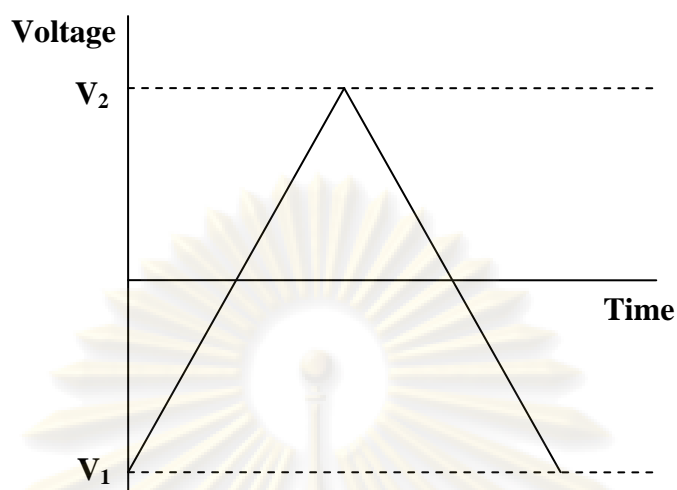


Figure 2.12 potential-time plot for cyclic voltammetry

(<http://www.bath.ac.uk/~chsacf/solartron/Electro/html/dl.ht>)

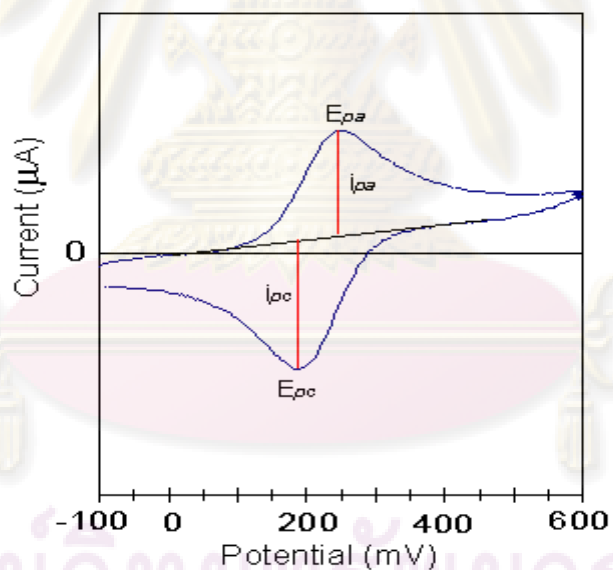


Figure 2.13 current-potential plot for cyclic voltammetry

(http://www-biol.paisley.ac.uk/marco/enzyme_electrode/chapter1/cv.gif)

Cyclic voltammogram (Figure 2.13) shows the anodic peak potential (E_{pa}), anodic peak current (i_{pa}) or oxidation current because the potential is scanned positively, anodic current occurs when the electrode becomes a sufficiently strong oxidant. When the scan direction is switched to negative for reverse scan. The

electrode becomes a sufficiently strong reductant. This causes the cathodic peak potential (E_{pc}), the cathodic peak current (i_{pc}) or reduction current occurs.

2.10.2 Amperometry

Amperometry is an electrochemical technique which a constant potential is applied at working electrode, the current is measured (Figure 2.14).

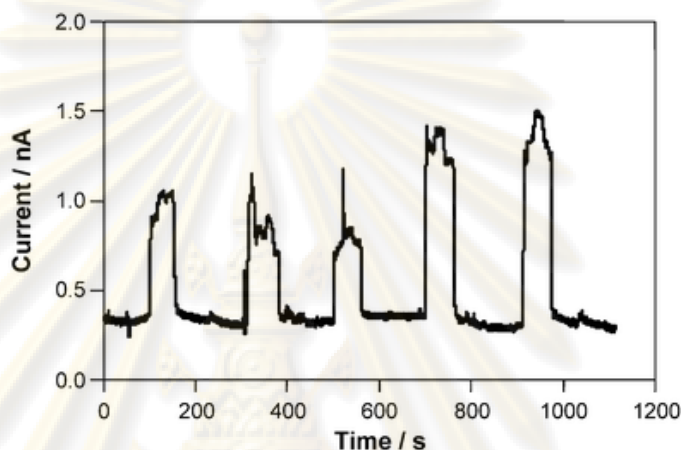


Figure 2.14 Current-time for constant potential amperometry

(www.rsc.org/ej/AN/2007/b611920d/b611920d-f5.gif)

2.11 Performance Factors

Biosensor can be considered as a new technique in analytical field. Thus, methods for determining the performance of biosensor and factors involved are necessary. Some important factors are defined to use in measuring of biosensor's performance. (Eggins, 1999)

1. Selectivity – a range of chemical species that responds to a particular sensor. A sensor may be so specific to one compound in group of related compounds. It must have narrow range.
2. Range and Linear range – the concentration range of substances that can be measured. At the lower limit is the detection limit, which is generally more than 10^{-5} M (0.01 mM). The detection limit can be found by plot the relationship between electrical potential and analyte's concentration. Then,

extending a linear portion of the graph to intersect the baseline. The intersection between these two lines is a detection limit as shown in Figure 2.15.

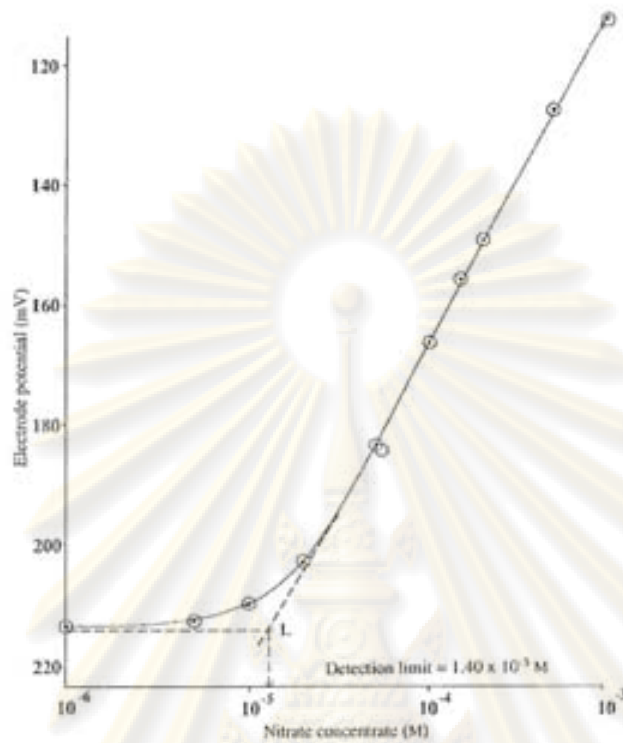


Figure 2.15 Method of determining the detection limit (Eggins, 1999)

3. Reproducibility – the ability of a test the biosensors to be accurately reproduced. Reproducibility is different from repeatability. The result is meaningless if the error of the experiment cannot be defined. Repetition of numbers of experiment must be performed followed by standard deviation in order to compare the result from new experiment to the standard value. The expected reproducibility between replicate determinations should be at least ± 5 to 10 %.
4. Response time – the amount of time required for the system to approach equilibrium. This response time can be varied for each biosensor; however, the typical value is less than 5-10 minutes.
5. Life time – the duration that the biological component on the biosensor lost its activity. There are three aspects of lifetime related to biosensor; the lifetime of the biosensor in use, the lifetime of the biosensor in storage and the lifetime of the biological material stored separately.

2.12 Literature reviews

2.12.1 HRP for phenol detection

Rosatto et al., 1999 studied immobilization of HRP on silica gel modified with titanium oxide. They found that the enzymatic mechanism involved in peroxidase based biosensor for phenol detection consists in the oxidation of native HRP (Fe^{3+}) by hydrogen peroxide (Figure 2.16) and become HRP (Fe^{5+}). Then HRP (Fe^{5+}) get one-electron by the electron donor (phenol), M_{red} and forms HRP (Fe^{4+}). Then HRP (Fe^{4+}) get one-electron by the electron donor (phenol), M_{red} again and forms native HRP (Fe^{3+}). In each step of HRP (Fe^{5+}) changed to HRP (Fe^{3+}), M_{red} get one-electron by electrode. In this step, the reduction current is occurring and proportional to the phenol concentration in the solution (Ruzgas et al., 1995). Nevertheless, peroxidase can also do the direct electron transfer (Figure 2.17) between HRP itself and electrode. Direct electron transfer is similar to mediator electron transfer but HRP (Fe^{5+}) get directly two electrons by electrode. However, direct electron transfer of the hydrogen peroxide reduction by HRP was blocked when immobilised on silica-titanium due to the insulator character of the matrix where the enzyme is immobilised.

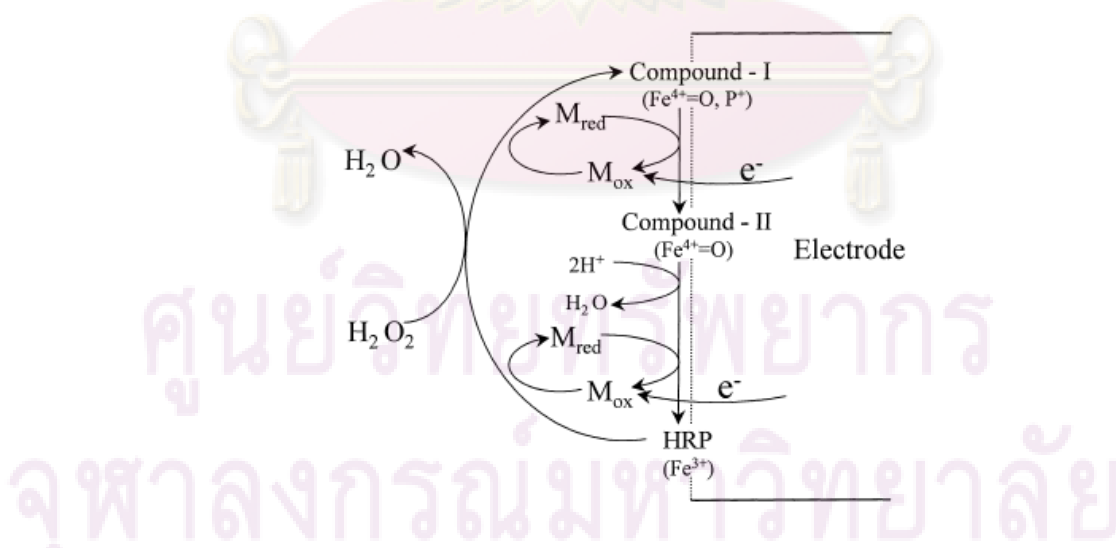


Figure 2.16 Mechanism of mediated electron transfer at HRP modified carbon paste electrode. M_{ox} and M_{red} are the oxidised and reduced forms of the mediator, respectively (Rosatto et al., 1999).

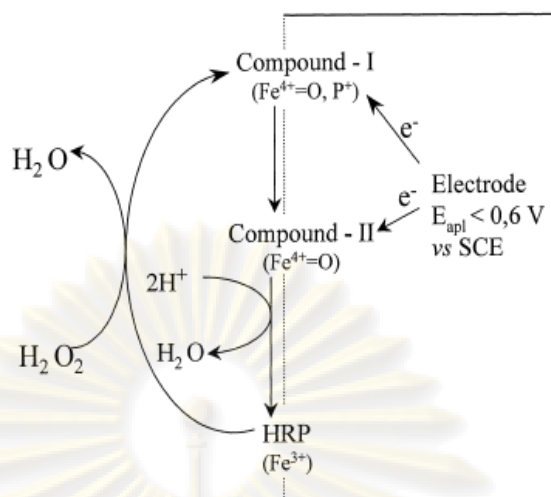


Figure 2.17 Mechanism of the direct electron transfer between HRP and base electrode (Rosatto et al., 1999).

The main parameters to operate of biosensor have many parameters such as optimal potential, scan rate. In each experiment which have differently value of these parameters (Table 2.4). In this study, we chose the applied potential at 0 V, potential range between -0.5 to 0.5 V because of the optimal range is -0.2 to 0 V (Varga et al., 1995) and in more negative values the enzymes molecules could be inactivated by the formation of reduced compound with HRP, decreasing the activity at time function (Rosatto et al., 1999).

ศูนย์วิทยทรัพยากร
จุฬาลงกรณ์มหาวิทยาลัย

Table 2.4 Condition of phenol and H₂O₂ biosensor by immobilized enzyme

Enzyme	Substrate	Matrices for immobilization on electrode	Potential range on Voltammetry (V)	Applied potential on Amperometry (V)	Scan rate (mV/s)	Reference
HRP	H ₂ O ₂ +Phenol	Adsorbed on solid graphite electrode	-0.2 to 0.4	-0.05	100	Ruzgas et al., 1995
HRP+Tyrosinase	H ₂ O ₂ +Phenol	Poly(amphiphilic pyrrole)	-	-0.2	-	Cosnier S. and Popescu I.C., 1996
HRP	H ₂ O ₂ +Phenol	Silica-titanium	-	0	-	Rosatto et al., 1999
HRP+Tyrosinase	H ₂ O ₂ +Phenol	poly(carbamoylsulfonate) /poly(vinyl alcohol) bearing styrylpyridinium groups	-0.75 to 0.75	-0.05	10	Chang et al., 2002
HRP+Tyrosinase	H ₂ O ₂ +Phenol	MCM-41/ poly(vinyl alcohol)	-0.4 to 0.4	-0.05	100	Dai et al., 2004

จุฬาลงกรณ์มหาวิทยาลัย

Enzyme	Substrate	Matrices for immobilization on electrode	Potential range on Voltammogram (V)	Applied potential on Amperometry (V)	Scan rate (mV/s)	Reference
HRP	H ₂ O ₂	Nanosized silver particles /silica sol-gel	-0.6 to 1	-0.3	10	Xu et al., 2004
HRP	H ₂ O ₂	Carboxymethyl chitosan/gold nanoparticle	-0.6 to 0.2	-0.4	100	Xu et al., 2006
HRP	H ₂ O ₂	Chitosan/silica sol-gel-potassium ferricyanide and gold nano particles	-0.1 to 0.6	-0.05	50	Yuan et al., 2007
HRP	H ₂ O ₂	Cyteamine/silver nanoparticle	-0.4 to 0.1	-0.2	10	Ren et al., 2008
HRP	H ₂ O ₂	Clay/chitosan/gold nanoparticle	-0.6 to 0.2	-0.3	200	Zhao et al., 2008

ศูนย์วิจัยทรัพยากร
จุฬาลงกรณ์มหาวิทยาลัย

2.12.2 Mesoporous silica on biosensor

Recently, a series of inorganic pore materials such as titania sol-gel, clay, mesoporous molecular sieves and pore alumina have been proven to be promising as the immobilization matrices due to their regular structure, good mechanical, thermal, and chemical stability. Among them, mesoporous silica has a large specific surface area, excellent mechanical, thermal, and chemical stability, good adsorption and penetrability. Thus it is a good matrix for protein immobilization through physical or chemical action (Dai et al., 2007).

Dai et al., (2004) studied the immobilization of tyrosinase-peroxidase on matrix of mesoporous silica type MCM-41 and PVA. The electrocatalytic response of bienzyme based biosensor to phenol was about 2 times larger than tyrosinase monoenzyme modified electrodes. The MCM-41 has an important role in enhancing the enzymatic activity of tyrosinase and suitable for enzyme loading. This matrix is very efficient for preventing the enzyme leakage out of the film. The sensor could retain 93% of initial activity within a storage period of 60 days at 4 °C. Another example on mesoporous silica is that of Dai et al., (2004), in which the direct electron transfer of horseradish peroxidase immobilized on matrix of hexagonal mesoporous silica (HMS) and PVA. They found that HMS could provide a microenvironment for HRP to undergo facile electron transfer reaction. The large specific surface area of HMS resulted in high enzyme loading and the electrochemical behavior which depended on the specific properties of the HMS. However, another enzyme was immobilized on mesoporous silica together. Glucose oxidase (GOD) was immobilized on matrix of mesoporous silica (MCM-41) and PVA. The porous structure of the MCM-41 film makes the immobilized enzyme easy to be accessed by its substrate and brings out a good performance of the modified electrode. After a storage period of 3 months the biosensor showed an 11% loss of activity (Dai et al., 2006). In addition, Dai et al., (2007) studied the glucose sensor was constructed by entrapping glucose oxidase and horseradish peroxidase in matrix of hexagonal mesoporous silica structures (SBA-15) and nafion. The modified electrode with SBA-15 showed greater responses than electrode without SBA-15. The SBA-15 mesoporous materials accelerated the electron transfer between the entrapped HRP and electrode and prevented the aggregation of enzyme on electrode. The activity to glucose retain 90% of initial activity when storage of 60 days at 4 °C.

2.12.3 Chitosan on biosensor

Chitosan has been found to be an interesting biopolymer for immobilization of desired biomolecules because of excellent film-forming ability, high permeability, mechanical strength, nontoxicity, biocompatibility, low cost and easy availability. With its attractive properties, chitosan has received much attention as material for design of modified electrodes (Khan et al., 2008; Wang et al., 2002).

In case of chitosan as a support on enzyme immobilization, chitosan showed good storage stability for enzyme support. Wang et al., (2002) studied a novel tyrosinase biosensor has been developed for detection of phenols, which is based on the immobilization of tyrosinase in a positively charged chitosan film. They were found that chitosan cross-linked with (3-aminooxyloxypropyl) dimethoxymethylsilane is beneficial for the immobilization of tyrosinase. The large microscopic surface area and porous morphology of chitosan matrix lead to high enzyme loading, and the enzyme entrapped in this matrix can retain its bioactivity. The catalytic current response could maintain about 75% after storage for 70 days at 4 °C. Abdullah et al., (2005) studied the immobilized tyrosinase enzyme in a chitosan film for the detection of phenol. The optimum chitosan concentrations were found to be 2% (w/v). The biosensor also demonstrated optimum activity of buffer solution at pH 6–7 and showed good stability for at least 2 months. Some researcher crosslink chitosan film with glutaraldehyde to provide a high enzyme loading because the widely present amino groups present in chitosan molecules facilitate immobilization of enzymes on chitosan by covalent binding loading and a stable film matrix for enzyme immobilization. Thus leading to less leakage of enzyme from the biosensor surface. It was found that the biosensor retained about 85% of its original response after one month (Miao et al., 2000). Another example on chitosan combined with other material to improve their properties is that of, Fan et al., (2006) studied an amperometric biosensor for phenol determination based on chitosan/laponite clay composite matrix. The composite film was used to immobilize polyphenol oxidase on the surface of electrode. Chitosan was utilized to improve the analytical performance of the pure clay-modified bioelectrode and decreased the electron-transfer resistance at the electrode surface. The chitosan/laponite clay/polyphenol oxidase bioelectrode retained about 88% of its original response after 60 days at 4 °C. In the study of Xu et

al., (2006), the results exhibit the presence O-carboxymethyl chitosan (CMCS) in silica sol-gel for HRP immobilization. The film would not crack. When there was no CMCS, the response time for analytic substrate became longer and not more enzyme activity was retained. Therefore, the presence of CMCS provided friendly surroundings for the immobilization of enzymes. Similarly, Yang et al., (2004) studied the immobilization of Glucose oxidase in surface treated nanoporous ZrO₂/Chitosan composite matrix was. ZrO₂ was treated with sodium dodecylbenene sulfonate to make the surface of ZrO₂ changed from hydrophilic to hydrophobic. The surface-treated ZrO₂/Chitosan film showed that the matrix was porous and highly homogeneous and in presence of chitosan which could overcome the cracking caused by inorganic material for enzyme immobilization in biosensor construction. Glucose oxidase immobilized in this material maintained its activity about 75.2% of its original response after 30 days of storage.

2.12.4 Metal on biosensor

Various metals have been studied as additive for enzyme immobilization in biosensor such as silver (Ag), gold (Au), platinum (Pt), and palladium (Pd). These metal nanoparticles have good interaction with the protein. Among these metals, silver is the best conductor. It can act as tiny conduction centers and can facilitate the transfer of electrons (Ren et al., 2005).

In case of silver loading in enzyme immobilization process, Xu et al., (2004) studied the nanosized silver particles are used to dope into the silica sol-gel film to prepare a biosensor. The HRP, mediator methylene blue (MB), nanosized silver particles and silica sol-gel solution are mixed and coated on the surface of electrode for biosensor. The Ag nanoparticles in the sol-gel film not only improve the conductivity, but also adsorb the enzyme molecules to keep the stability of the biosensor. So the biosensor has higher sensitivity than the traditional sol-gel biosensor. The current response decreased about 18% in 2 weeks. Ren et al., (2005) studied an immobilization of glucose oxidase in Ag nanoparticles sol cross-linked with a polyvinyl butyral (PVB). The result indicates that the current response of the electrode containing Ag nanoparticles is much larger than the enzyme electrode containing no Ag nanoparticles. The Ag nanoparticles function as electron-conducting

pathways between the enzyme and the electrode surface, therefore the electron transfer rate between the enzyme and the electrode is increased significantly and the time reaching the steady-state current response reduced from 60 to 20 s. Ren et al., (2005) studied immobilized HRP on silver nanoparticles adsorbed on a cysteamine monolayer-modified electrode, and detected H_2O_2 . The catalytic current at the HRP/cysteamine electrode was very slight compared to that at the HRP/silver nanoparticles/cysteamine electrode. Silver nanoparticles play an important role in the catalysis process because the silver nanoparticles facilitate electron transfer between HRP and the bulk electrode surface and provide more binding sites for the immobilization of HRP, thus increasing the biosensor's sensitivity. When it was stored at 4 °C for two weeks, the sensor retained more than 86.2% of its initial response.

Recently, many published works gave the relation between nanoparticles and inorganic material to improve the conductivity of inorganic material. Lin et al., (2008) studied the catalytic activity of silver nanoparticles confined in the mesoporous silica SBA-15 to the reduction of hydrogen peroxide (H_2O_2). The Ag-SBA-15 modified electrode exhibited an excellent electrocatalytic activity toward the reduction of hydrogen peroxide (H_2O_2). The electrode can maintain over 97% of the initial value in the response to H_2O_2 after 100 days. In the same way of the study of Bai et al., (2007), have proposed gold nanoparticles-mesoporous silica (SBA-15) composite as a support for glucose oxidase immobilization. The result reveals the introduction of gold nanoparticles improved the conductivity of SBA-15. Besides, gold-nanoparticle were assembled on the surface of porous calcium carbonate microspheres ($CaCO_3$) hybrid material for immobilized HRP in the determination of H_2O_2 . When without the gold-nanoparticle, HRP- $CaCO_3$ are not stable in aqueous solution. Therefore, the direct and stable electron transfer of HRP was suggested to be the result of the synergic effect of both $CaCO_3$ and gold-nanoparticle. The hybrid material provided a biocompatible environment for HRP to orient the heme edge toward its electron donor or acceptor and facilitate its electron-transfer process. When the biosensor was stored in a dry state at 4 °C, the current response for H_2O_2 decreased by only about 6% of the original value after 20 days (Cai et al., 2005).

CHAPTER III

MATERIALS & METHODS

3.1 Chemicals

1. Horseradish peroxidase (HRP, EC 1.11.1.7), available from Toyobo, Japan.
2. Phenol (C₆H₅OH), available from Carlo Erba Regent Co.
3. potassium hydrogen phosphate (K₂HPO₄), available from Ajax Fine Chem.
4. potassium dihydrogen phosphate (KH₂PO₄), available from Ajax Fine Chem.
5. Hydrogen peroxide (H₂O₂) 30%, available from E.Merck, Darmstadt.
6. Chitosan (deacetylation degree 95 %, MW 1,450 kDa), available from Seafresh chitosan Co., Ltd., Thailand.
7. Acetic acid (CH₃COOH), available from BDH laboratory supplies.
8. Silver nitrate (AgNO₃), available from Poch S.A.
9. Hydrochloric Acid (HCl), available from J.T. Baker.
10. Tetraethyl orthosilicate (TEOS), available from Sigma Aldrich.
11. Pluronic P123, available from BASF.
12. 1,3,5-Trimethylbenzene (TMB), available from Supelco.
13. Sodium Borohydride (NaBH₄), available from Ajax Fine Chem.
14. Sodium Hydroxide (NaOH), available from Ajax Fine Chem.
15. Toluene Anhydrosol (C₆H₅CH₃), available from Lab Scan.
16. Dichloromethane (CH₂Cl₂), available from Fisher scientific.
17. Silica dioxide nanopowder (SiO₂), commercial grade, available from Sigma Aldrich.

* All chemicals were of analytical grade and used without further purification.

3.2 Apparatus

1. Cyclic voltammetry (CV) and amperometry was performed using a Glucosen potentiostat (Chulalongkorn University, Thailand). All electrochemical experiments were performed in three-electrode cell using a glassy carbon electrode

(GC) as working electrode, a silver/silver chloride (Ag/AgCl) reference electrode and a platinum counter electrode (figure 3.1).

2. The working electrode was cleaned by sonication using ultrasonic cleaner (CREST, model D, Malaysia).

3. Vacuum oven (Binder model VD23, USA) used for synthesis of MCF.

4. Magnetic stirrer (Barnstead Thermolyne, Canada).

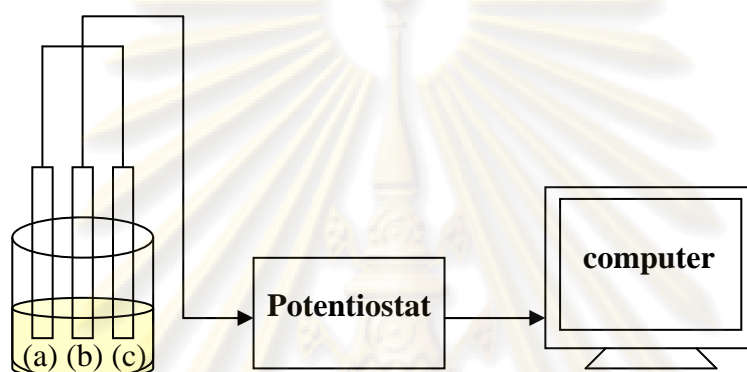


Figure 3.1 Schematic diagram of experiments: (a), (b) and (c) shown in figure 3.2 and potentiostat shown in figure 3.3

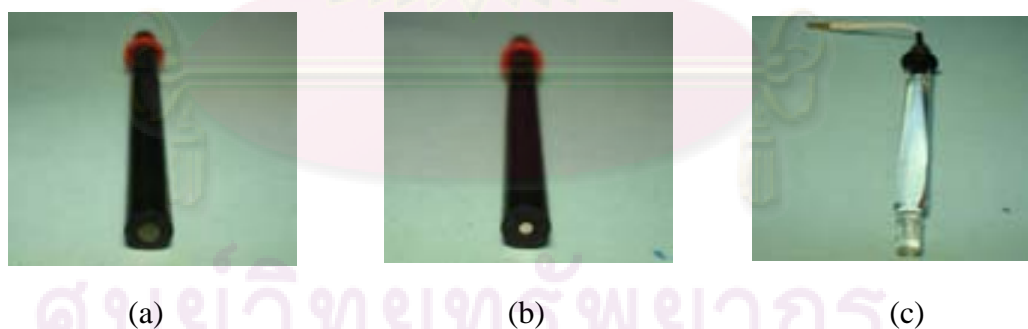


Figure 3.2 (a) working electrode (WE), (b) counter electrode (CE) and (c) reference electrode (RE).



Figure 3.3 Glucosen potentiostat

3.3 Synthesis of mesoporous silica (MCF)

Pluronic P123 (MW = 5800, 2.0 g, 0.4 mmol) was added to 75 mL of 1.6 M HCl at 35-40 °C using magnetic stirrer. One gram of TMB was then added to the polymer solution, and the mixture was stirred for at least 1 h. Tetraethyl orthosilicate (TEOS, 4.25 g, 21 mmol) was added as the silica source. After the mixture was stirred for 24 h at 35-40 °C and aged for 24 h at 100-120 °C in vacuum oven, the solids were collected by filtration with filter paper no.5 and dried in air for 24 h. The resulting powder was calcined at 500 °C for 6 h to produce the mesoporous silica material (Lettow et al., 2000).

3.4 Synthesis of Ag/MCF and Ag/SiO₂

In our method, we used the in situ reduction method to synthesis Ag/MCF. This method had 2 steps, surface functionalization to produce MCF-NH₂ for host of the incorporation of Ag nanoparticle and Ag loading as describe below.

In the functionalization step, surface of MCF was functionalized follow method of Zhao et al. (2004). In this process, 1 g of calcined MCF and 10 ml of ATPS were added in 150 ml toluene anhydrous in teflon bottle then the mixture was heated at 100 °C for 24 h in vacuum oven. Subsequently, the solid was filtrated off by filter paper no.5 and washed with 150 ml of toluene anhydrosan and 30 ml of dichloromethane . Finally, resulting solid was dried under vacuum at 50 °C for 10 h to produce the modified MCF.

In the metal loading step, silver nitrate was used as Ag^+ precursor. The chemical sonocation technique was selected for reduction silver nanoparticle. The functionalized MCF (0.1 g) was poured in 50 ml AgNO_3 solution of various concentrations (20, 100, 500, 1000 ppm) in flask 125 ml and the solid-mixture was stirred with magnetic stirrer for 6 h at room temperature. Then the mixture in flask was put in ultrasonic cleaner and irradiation at frequency of 40 kHz for 12 h. During the mixture in flask was react, the flask was purged with argon gas to eliminated oxygen all the time. And flow cool water to control temperature in ultrasonic bath at 20 °C all the time. After the reduction, the resulting solid was filtrated by filter paper no.5 and dried in vacuum oven at 50 °C for 10 h to produce Ag/MCF. The synthesis of Ag/SiO₂ was same to the synthesis of Ag/MCF but we changed MCF to SiO₂ nanopowder.

3.5 Characterization of MCF, Ag/MCF and Ag/SiO₂

The specific surface area and pore volumes of MCF were measured and calculated according to the Brunauer-Emmett-Teller (BET) method. The weight of the sample was 0.3 g. And the sample was degassed at 300 °C prior to the measurement. Transmission Electron Microscopy (TEM) to determination of surface characteristics such as pore diameter by using JEOL JEM-2100. Fourier transform infrared (FT-IR) spectrometer for identifying the chemical structure of modified MCF by using FT-IR model 1760x. X-ray diffraction (XRD) for the structure of MCF by using XRD model JDX-8030. UV-vis absorption spectrum was recorded on a Shimadzu UV-2450 spectrophotometer for identifying Ag nanoparticles in MCF and on Si, the absorbance spectra of Ag/MCF and Ag/SiO₂ in the wavelength range of 200-700 nm.

3.6 Synthesis of Ag

The preparation of Ag solution were obtained by chemical reduction of metal salts to yield the corresponding zero valent metal nanoparticles with NaBH_4 . To ensure the entire reduction, the concentration of NaBH_4 was 10 times that of metal salt (Huang et al., 2004). Prepare 50 ml of (20, 100, 500 ppm) AgNO_3 solution in flask 250 ml controlled at 70 °C all the time using magnetic stirrer and mixed with 50 ml of the concentration of NaBH_4 was 10 times that of each AgNO_3 concentration,

then stirred for 90 minutes and mixtures will change to yellow. Silver nanoparticle solution was stored in dark brown bottle at 4°C.

3.7 Preparation of chitosan solution

In this study, we prepare the chitosan concentration (0.1-0.7 %w/v). For example, chitosan solution (0.5 %w/v) was prepared by dissolving 0.5 g of chitosan powder in 100 mL of acetic acid (1%, v/v). The viscous chitosan solution was stirred by magnetic stirrer overnight at room temperature. Then, adjusted the pH of all chitosan concentration to 5.0 with 0.1 M NaOH solution.

3.8 Preparation of Ag/chitosan solution

0.1 ml silver nanoparticle solution of various concentration (100, 500, 1000 ppm) add in 1 ml chitosan 0.5 %w/v in beaker 10 ml and stirred for 30 minutes.

3.9 Procedures for modified working electrode

3.9.1 Working electrode cleaning

Before each experiment, working electrode was first polished with 0.3 μm alumina slurry and rinsed with distilled water. The electrode was then sonicated using ultrasonic cleaner at frequency of 40 kHz in absolute ethanol for 5 minutes and distilled water 5 minutes, respectively. After dried in ambient condition for 30 minutes, the electrode was ready to use as bare electrode.

3.9.2 Preparation of the modified working electrode with different composite

3.9.2.1 Chitosan film

32 μl of 10 mg/ml HRP (in pH 6.0 phosphate buffer) was dropped into 1 ml of chitosan solution (0.5 %w/v) in beaker 10 ml and stirred at 4 °C for 6 h. 5 μl of the prepared solution was dropped on the pretreated WE surface and allowed to dry under ambient condition for 2 h.

3.9.2.2 Chitosan/MCF composite film

In this study, we prepare the amount of MCF in chitosan solution (0.1-0.7 %w/v). For example, MCF (0.1 %w/v) was prepared by 1 mg of MCF were dispersed in 1 ml of various chitosan concentration (0.1-0.7 %w/v) in beaker 10 ml and stirred at 4 °C for 90 minutes to produce a MCF colloid. 32 µl of 10 mg/ml HRP (in pH 6.0 phosphate buffer) was dropped into MCF colloid and stirred at 4 °C for 6 h. 5 µl of the prepared solution was dropped on the pretreated WE surface and allowed to dry under ambient condition for 2 h.

3.9.2.3 Chitosan/(Ag/MCF) and Chitosan/(Ag/SiO₂) composite film

7 mg of various Ag in MCF (section 3.4) were dispersed in 1 ml of chitosan 0.5 %w/v in beaker 10 ml and stirred at 4 °C for 90 minutes to produce a Chitosan/(Ag/MCF) colloid. 32 µl of 10 mg/ml HRP (in pH 6.0 phosphate buffer) was dropped into Chitosan/Ag/MCF colloid and stirred at 4 °C for 6 h. 5 µl of the prepared solution was dropped on the pretreated WE surface and allowed to dry under ambient condition for 2 h. In case of chitosan/(Ag/SiO₂) was same to chitosan/(Ag/MCF) but changed Ag/MCF to Ag/SiO₂.

3.9.2.4 (Ag/Chitosan solution)/MCF composite film

7 mg of MCF were dispersed in 1 ml of various solution of Ag/chitosan 0.5 %w/v (section 3.8) and stirred at 4 °C for 90 minutes to produce an Ag/Chitosan solution/MCF colloid. 32 µl of HRP was dropped into (Ag/Chitosan solution)/MCF colloid and stirred at 4 °C for 6 h. 5 µl of the prepared solution was dropped on the pretreated WE surface and allowed to dry under ambient condition for 2 h.

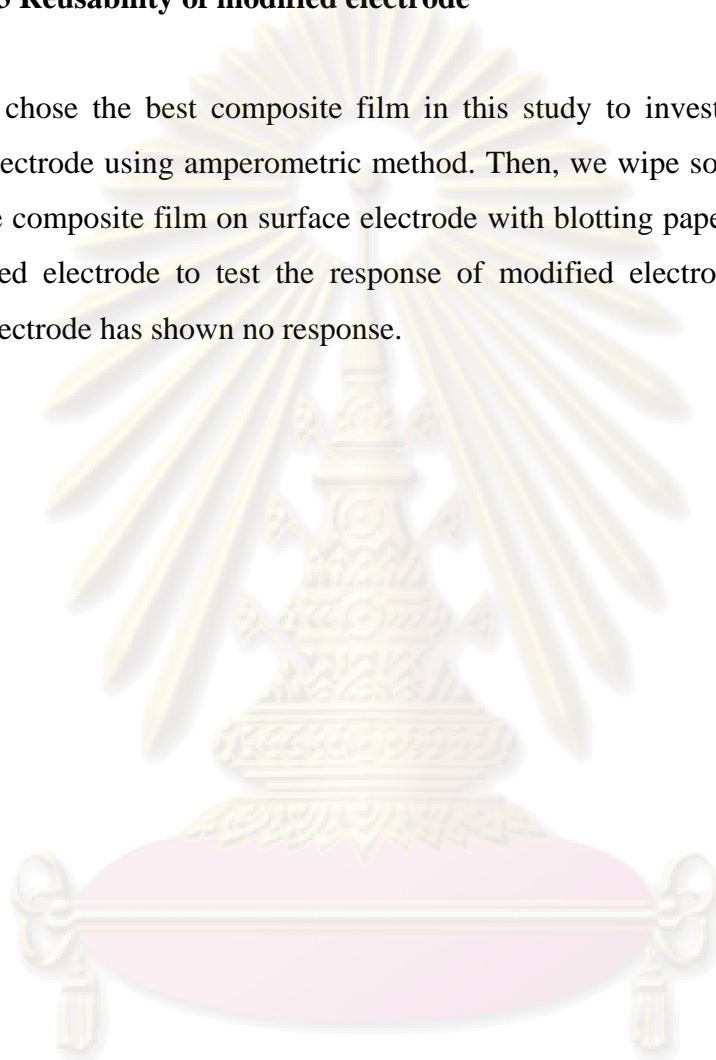
3.9.2.5 Cyclic voltammetric and Amperometric phenol sensor

The cyclic voltammogram response of modified electrode to phenol was measured by add the 60 µl of 0.1 M phosphate buffer solution pH 7 (PBS pH 7) containing 0.1 mM hydrogen peroxide into 5.94 ml of 0.1 M PBS pH 7 containing 0.1 mM phenol in beaker 10 ml as substrate solution. The solution was stirred at a constant rate using a magnetic stirrer bar. Cyclic voltammogram were recorded at scan rate 50 mV/s and the potential between -500 mV and 500 mV.

The amperometric response of modified electrode to phenol was measured same as cyclic voltammetric but fixed potential at 0 mV. The solution was stirred at a constant rate using a magnetic stirrer. Current was measured as a function of time.

3.9.3 Reusability of modified electrode

We chose the best composite film in this study to investigate the reuse of modified electrode using amperometric method. Then, we wipe some solution which attaches the composite film on surface electrode with blotting paper after that we use this modified electrode to test the response of modified electrode again until the modified electrode has shown no response.



ศูนย์วิจัยทรัพยากร
จุฬาลงกรณ์มหาวิทยาลัย

CHAPTER IV

RESULTS AND DISCUSSION

The results in this chapter are divided into three sections. Firstly, the physical and chemical properties of MCF, modified MCF, SiO₂ nanopowder, and modified SiO₂ nanopowder. In addition, results from UV-vis spectroscopy and TEM micrographs for Ag/SiO₂ nanopowder, and Ag/MCF were described. Please be noted that only modified MCF and modified SiO₂ nanopowder (modified SiO₂) were used for syntheses of Ag/MCF and Ag/SiO₂ nanopowder (Ag/SiO₂), since aminopropyl groups which was added to the surface after modification were used for incorporation of Ag nanoparticles. Secondly, effects of amounts of MCF, chitosan, and Ag particles on biosensor responses are discussed. Finally, reproducibility of the modified biosensor electrodes are illustrated.

4.1 Characterization of MCF and SiO₂ nanopowder

Figure 4.1 shows the nitrogen adsorption-desorption isotherm of MCF. From the isotherm characteristics of H1 hysteresis loop of type-IV mesoporous material, it could be concluded that MCF synthesized in this work was of approximately uniform spheres in fairly regular array as classified by IUPAC (See Section 2.7).

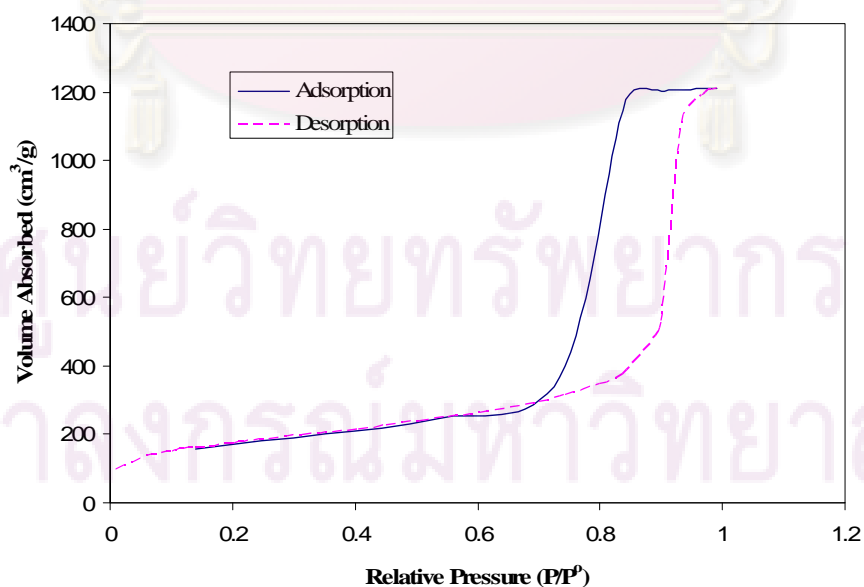


Figure 4.1 N₂ adsorption-desorption isotherm of MCF

The pore size and pore size distribution were calculated from adsorption branches of isotherms by the Barrett–Joyner–Halenda (BJH) method and are displayed in Figure 4.2. The pore size distribution peak is narrow and of one peak with the average pore diameter of 23.7 nm.

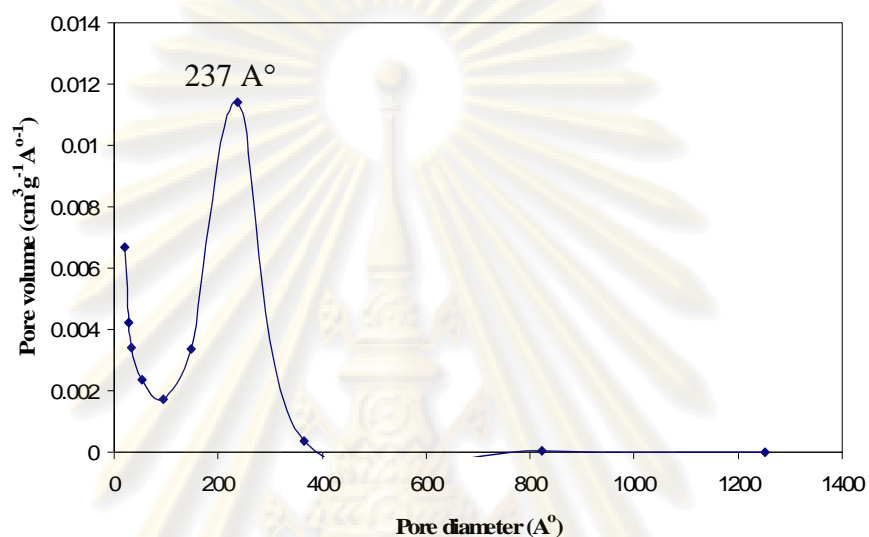


Figure 4.2 Pore size distribution of MCF

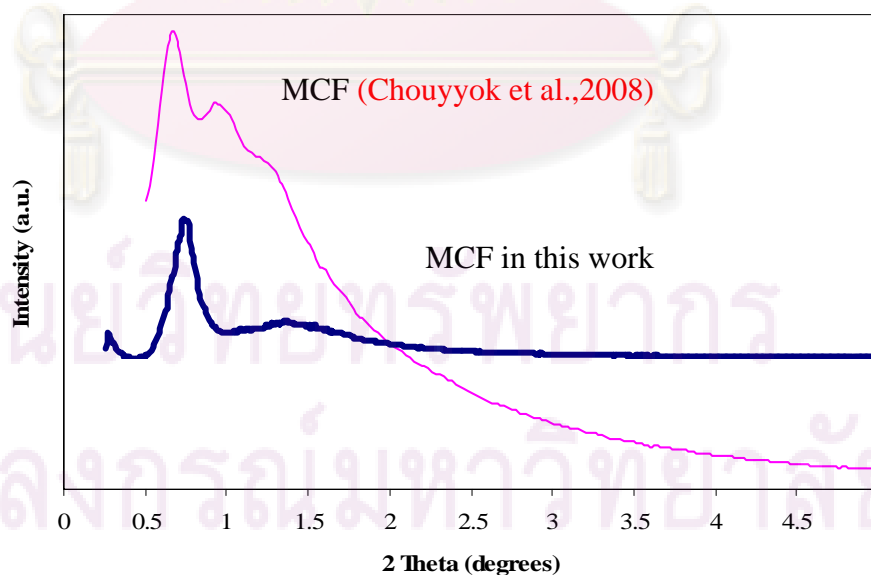


Figure 4.3 XRD patterns of MCF

XRD pattern of the synthesized material, as shown in Figure 4.3, confirms that the mesoporous silica synthesized was of mesocellular foam characteristics or uniform arrays of sphere as already mentioned. In addition, XRD pattern of MCF which was synthesized in this study was of the same pattern as that of [Chouyyok et al.\(2008\)](#).

The specific surface area, pore size, and pore volume of MCF were determined from nitrogen adsorption isotherms and are displayed in Table 4.1. It is noticed that, the pore size and pore volume of MCF are indicated, while that of SiO₂nanopowder are not. This is because SiO₂ nanopowder used was of a nonporous type. On the other hand, MCF average pore size was determined at 23.7 nm which corresponds to an IUPAC classified mesoporous material. Therefore, it is not surprising that MCF contained much higher surface area (approximately 4 folds higher) than SiO₂ nanopowder.

Table 4.1 Physical properties of MCF and SiO₂ nanopowder.

Support	Pore size* (nm)	Surface area (m ² /g)	Pore volume (cm ³ /g)
MCF	23.7	629.97	1.85
SiO ₂ nanopowder**	-	140-180	-

*From figure 4.1 Pore size distribution of MCF.

**Specification from Sigma-Aldrich.

The surface of MCF and SiO₂ nanopowder were modified to host Ag. Similar to what was already mentioned in section 2.6.2, the surface silanol groups allow covalent linkage with functionalized organic moieties, APTS in this case. Therefore, the aminopropyl groups with amine functional groups at the far end were linked to the silanol groups (Figure 4.4).

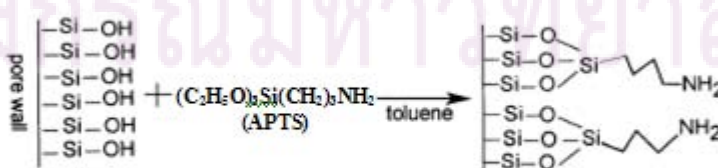


Figure 4.4 Schematic illustration of modified surface of silica with APTS

Silver nitrate was used as Ag^+ source. The interaction between the surface NH_2 species and Ag^+ was same as Long et al.(2007). The surface NH_2 groups may act as anchors to help immobilizing Ag^+ . Changing of Ag^+ to Ag can be obtained by using H_2O (Long et al., 2007) associate with ultrasound at frequency of ca. 40 kHz shown in Figure 4.5.

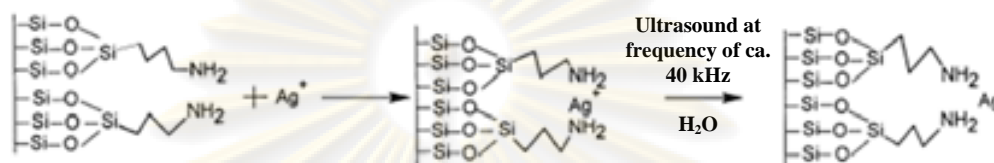


Figure 4.5 Schematic illustration of in situ formation of Ag nanoparticle on modified surface silica (Zhao et al., 2004)

In order to confirm the surface modification, Figure 4.6 exhibits the FTIR spectra of MCF and SiO_2 nanopowder before and after surface modification. For MCF, 1200-1000 cm^{-1} band was attributed to siloxane, Si-O-Si, vibrations while the band between 3700 and 3200 cm^{-1} was attributed to Si-OH stretching (silanol group). For the surface modified materials, the presence of aminopropyl groups were identified by the appearance of C-H stretching band between 2935-2945 cm^{-1} (Luan et al., 2005). Zhao et al. (2004) also confirmed the similar FTIR patterns on MCM-41 (See Figure 4.6).

ศูนย์วิทยทรัพยากร
จุฬาลงกรณ์มหาวิทยาลัย

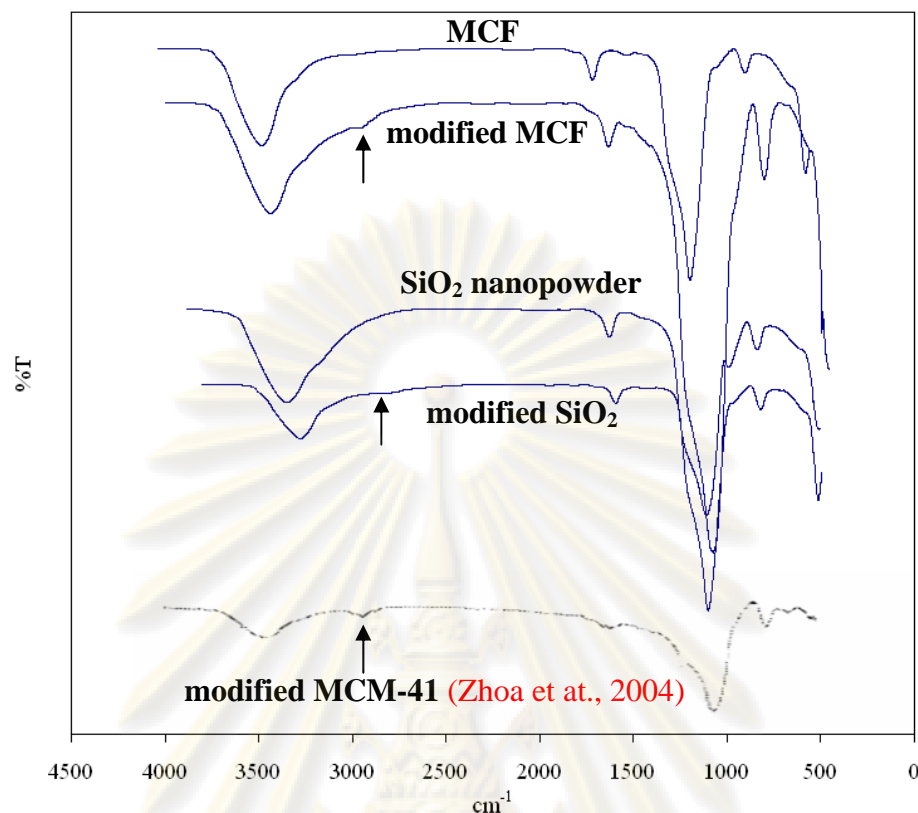


Figure 4.6 FTIR of MCF, modified MCF, SiO₂ nanopowder and modified SiO₂ compare with modified MCM-41 (Zhao et al., 2004).

After modified surfaces of MCF and SiO₂ nanopowder with aminopropyl groups, the presence of C–H stretching occurred. The modification of MCF in this amount of aminopropyl groups does not decrease both surface area and pore diameter (Luan et al., 2005).

4.2 Characterization of Ag/MCF and Ag/SiO₂

In order to confirm the attachment of Ag on modified MCF and SiO₂ nanopowder, we used the UV-vis spectrophotometer and TEM to test the UV–visible light absorption and size of Ag respectively. UV–visible light spectrum of Ag/SiO₂, and Ag/MCF at different Ag concentrations (100, 500, 1000 ppm) are demonstrated in Figure 4.7, and 4.8, respectively. It is obviously noticed that Si nanopowder without Ag does not show any peak at 420 nm. Therefore, absorbance peak at a wavelength of 420 nm was most likely indicated the Ag particle. This is also in accordance to Zhao et al., (2004) who reported the same 420 nm wavelength for Ag particle. Moreover,

the Figure demonstrates the increase in absorbance intensity with increased Ag concentration. Therefore, it could be concluded that Ag particles were incorporated on the surface of SiO₂ nanopowder. Similarly, MCF and Ag/MCF were tested using UV-vis spectrophotometry, and the results are shown in Figure 4.8. It is obviously noticed that MCF without Ag does not show any peak. However, the absorbance peaks show almost same pattern of all the Ag concentrations and have been appeared at the wavelength of 440 nm. However, it is believed that the revealed peak may have Ag attachment.

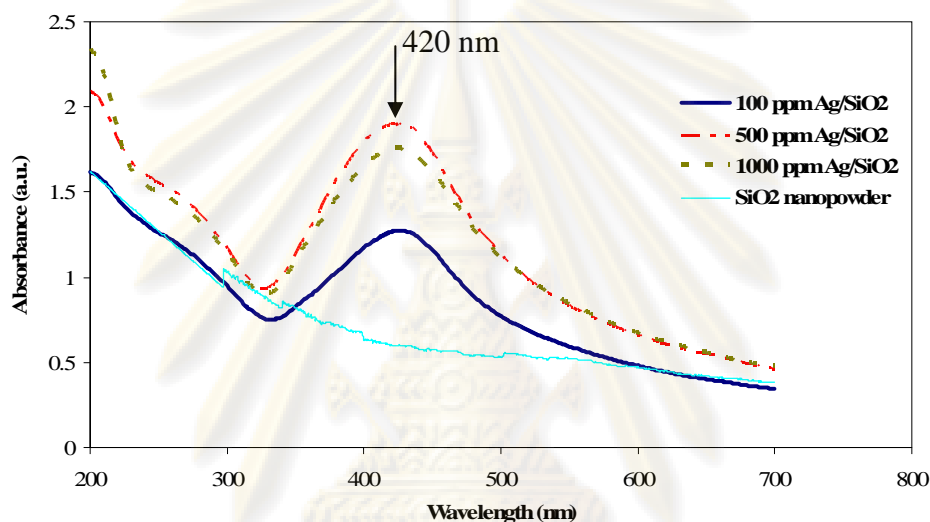


Figure 4.7 UV-vis spectrums of Ag/SiO₂ with various amount of Ag

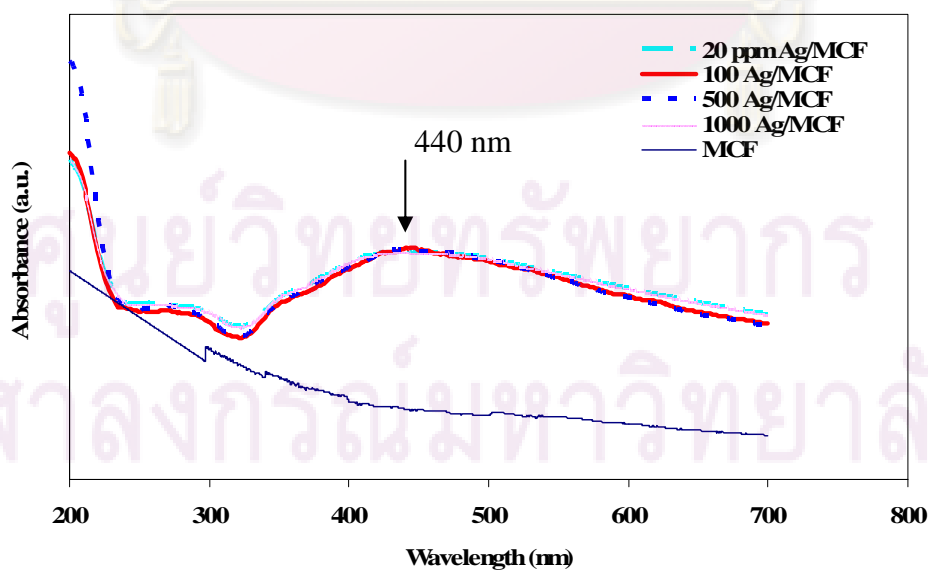


Figure 4.8 UV-vis spectrums of Ag/MCF with various amount of Ag

In order to confirm the UV-vis results regarding Ag attachment on the surfaces as well as to determine rough sizes, and distribution of Ag particles on these surfaces, Transmission electron microscopy (TEM) were used. The micrographs are shown in Figure 4.9, which Figure 4.9(a) demonstrates spherical cells and frame structure of MCF synthesized in this work. This is in accordance to Chouyyok et al. 2008 who reported the very similar TEM image. The Ag nanoparticles were attached on surface of MCF shown in figure 4.9(b). The dark spots in figure 4.9(b) are the Ag nanoparticles integrated with the pore structure of MCF with average size of 19 nm. It was likely that more surface area of MCF caused higher silver nitrate entrapment than the case of nonporous SiO₂ nanopowder. Therefore, bigger Ag particles were observed. The dark spots on surface of Si in figure 4.9(c) are the Ag nanoparticles which good distribution on surface of Si nanopowder and average size of about 9 nm.

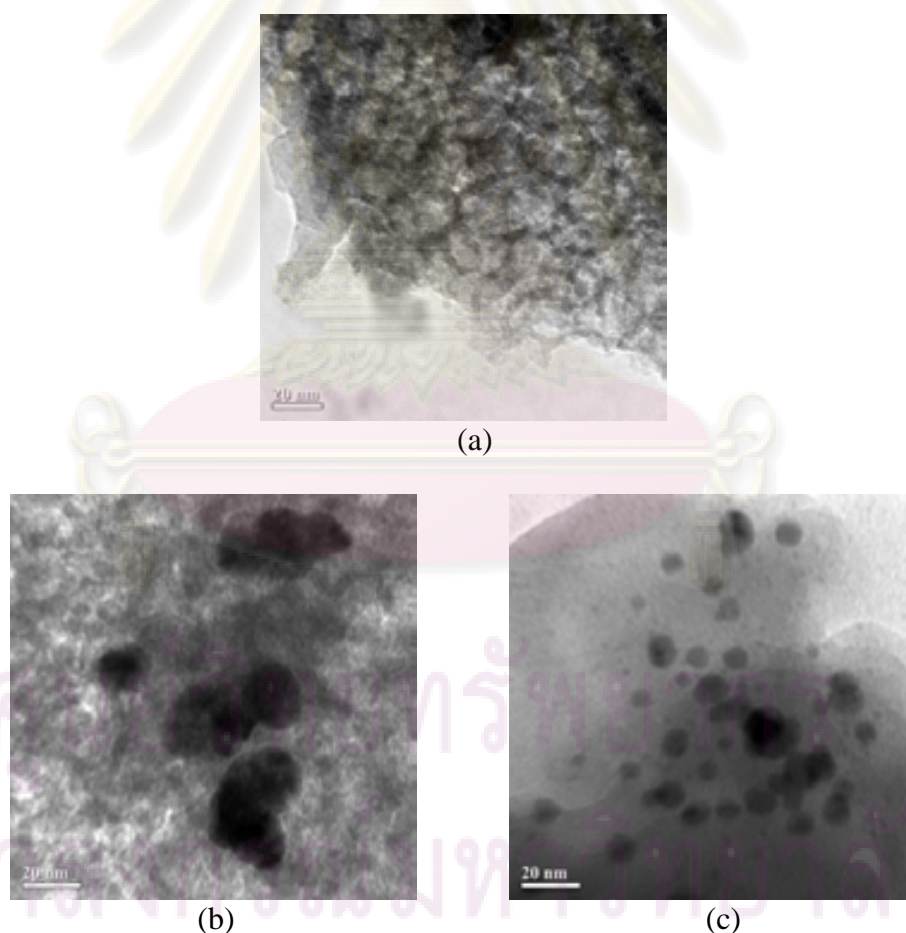


Figure 4.9 TEM micrograph of synthesized MCF (a), Ag/MCF (b), Ag/SiO₂ (c).

When the surface area, pore volume and pore size were checked again after Ag loading on silica with nitrogen adsorption isotherms and pore size was calculated from adsorption branches of isotherms by the Barrett–Joyner–Halenda (BJH) method and were shown in Table 4.2

Table 4.2 Physical properties of MCF, SiO₂ nanopowder and Ag/MCF

Support	Pore size (nm)	Surface area (m ² /g)	Pore volume (cm ³ /g)
MCF	23.7	629.97	1.85
Ag/MCF	24.5	300.13	1.47
SiO ₂ nanopowder	-	140-180	-

Considering pore size, surface area, and pore volume of MCF before and after Ag loading, it was likely that Ag was entrapped in the pore of MCF. In addition, Ag attachment on the outer surface of MCF was possible. When comparing a 23.7 nm pore size of MCF and 4.8 nm average molecular diameter of HRP (Takahashi et al., 2001), it was possible that HRP could be entrapped in the pore of MCF in addition to adsorption on the outer surface of the mesoporous material. The proposed schematic diagrams for HRP entrapment in various matrices are shown in Figure 4.10

ศูนย์วิทยทรัพยากร
จุฬาลงกรณ์มหาวิทยาลัย

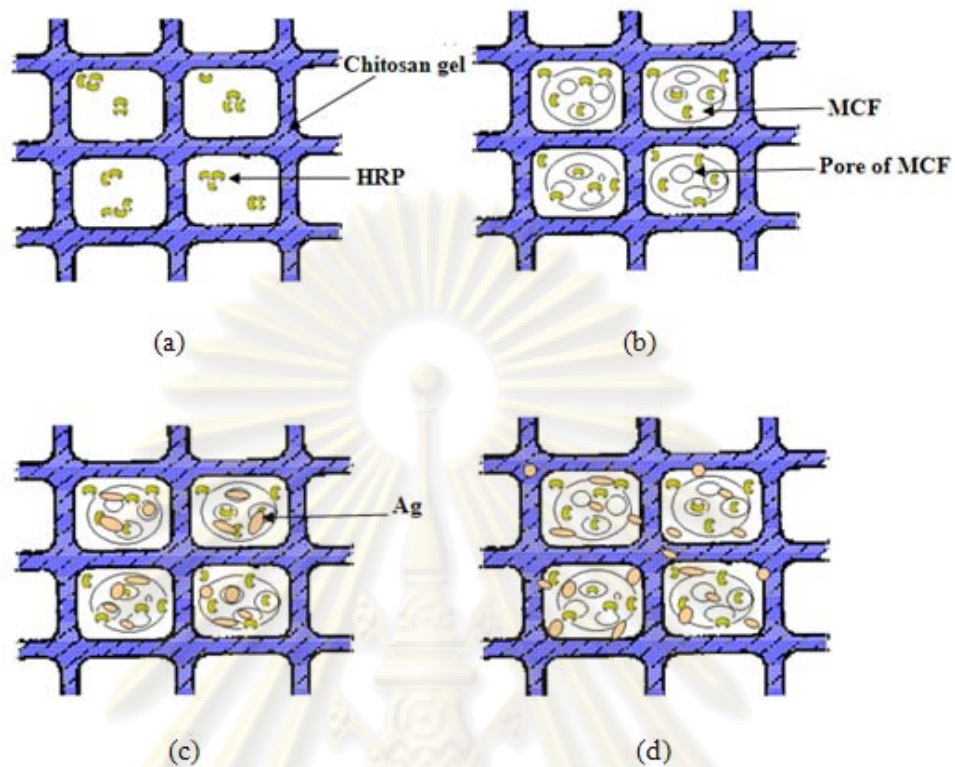


Figure 4.10 Proposed schematic diagrams for HRP were entrapped in chitosan (a), MCF and chitosan (b), Ag/MCF and chitosan (c) and Ag/chitosan and MCF (d)

4.3 The effect of amount of MCF, chitosan concentration, and amount of Ag in each composite film on cyclic voltammogram.

The factor which is really the most important contributing component to the performance of an immobilized enzyme system are physical and chemical properties of support. They have effect on activity and stability of enzyme. The support functional group which is chemical properties have effect on immobilized enzyme whereas physical properties such as pore size, specific area and tortuosity have effect on Effective Diffusivity (D_{eff}) as shown in equation 4.1 which concern in mass transfer limitation.

$$D_{\text{eff}} = D_s \frac{\varepsilon}{\tau} H \quad (4.1)$$

Where D_{eff} is a function of bulk diffusivity (D_s), particle porosity (ε), tortuosity (τ) and hindrance factor (H)

The schematic diagram of mass transport processes in this study was shown in Figure 4.11. In Figure 4.11 exhibit that the diffusivity of substrate solution must thought the matrix which is the support for enzyme immobilization so diffusivity is more important

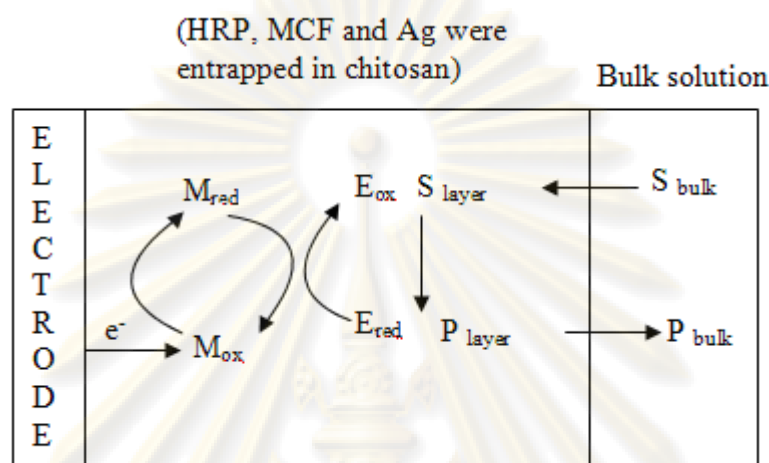


Figure 4.11 Proposed schematic diagram of mass transport processes in this study. E is enzyme, M is mediator, S is substrate and P is product. The subscripts red and ox indicate that the reduced and oxidized forms of enzyme or mediator

4.3.1 The effect of base solutions on cyclic voltammogram

In this section, we tested the response of bare electrode in presence of base solutions. The base solutions in this study is consist of PBS pH 7 as buffer solution for dissolve the substance solutions, Hydrogen peroxide and Phenol which acted as substance solutions to determine the interfere of each solution in electrochemical reaction with 50 mV/ s of scan rate and potential range between -0.5 – 0.5 volts.

ศูนย์วิทยทรัพยากร
 จุฬาลงกรณ์มหาวิทยาลัย

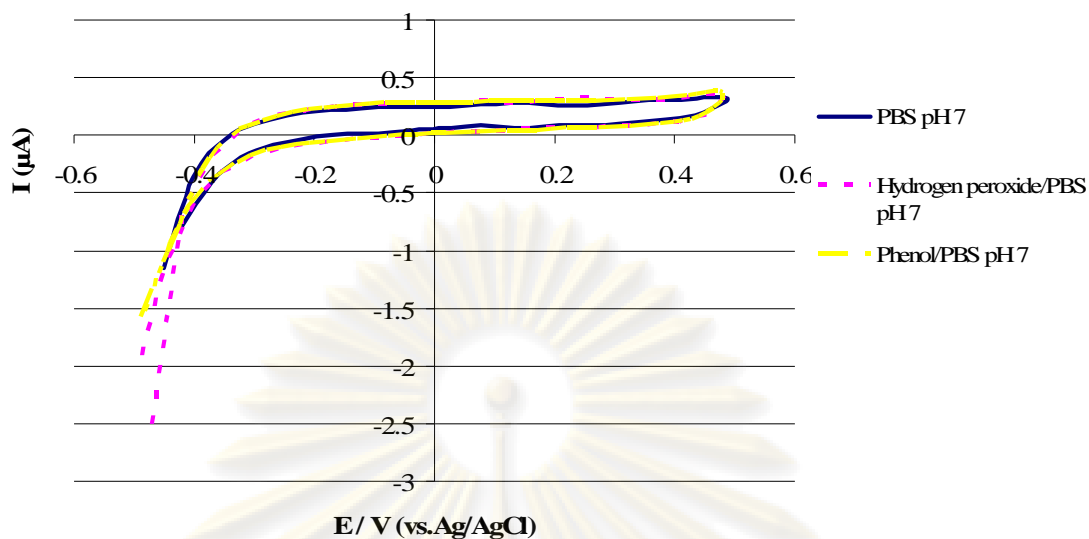


Figure 4.12 Cyclic voltammograms of bare electrode of base solutions: PBS (pH 7), H_2O_2 and Phenol. Scan rate is 50 mV/s.

4.3.2 The effect of HRP on cyclic voltammogram

In order to test the effect of HRP, we would like to test the modified WE with HRP and without HRP. When compare between the modified WE with HRP/chitosan 0.5% and bare electrode in presence of 0.1 mM of Phenol and 0.1 mM of H_2O_2 is shown in Figure 4.13. It was found that the couple of redox peak of HRP occurred while nothing happened without HRP. The anodic peak current or oxidation current (A) occurred when the potential is scanned positively, which may come from the oxidation of HRP by H_2O_2 . The cathodic peak current or reduction current (B) occurred when the potential is scanned negatively, which came from the reduction of phenol by electrode (see figure 2.12). This reduction current is proportional to the phenol concentration in the solution (Ruzgas et al., 1995).

ศูนย์วิทยทรัพยากร
จุฬาลงกรณ์มหาวิทยาลัย

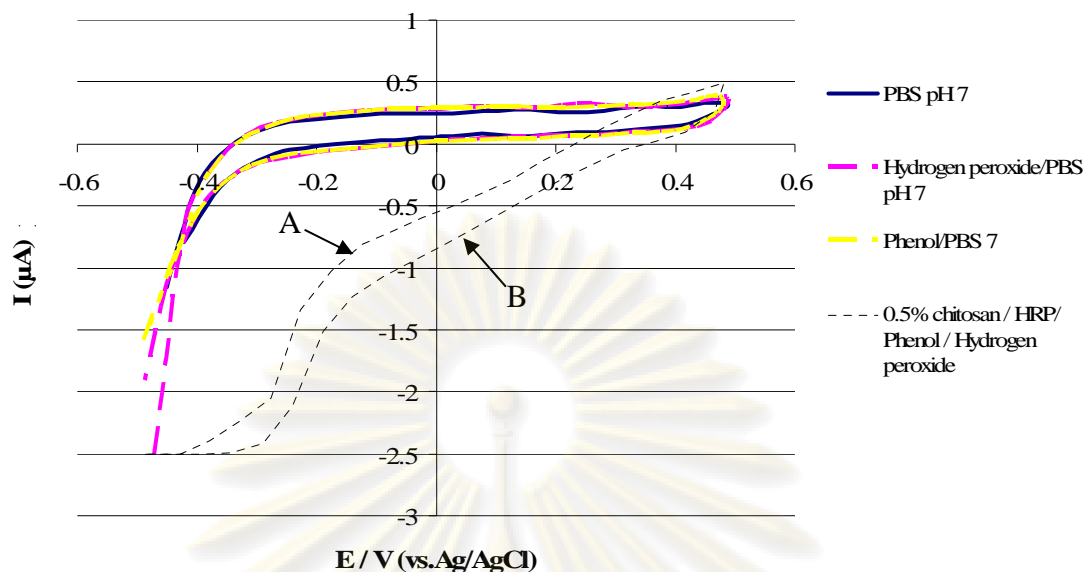


Figure 4.13 Cyclic voltammograms of modified electrode with 0.5% w/v chitosan / HRP in presence of 0.1 mM of Phenol and 0.1 mM of H_2O_2 compared with base solutions. Scan rate is 50 mV/s.

4.3.3 The effect of MCF on cyclic voltammogram

In previous work of Dai et al., (2008), the mesoporous materials prevented the aggregation of enzyme on electrode include the mesoporous silica has a high surface area, controlled porosity and mechanical resistance, which to get high sensitivity. In this section, MCF was loaded in film of HRP and chitosan to determine the effect of MCF in this composite film. The composite film of 0.1 %w/v MCF / HRP / 0.5 %w/v chitosan modified WE was shown in Figure 4.14. When compare between the composite film which loaded and not loaded MCF. The presence of MCF in composite film improves greatly the electron transfer between the electrode and the immobilized HRP, because of we found that the reduction current of this composite film was higher than the reduction current of composite film without MCF. According to Dai et al. (2008), though MCF is not conductive, it prevented the aggregation of proteins on electrode, thus was in favor of the electron transfer.

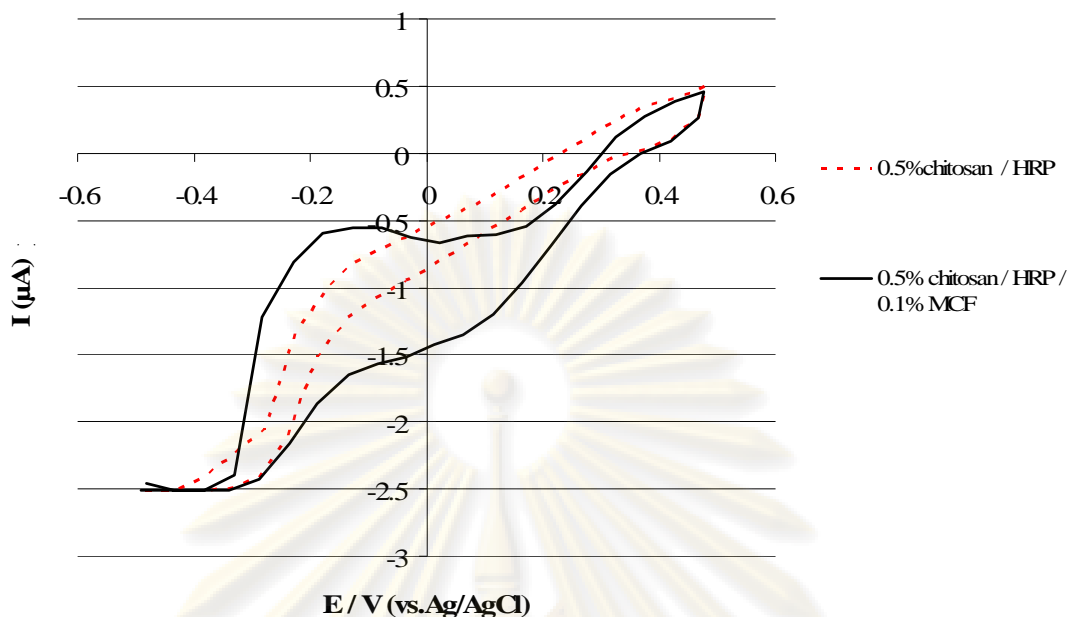


Figure 4.14 Cyclic voltammograms of modified electrode with 0.5% w/v chitosan /HRP and 0.5% w/v chitosan / HRP / 0.1% w/v MCF in presence of 0.1 mM of Phenol and 0.1 mM of H_2O_2 . Scan rate is 50 mV/s.

For next section, the amount of MCF in composite film of chitosan and HRP was investigated. The couple of redox peak for the results shown in Figure 4.15. The results indicate that the response of reduction current of sensor increased when the amount of MCF increased in range of 0.1 - 0.7 %w/v of MCF in chitosan. However, the response of the biosensor decreased when MCF content was more than 0.7%w/v. The increase of MCF content up to 0.7 %w/v may be attributed to the good distribution of enzyme in chitosan because of MCF have a large specific surface area and good adsorption (Dai et al., 2005). However, the increase of MCF content up to 0.9 %w/v decreased the reduction current, it was possible that the excessive MCF obstructed the diffusion of substrate.

จุฬาลงกรณ์มหาวิทยาลัย

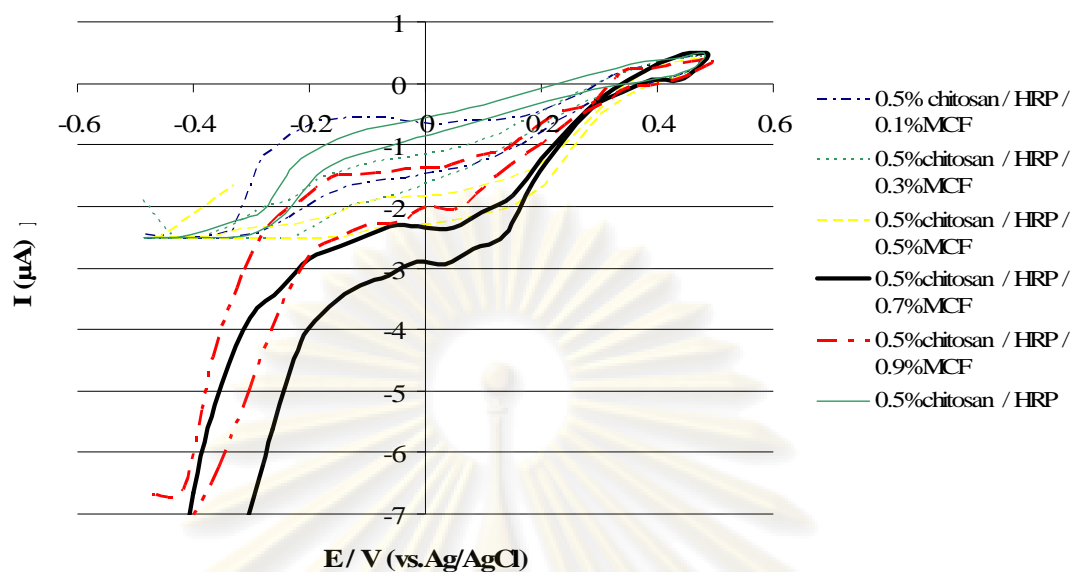


Figure 4.15 Cyclic voltammograms of modified electrode with 0.5% w/v chitosan / HRP / various amount of MCF compared with 0.5% w/v chitosan / HRP in presence of 0.1 mM of Phenol and 0.1 mM of H_2O_2 . Scan rate is 50 mV/s.

Based on these results, the suitable amount of MCF in composite film was 0.7% w/v and this content was used for the subsequent study on effect of chitosan concentration.

4.3.4 The effect of chitosan concentration on cyclic voltammogram

The chitosan concentration has affect on mass transfer limitation because the concentration of chitosan was higher lead to the film was thicker and brittle, it would lead to a higher diffusion barrier for the substrate and mediator. Thus, Effective Diffusivity (D_{eff}) decreased lead to the mass transfer was limited. In this case, A composite film which were prepared with different concentrations of chitosan (0.1–0.7 %w/v), MCF 0.7%w/v and HRP were investigated. Figure 4.16 shows that the highest reduction response was observed at 0.5 %w/v of chitosan. When the concentration of chitosan was higher than 0.5 % w/v result in the immobilization film was thicker and rigid, it would lead to a lower diffusion for the substrate and mediator (Wang et al., 2005). On the other hand, the concentration of chitosan was lower than 0.5 %w/v, the sensor response was lower than 0.5 %w/v together because the immobilization of HRP with low chitosan concentration might be the three-dimensional structure of HRP changed lead to decreasing activity of enzyme and the

leakage of enzyme. Based on these results, the suitable chitosan concentration in composite film was 0.5% w/v and this content was used for all subsequent studies.

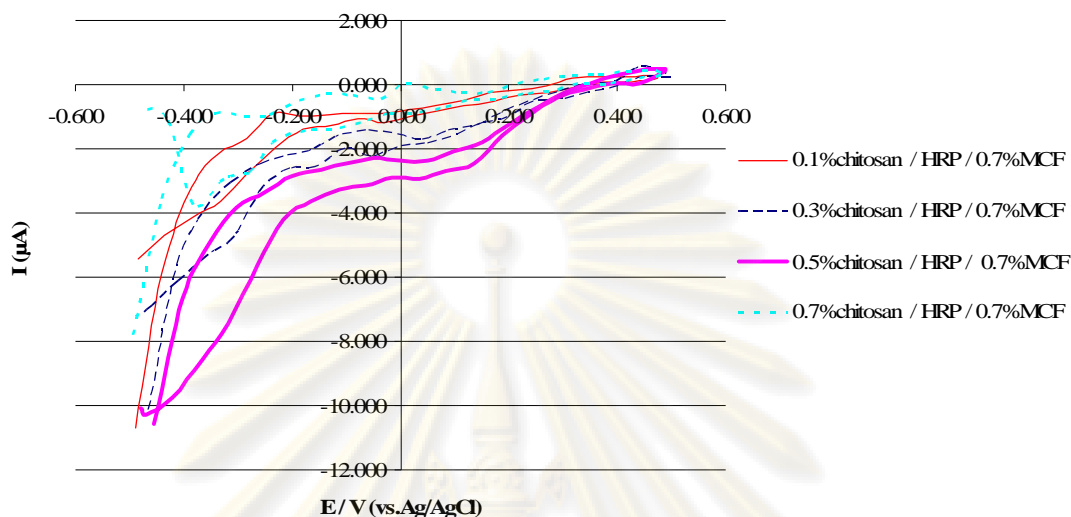


Figure 4.16 Cyclic voltammograms of modified electrode with various chitosan concentration / HRP / 0.7% w/v MCF in presence of 0.1 mM of Phenol and 0.1 mM of H_2O_2 . Scan rate is 50 mV/s.

4.3.5 The effect of amount of Ag in MCF on cyclic voltammogram

Silver (Ag) is the best conductor among metals, and so Ag nanoparticles may facilitate more efficient electron transfer than gold nanoparticles in biosensors not only improve the conductivity, but also adsorb the enzyme molecules to keep the stability of the biosensor (Ren et al., 2005). However, the excessive Ag in enzyme immobilization may be attributed to inhibition of enzyme activity. For the different structure of MCF and Silica nanopowder, the response of each composite film may be differently. The MCF which has pore size and high surface area may be the higher attachment of Ag than Si nanopowder which is non porous and can help more electron transfer. In this section, the amount Ag precursor which was attached in MCF were varied. Figure 4.17 exhibit the behavior of modified WE with 0.5% w/v chitosan / HRP / various amount of Ag precursor which was attached in MCF. The results indicate that the increase of amount Ag in MCF, all the response peak of Ag/MCF almost remained same pattern and all the reduction peaks were lower than composite film without Ag, in spite of the fact that the Ag possess good conductivity which can make possible conducting channels to facilitate electron transfer between the active

center of HRP and the electrode surface (Ren et al., 2005; Xu et al., 2004). The decrease in activity of enzyme may be attributed to the aggregation of Ag on MCF obstructed the diffusion of bulk solution.

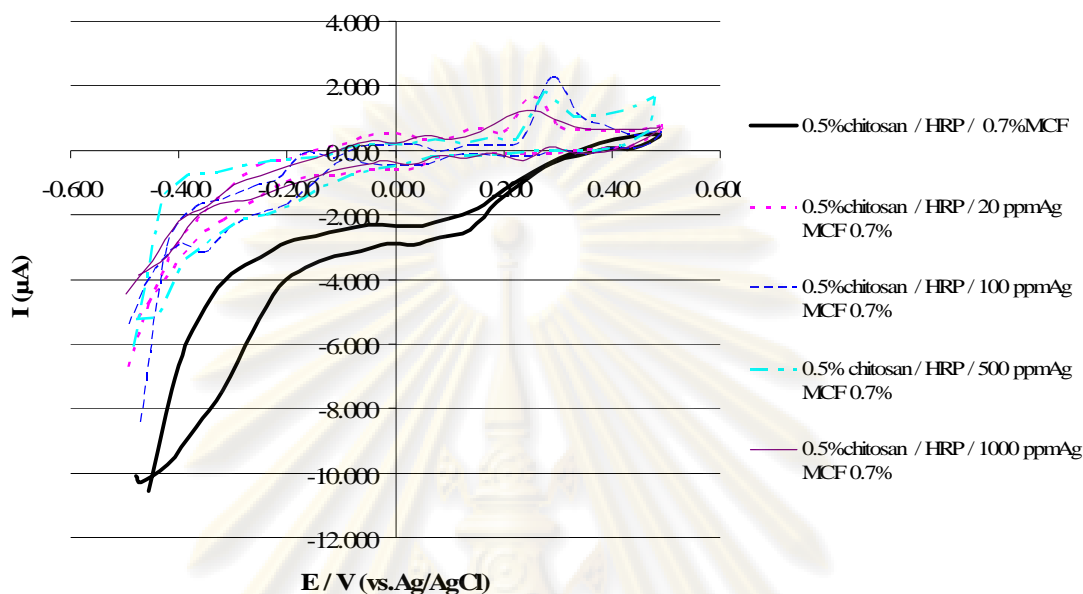


Figure 4.17 Cyclic voltammograms of modified electrode with 0.5% w/v chitosan / HRP / various amount of Ag in 0.7% w/v MCF compared with 0.5% chitosan / HRP / 0.7% w/v MCF in presence of 0.1 mM of Phenol and 0.1 mM of H_2O_2 . Scan rate is 50 mV/s.

4.3.6 The effect of amount of silver in SiO_2 nanopowder on cyclic voltammogram

In the case of the amount Ag precursor which was attached in SiO_2 nanopowder were varied. The suitable amount of Ag precursor which was attached in SiO_2 nanopowder was 500 ppm because the reduction peak is highest than all amount Ag precursor which was attached in SiO_2 nanopowder when observed at 0 volt (Figure 4.18). It was possible that the distribution of Ag on SiO_2 nanopowder was good lead to facilitate the electron transfer.

จุฬาลงกรณ์มหาวิทยาลัย

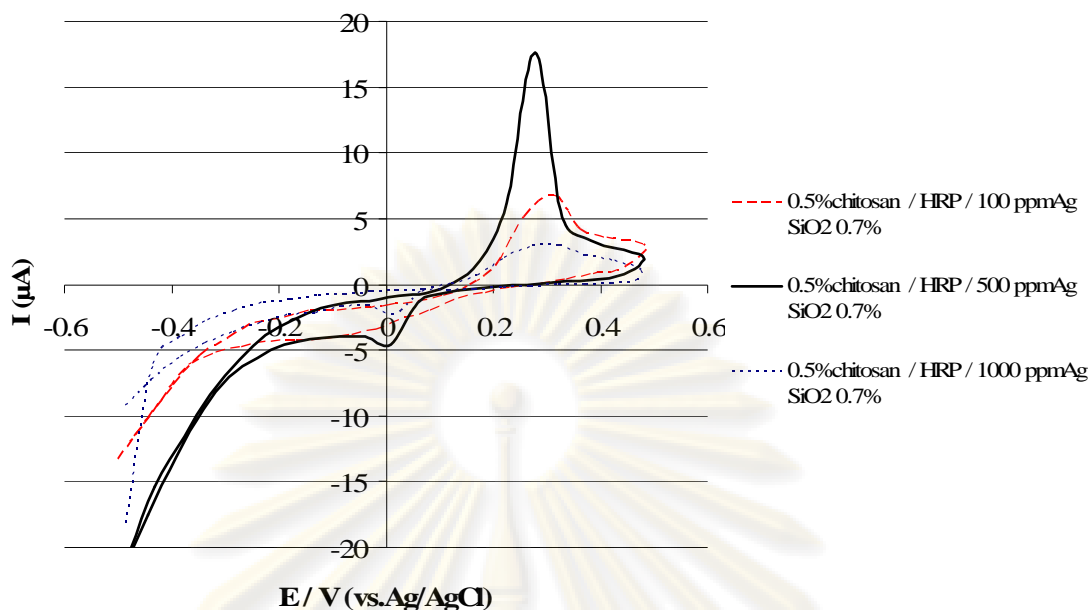


Figure 4.18 Cyclic voltammograms of modified electrode with 0.5% w/v chitosan / HRP / various amount of Ag in 0.7% w/v SiO₂ nanopowder in presence of 0.1 mM of Phenol and 0.1 mM of H₂O₂. Scan rate is 50 mV/s.

4.3.7 The effect of amount of silver in chitosan on cyclic voltammogram

After Ag attached on MCF and SiO₂ nanopowder were discussed in section 4.2.5 and 4.2.6, respectively. It is probable that the Ag was confined in silica host. Therefore, Ag solution was dispersed in chitosan solution to produce Ag/chitosan solution so Ag was spread all in matrix in this section. Figure 4.19 exhibited the response of modified electrode with various amount of Ag solution in chitosan 0.5% w/v. The highest reduction current appear in the modified electrode with 0.5% w/v chitosan mixed with 20 ppm Ag solution, HRP and 0.7% w/v modified MCF due to this composite has amount of Ag which suitable for facilitate the electron transfer including may help the distribution of enzyme in matrix.

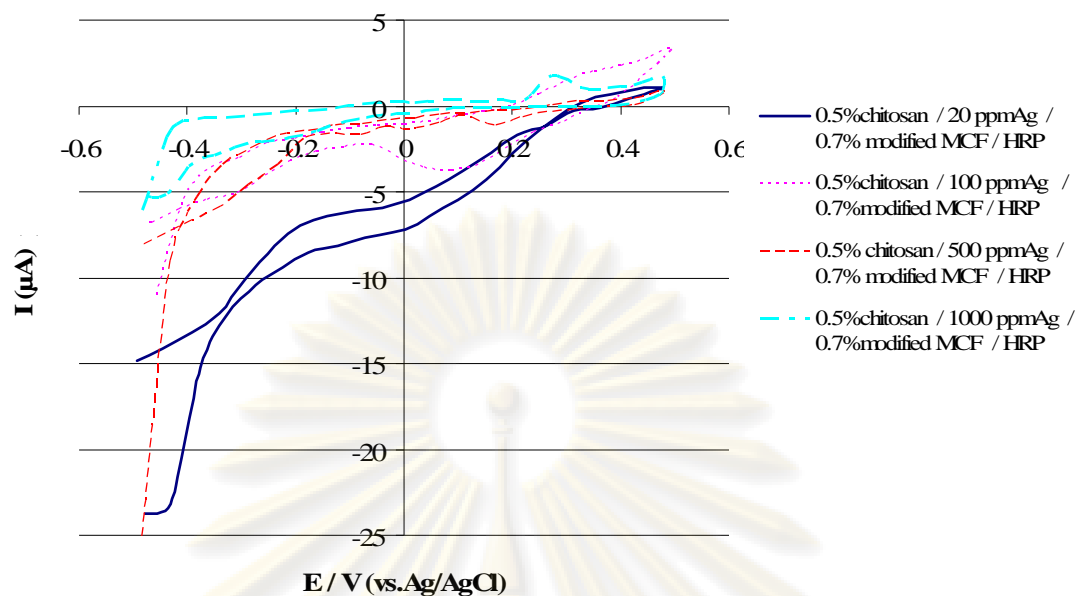


Figure 4.19 Cyclic voltammograms of modified electrode with 0.5% w/v chitosan / various amount of Ag solution / HRP / 0.7% w/v modified MCF in presence of 0.1 mM of Phenol and 0.1 mM of H_2O_2 . Scan rate is 50 mV/s.

4.3.8 The effect of various matrices on cyclic voltammogram

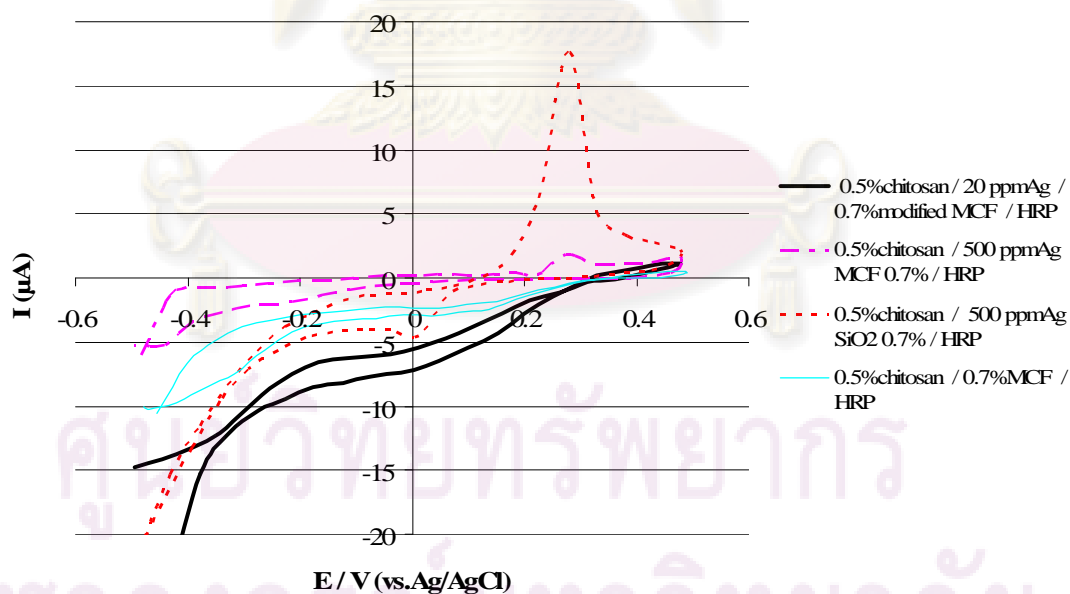


Figure 4.20 Cyclic voltammograms of modified electrode with various matrices in presence of 0.1 mM of Phenol and 0.1 mM of H_2O_2 . Scan rate is 50 mV/s.

The best matrices in each section were shown in Figure 4.20 in order to choose the best matrix to use for the study in reusability. The results indicate that the composite film consist of 0.5%w/v chitosan mixed with 20 ppm Ag solution, HRP and 0.7%w/v modified MCF showed the highest response on phenol detection because its has highest the reduction current than all composite.

4.4 Reusability

From section 4.3.8, the highest response on phenol detection appear in composite film consist of 0.5%w/v chitosan mixed with 20 ppm Ag solution, HRP and 0.7%w/v modified MCF. Thus, we chose this composite film to reuse for phenol detection with amperometry method. The potential was fixed at 0 V because in more negative values the enzymes molecules could be inactivated by the formation of reduced compound with HRP, decreasing the activity at time function (Rosatto et al., 1999). Figure 4.21 exhibited when modified electrode with this composite material was used in first time, the current had occurred immediately but when the modified electrode was used in second and third times, the current had not reacted. The assumptions for the cause of only one time use of enzyme; the leaching of enzyme from matrix, the denature of enzyme from other material added in composite film, the adsorption of product in composite film in first used cause the fresh substrate cannot diffuse through the film to react with HRP again and the potential was applied in electrochemical reaction to make enzyme denature.

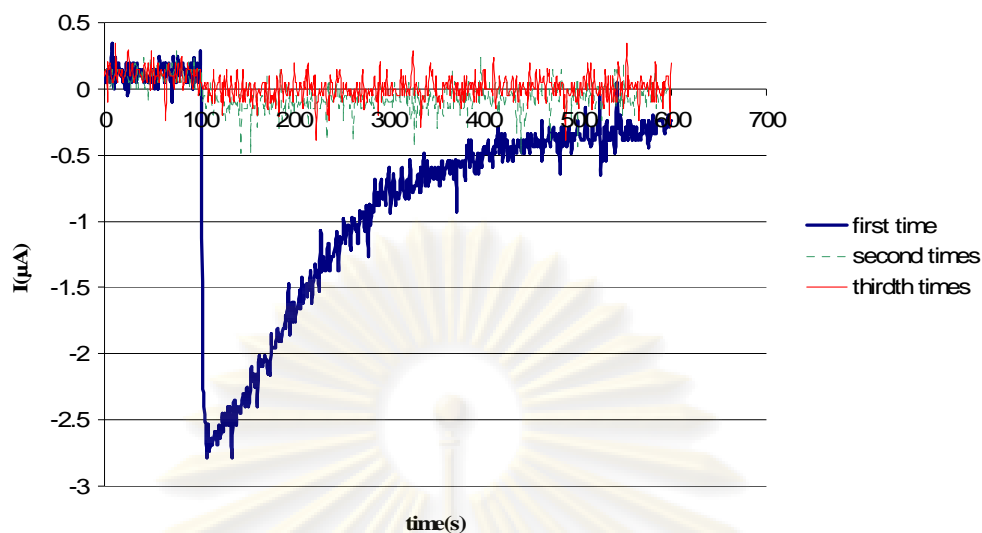


Figure 4.21 Amperometric of modified electrode with 0.5% w/v chitosan mixed with 20 ppm Ag solution, HRP and 0.7% w/v modified MCF in presence of 0.1 mM of Phenol and 0.1 mM of H_2O_2 at 0 volt.

For the leaching of enzyme from matrix, the residue solution after the chemical reaction in first used was tested with chemical reaction in order to confirm enzyme leak to the residue solution. After we checked the activity of enzyme from residue solution, the result indicates that the residue solution had enzyme activity about 31.43% of initial activity. It can be concluded that the enzyme leaked out the composite film. Therefore, it causes only one time use of enzyme

For the denature of enzyme from other material added in composite film, we will seek that what material in this composite materials pose for the modified electrode with these material used once. First step, we eliminated the 20 ppm Ag solution get off these composite materials so the composite material will consist 0.5% w/v chitosan, HRP and 0.7% w/v modified MCF (Figure 4.22). The figure indicates that when we eliminated the Ag solution, the modified electrode was used only first time together thus the Ag solution did not concern to make the modified electrode cannot reuse.

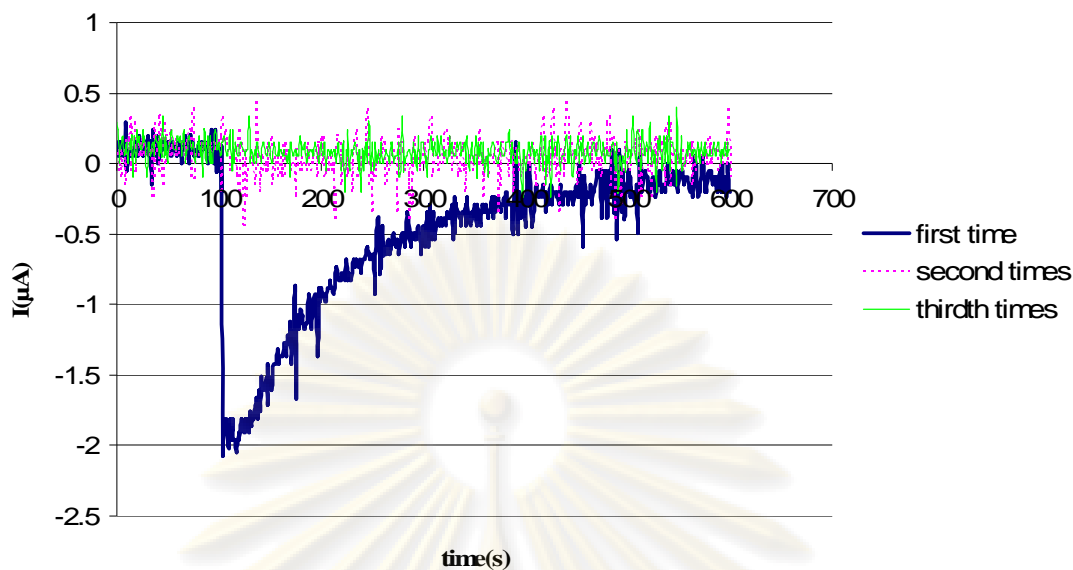


Figure 4.22 Amperometric of modified electrode with 0.5% w/v chitosan, HRP and 0.7% w/v modified MCF in presence of 0.1 mM of Phenol and 0.1 mM of H_2O_2 at 0 volt

Second step, we eliminated the 0.7% w/v modified MCF get off these composite materials so the composite material will consist 0.5% w/v chitosan, HRP and 20 ppm Ag solution (Figure 4.23). The Figure indicates that when we eliminated the MCF modified, the modified electrode was used only first time together thus the MCF modified did not concern to make the modified electrode cannot reuse.

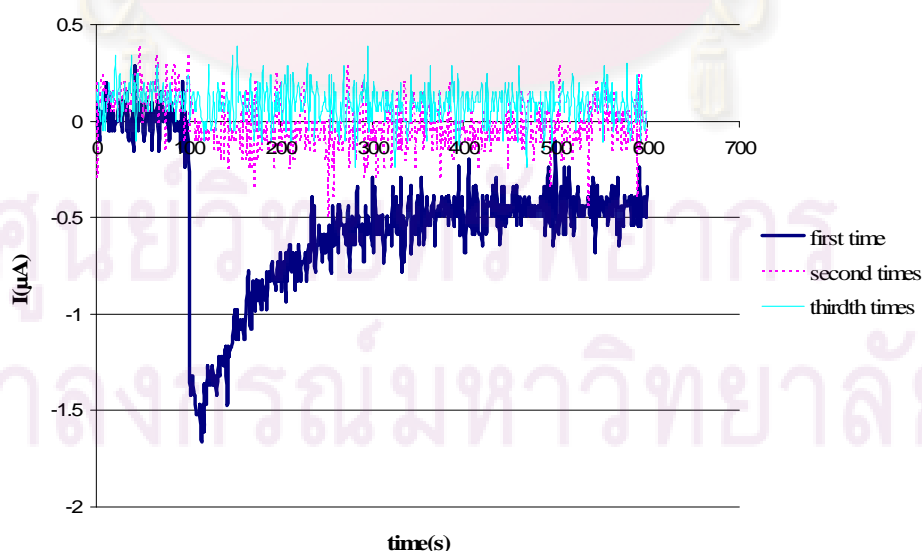


Figure 4.23 Amperometric of modified electrode with 0.5% w/v chitosan, HRP and 20 ppm Ag solution in presence of 0.1 mM of Phenol and 0.1 mM of H_2O_2 at 0 volt

Third step, we eliminated both 0.7% w/v modified MCF and 20 ppm Ag solution get off the composite film (Figure 4.24). The response of modified electrode had been active in first time in the same way, composite film which eliminated 20 ppm Ag solution (first step) and 0.7% w/v modified MCF (second step).

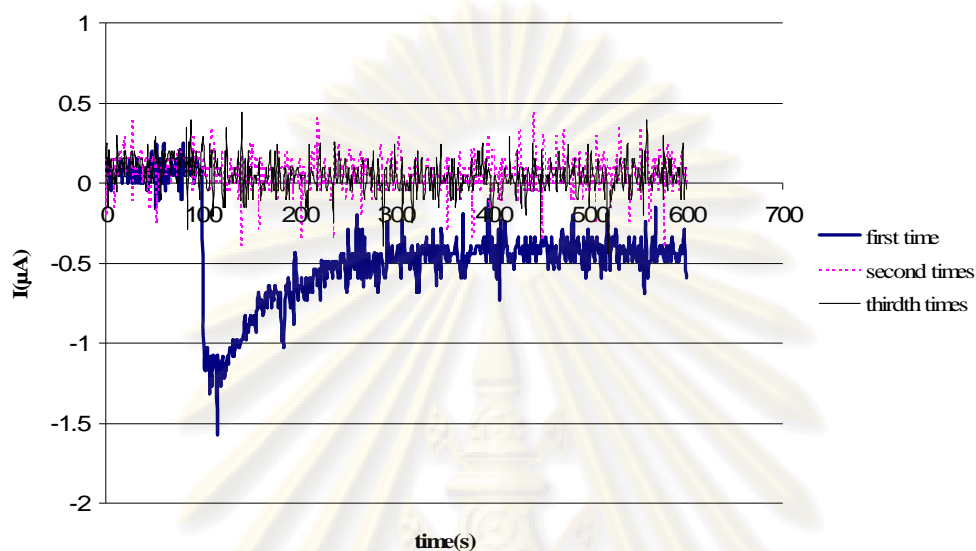


Figure 4.24 Amperometric of modified electrode with 0.5% w/v chitosan and HRP in presence of 0.1 mM of Phenol and 0.1 mM of H_2O_2 at 0 volt

The all materials were eliminated from composite film except chitosan. The reuse of modified electrode had first time together. Therefore, all materials except chitosan did not concern to make the modified electrode cannot reuse. However, the properties chitosan may cause one time use of enzyme. Because of when we used the composite film in first time, the film color changed from light yellow to dark brown (data not shown) which the reason of the change of film color probably to adsorption of product in the film.

To confirm that chitosan had more affected in enzyme immobilization, the various chitosan concentration were tested again with amperometry method (Figure 4.25). The result indicate that 1% w/v of chitosan concentration has been slightly response while concentration of chitosan of 0.1, 0.3, 0.5 and 0.7% (w/v), almost same pattern which higher response than 1% w/v of chitosan concentration because these concentration had not impact from mass transfer whereas 1% w/v of chitosan concentration may impact on diffusivity. However, all chitosan concentration cannot reuse.

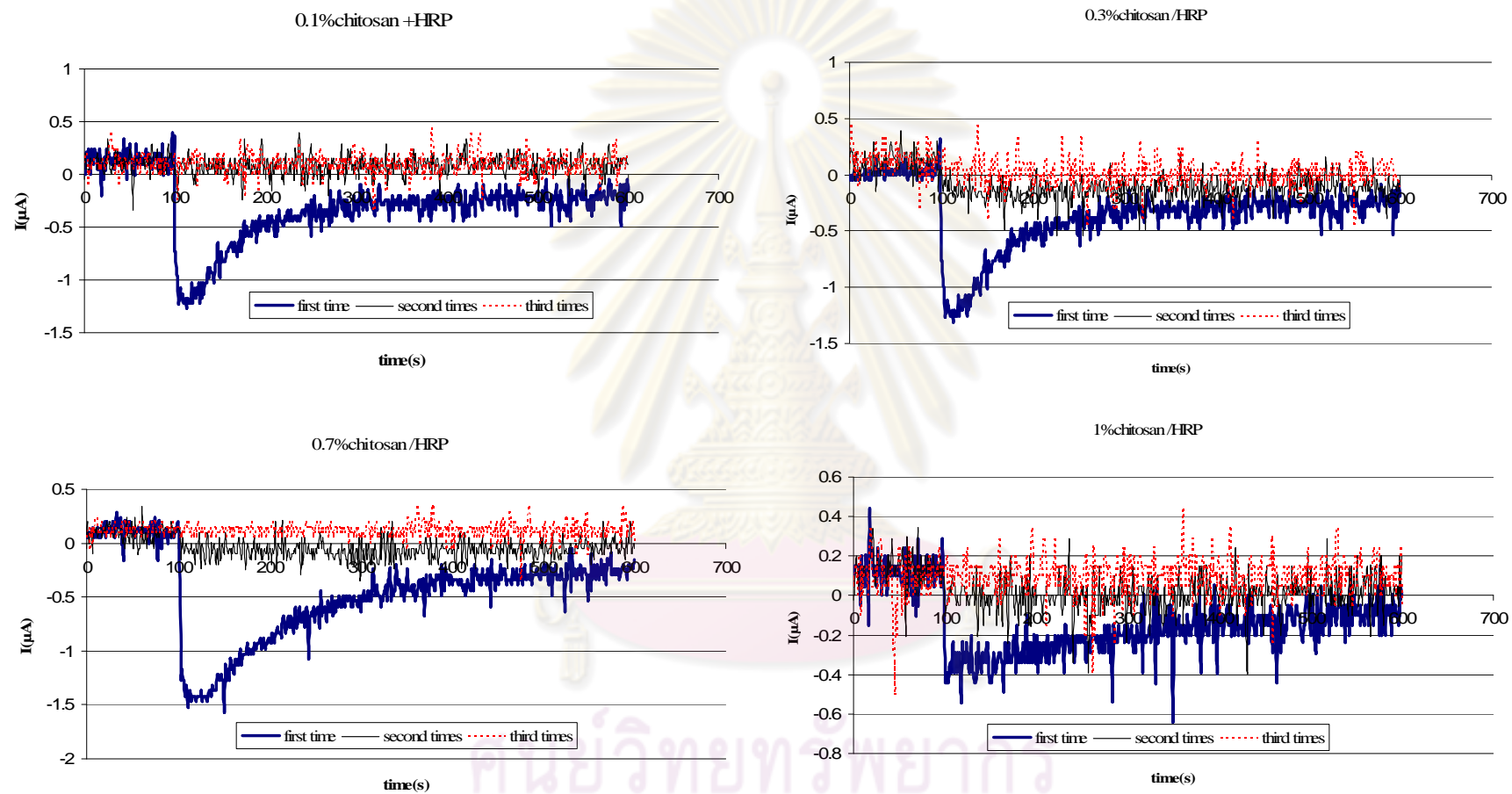


Figure 4.25 Amperometric of modified electrode with various chitosan concentration and HRP in presence of 0.1 mM of Phenol and 0.1 mM of H_2O_2 at 0 volt

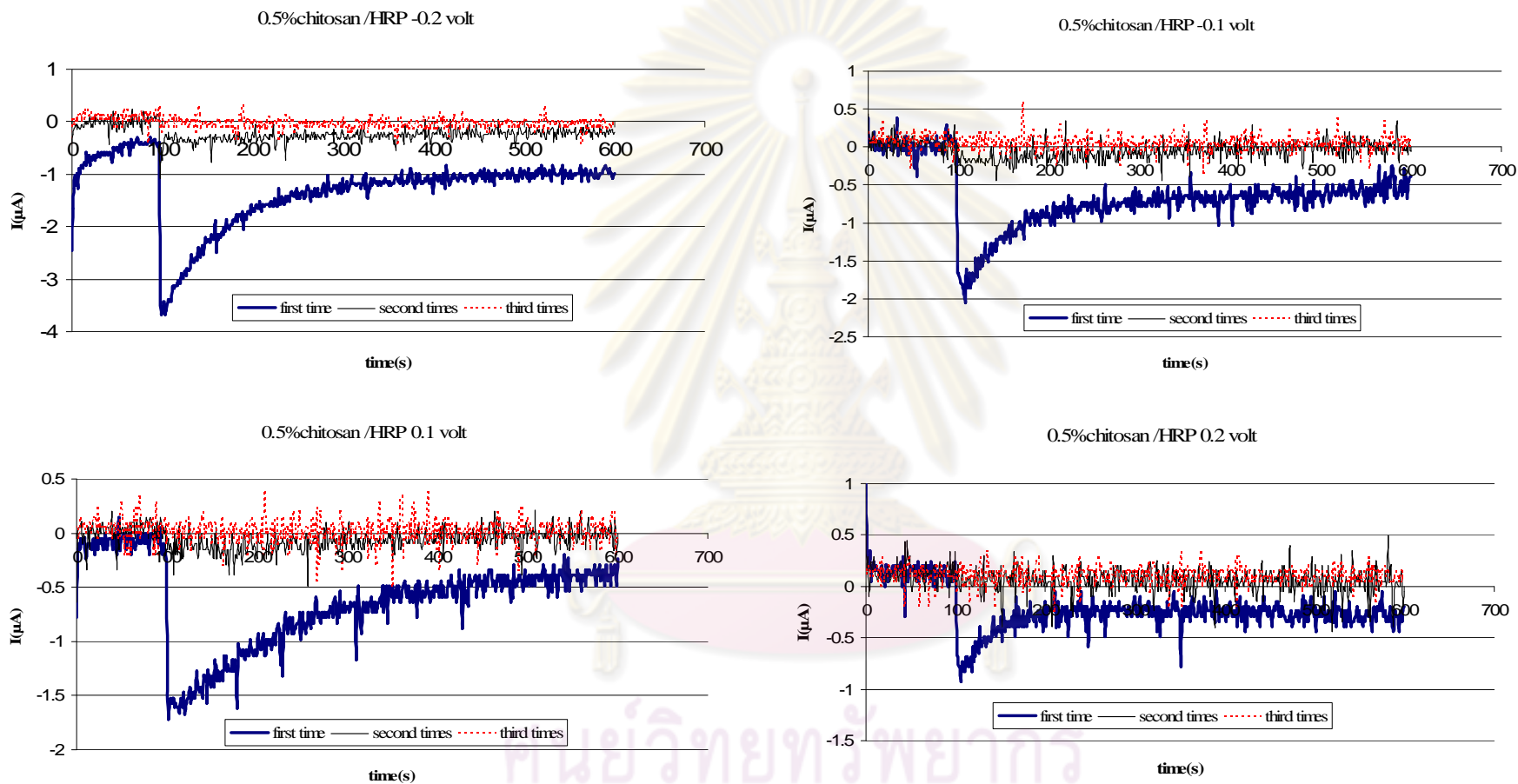


Figure 4.26 Amperometric of modified electrode with 0.5% w/v chitosan and HRP in presence of 0.1 mM of Phenol and 0.1 mM of H_2O_2 at various volt

While the response of various voltage on amperometric shown in figure 4.26. The result indicates that all various voltage had been shown one time use of enzyme together. Therefore, the voltage did not cause the denature of enzyme. However, when various voltages in electrochemical reaction, the response of modified electrode have difference clearly. The applied potential had an important influence over the sensor response, because the applied potential contributes to the sensitivity and selectivity of the system (Mello et al., 2003).



ศูนย์วิจัยทรัพยากร
จุฬาลงกรณ์มหาวิทยาลัย

CHAPTER V

CONCLUSION AND RECOMMENDATIONS

5.1 Conclusion

The immobilization of Horseradish peroxidase in mesoporous silica/silver nanoparticle/chitosan composite material. Major findings from this work can be summarized as follows:

5.1.1 The physical properties of MCF

The specific surface area, pore size, and pore volume of MCF were 629.97 m²/g, 23.7 nm and 1.85 cm³/g, respectively.

5.1.2 The physical properties of Ag/MCF and Ag/SiO₂

The specific surface area, pore size, and pore volume of Ag/MCF were 300.13 m²/g, 24.5 nm and 1.47 cm³/g, respectively. It was revealed that Ag particles were possibly entrapped in MCF pores as well as on the outside surface. The Ag nanoparticles were attached on MCF have average size 19 nm while the Ag nanoparticles were attached on SiO₂ nanopowder have average size 9 nm.

5.1.3 Additives such as MCF and Ag particles helped enzyme dispersion to a certain concentration, however, higher concentration of additives results in higher substrate/product mass transfer limitation.

5.1.4 Ag particles were found to help enhancing electrical response.

5.1.5 Optimal compositions of modified electrode are 20 ppm Ag solution, chitosan 0.5 % w/v, modified MCF 0.7% w/v and HRP.

5.1.6 The use of modified electrode was limited to only once. The main cause was probably enzyme leakage from chitosan matrix.

5.2 Recommendations for the future studies

5.2.1 Ag should be made to distribute thoroughly on silica.

5.2.2 The effect of the other metals (Au or Pt) on HRP activity should be studied.

5.2.3 The effect of other parameter on biosensor such as scan rate should be studied.

5.2.4 The effect of molecular weight and %deacetylation of chitosan should be studied.



ศูนย์วิทยทรัพยากร
จุฬาลงกรณ์มหาวิทยาลัย

REFERENCES

- Abdullah J, Ahmad M, Karuppiah N. Immobilization of tyrosinase in chitosan film for an optical detection of phenol. Sensors and Actuators B 114(2006): 604–609.
- Aiba Sei-ichi. Studies on chitosan: 3. Evidence for the presence of random and block copolymer structures in partially N-acetylated chitosans. Int. J. Biol. Macromol. 13(1991): 40-44.
- Alsarra I. A., Betigeri S. S., Zhang H., Evans B. A., Neau S. H. Molecular weight and degree of deacetylation effects on lipase-loaded chitosan bead characteristics. Biomaterials 23(2002): 3637–3644.
- Amatani T., Nakanishi K., Hirao K., Kodaira T. Monolithic Periodic Mesoporous Silica with Well-Defined Macropores. Chem. Mater. 17(2005): 2114-2119.
- Ayral A, Julbe A, Roualdes S, Rouessac V, Durand J, Sala B. Silica membranes-Basic principles. Periodica Polytechnica Ser. Chem. Eng. 50(2006): 67-79.
- Bai Y, Yang H, Yang W, Li Y, Sun C. Gold nanoparticles-mesoporous silica composite used as an enzyme immobilization matrix for amperometric glucose biosensor construction. Sensors and Actuators B 124(2007): 179–186.
- Beck J.S., Vartuli J.C., Roth W.J., Leonowicz M.E., Kresge C.T., Schmitt K.D., Chu C.T-W., Olson D.H., Sheppard E.W., McCullen S.B., Higgins J.B., Schlenker J.L. A New Family of Mesoporous Molecular Sieves Prepared with Liquid Crystal Templates. J. Am. Chem. Soc. 114(1992): 10834-10843.
- Biró E., Németh Á. Sz., Sisak C., Feczko T, Gyenis Já. Preparation of chitosan particles suitable for enzyme immobilization. J. Biochem. Biophys. Methods 70(2008): 1240–1246.
- Cai W-Y, Xu Q, Zhao X-N, Zhu J-J, Chen H-Y. Porous Gold-Nanoparticle-CaCO₃ Hybrid Material: Preparation, Characterization, and Application for Horseradish Peroxidase Assembly and Direct Electrochemistry. Chem. Mater. 18(2006): 279-284.

- Carvalho R.H., Lemos F., Lemos M.A.N.D.A., Cabral J.M.S., Ribeiro F.R. Electro-oxidation of phenol on a new type of zeolite/graphite biocomposite electrode with horseradish peroxidase. Journal of Molecular Catalysis A: Chemical 278(2007): 47–52.
- Chaubey A, Malhotra B.D. Review Mediated biosensors. Biosensors & Bioelectronics 17(2002): 441–456.
- Chen P.C., Hsieh B.C., Chen R. L.C., Wang T.Y., Hsiao H.Y., Cheng T.J. Characterization of natural chitosan membranes from the carapace of the soldier crab *Mictyris brevidactylus* and its application to immobilize glucose oxidase in amperometric flow-injection biosensing system. Bioelectrochemistry 68(2006): 72 – 80.
- Chen W, Zhang J, Shi L, Di Y, Fang Q, Cai W. Characterization of sonochemically prepared silver–silica monolithic mesoporous nanocomposite. Composites Science and Technology 63(2003): 1209–1212.
- Chouyyok W, Panpranot J, Thanachayanant C, Prichanont S. Effects of pH and pore characters of mesoporous silicas on horseradish peroxidase immobilization. Journal of Molecular Catalysis B: Enzymatic (2008).
- Dai Z.H., Bao J., Yang X, Ju H. A bienzyme channeling glucose sensor with a wide concentration range based on co-entrapment of enzymes in SBA-15 mesopores. Biosensors and Bioelectronics 23(2008): 1070–1076.
- Dai Z.H., Ju H., Chen H. Mesoporous Materials Promoting Direct Electrochemistry and Electrocatalysis of Horseradish Peroxidase. Electroanalysis 17(2005): 10.
- Dai Z.H., Xu X, Wu L, Ju H. Detection of Trace Phenol Based on Mesoporous Silica Derived Tyrosinase-Peroxidase Biosensor. Electroanalysis 17(2005): 17.
- Dai Z.H., Ni J., Huang X.H., Lu G.F., Bao J.C. Direct electrochemistry of glucose oxidase immobilized on a hexagonal mesoporous silica-MCM-41 matrix. Bioelectrochemistry 70(2007): 250–256.
- Eggins B.R., Biosensors: An Introduction. John Wiley & Sons Ltd, chichester, 1999.
- Fan Q, Shan D, Xue H, He Y, Cosnier S. Amperometric phenol biosensor based on laponite clay–chitosan nanocomposite matrix. Biosensors and Bioelectronics 22(2007): 816–821.

- Fernandes KF, Lima CS, Pinho H, Collins CH. Immobilization of horseradish peroxidase onto polyaniline polymers. Process Biochemistry 38,(2003): 1379 - 1384.
- Haizhen Huang, Qiang Yuanb , Xiurong Yanga. Preparation and characterization of metal–chitosan nanocomposites. Colloids and Surfaces B: Biointerfaces 39(2004): 31–37.
- He J., Xu Y., Ma H., Evans D. G., Wang Z., Duan X. Inhibiting the leaching of lipase from mesoporous supports by polymerization of grafted vinyl groups. Microporous and Mesoporous Materials 94(2006): 29–33.
- Khan T. A., Peh K. K., Ching H. S. Reporting degree of deacetylation values of chitosan: the influence of analytical methods. J Pharm Pharmaceut Sci 5(2002):205-212.
- Khan R, Kaushik A, Solanki P.R., Ansari A.A., Pandey M.K., Malhotra B.D. Zinc oxide nanoparticles-chitosan composite film for cholesterol biosensor. analytica chimica acta 616(2008): 207–213.
- Kim K.D., Han D.N., Kim H.T. Optimization of experimental conditions based on the Taguchi robust design for the formation of nano-sized silver particles by chemical reduction method. Chemical Engineering Journal 104(2004): 55–61.
- Krajewska B. Application of chitin and chitosan based materials for enzyme immobilizations. Enzyme and Microbial Technology 35(2004): 126–139.
- Kumar M.N.V.R, A review of chitin and chitosan applications. Reactive & Functional Polymers 46(2000): 1–27.
- Lei C-X, Hu SQ, Shen G-L, Yu R-Q. Immobilization of horseradish peroxidase to a nano-Au monolayer modified chitosan-entrapped carbon paste electrode for the detection of hydrogen peroxide. Talanta 59(2003): 981–988.
- Leofanti G., Padovan M., Tozzola G., Venturelli B. Surface area and pore texture of catalysts. Catalysis Today 41(1998): 207-219.
- Lettow J.S., Han Y.J, Schmidt-Winkel P, Yang P, Zhao D, Stucky G.D., Ying J.Y., Hexagonal to Mesocellular Foam Phase Transition in Polymer-Templated Mesoporous Silicas. Langmuir 16(2000): 8291-8295.
- Lindgren A, Emneus J, Ruzgas T, Gorton L, Marko-Varga G. Amperometric detection of phenols using peroxidase-modified graphite electrodes. Analytica Chimica Acta 347(1997): 51-62.

- Lin D-H, Jiang Y-X, Wang Y, Sun S-G. Silver Nanoparticles Confined in SBA-15 Mesoporous Silica and the Application as a Sensor for Detecting Hydrogen Peroxide. Journal of Nanomaterials (2008).
- Liu Y-M, Feng W-L, Li T-C, He H-Y, Dai W-L, Huang W, Cao Yong, Fan K-N. Structure and catalytic properties of vanadium oxide supported on mesocellulose silica foams (MCF) for the oxidative dehydrogenation of propane to propylene. Journal of Catalysis 239(2006): 125–136.
- Li W, Yuan R, Chai Y, Zhou L, Chen S, Li N. Immobilization of horseradish peroxidase on chitosan/silica sol–gel hybrid membranes for the preparation of hydrogen peroxide biosensor. J. Biochem. Biophys. Methods 70(2008): 830–837.
- Liu Z-M, Tingry S, Innocent Christophe, Durand J, Xua Z-K, Seta Patrick. Modification of microfiltration polypropylene membranes by allylamine plasma treatment Influence of the attachment route on peroxidase immobilization and enzyme efficiency. Enzyme and Microbial Technology 39(2006):868-876.
- Long D., Wu G., Chen S. Preparation of oligochitosan stabilized silver nanoparticles by gamma irradiation. Radiation Physics and Chemistry 76(2007): 1126–1131.
- Luo X-L , Xu J-J , Du Y, Chen H-Y. A glucose biosensor based on chitosan–glucose oxidase–gold nanoparticles biocomposite formed by one-step electrodeposition. Analytical Biochemistry 334(2004):284–289.
- Luo X-L , Xu J-J , Zhang Q, Yang G-J , Chen H-Y. Electrochemically deposited chitosan hydrogel for horseradish peroxidase immobilization through gold nanoparticles self-assembly. Biosensors and Bioelectronics 21(2005): 190–196.
- Marko-Varga G., EmnCUS J., Got-ton L., Ruzgas T. Development of enzyme-based amperometric sensors for the determination of phenolic compounds. trends in analytical chemistry 14(1995): 319-328.
- Mello LD, Sotomayor M, Kubota T. HRP-based amperometric biosensor for the polyphenols determination in vegetables extract. Sensors and Actuators B 96(2003): 636–645.

- Miao Y, Tan SN. Amperometric hydrogen peroxide biosensor based on immobilization of peroxidase in chitosan matrix crosslinked with glutaraldehyde. Analyst 125(2000): 1591–1594.
- Mou C-Y, Lin H-P. Control of morphology in synthesizing mesoporous silica. Pure Appl. Chem 72(2000): 137–146.
- Nunthanid J., Puttipipatkachorn S., Yamamoto K., Peck G. E. Physical Properties and Molecular Behavior of Chitosan Films. Drug Development and Industrial Pharmacy 27(2001): 143–157.
- Ren C, Song Y, Li Z, Zhu G. Hydrogen peroxide sensor based on horseradish peroxidase immobilized on a silver nanoparticles / cysteamine /gold electrode. Anal Bioanal Chem 381(2005): 1179–1185.
- Ren D., Yi H., Wang W., Ma X. The enzymatic degradation and swelling properties of chitosan matrices with different degrees of N-acetylation. Carbohydrate Research 340(2005): 2403–2410.
- Ren X , Meng X , Chen D, Tang F, Jiaob J. Using silver nanoparticle to enhance current response of biosensor. Biosensors and Bioelectronics 21(2005): 433–437.
- Rosatto SS., Kubota LT., Neto G. Biosensor for phenol based on the direct electron transfer blocking of peroxidase immobilising on silica-titanium. Analytica Chimica Acta 390(1999): 65-72
- Ruzgas T., Csoregi E, Emneus J., Gorton L, Marko-Varga G. Review Peroxidase-modified electrodes: Fundamentals and application. Analytica Chimica Acta 330(1996): 123-138.
- Ruzgas T., Emneus J., Gorton L., Marko-Varga G. The development of a peroxidase biosensor for monitoring phenol and related aromatic compounds. Analytica Chimica Acta 311(1995): 245-253.
- Ruzgas T., Gorton L., Emneus J., Marko-Varga G. Kinetic models of horseradish peroxidase action on a graphite electrode. Journal of Electroanalytical Chemistry 391(1995): 41-49.
- Sato K, Hasumi H, Tsukidate A, Sakurada J, Nakamura S, Toichiro H. Effects of mixed solvents on three elementary steps in the reactions of horseradish peroxidase and lactoperoxidase. Biochimica et Biophysica Acta 1253(1995): 94-102.

- Scragg A.H., Biotechnology for engineers. Ellis Horwood Limited, Chichester, 1988.
- Shuler, M.L., and Kargi, F., *In: Bioprocess engineering: Basic concepts*, Prentice Hall, New Jersey, 1992.
- Shan D, Zhu M, Han E, Xue H, Cosnier S. Calcium carbonate nanoparticles: A host matrix for the construction of highly sensitive amperometric phenol biosensor. Biosensors and Bioelectronics 23(2007): 648–654.
- Sing K. S. W., Everett D. H., Haul R. A. W., Moscou L., Pierotti R. A., Rouquerol J., Siemieniowska T. REPORTING PHYSISORPTION DATA FOR GAS/SOLID SYSTEMS with Special Reference to the Determination of Surface Area and Porosity. Pure & Appl. Chem. 57(1985): 603—619.
- Takahashi H, Li B, Sasaki T, Miyazaki C, Kajino T, Inagaki S. Immobilized enzymes in ordered mesoporous silica materials and improvement of their stability and catalytic activity in an organic solvent. Micropor and Mesopor Mater 44-45(2001):755-762 .
- Tanguaram T, Ponchio C, Kangkasomboon T, Katikawong P, Veerasai W. Design and development of a highly stable hydrogen peroxide biosensor on screen printed carbon electrode based on horseradish peroxidase bound with gold nanoparticles in the matrix of chitosan. Biosensors and Bioelectronics 22(2006): 2071–2078.
- Wang G, Xu J-J, Ye L-H, Zhu J-J, Chen H-Y. Highly sensitive sensors based on the immobilization of tyrosinase in chitosan. Bioelectrochemistry 57(2002): 33– 38.
- Wang G, Xu J-J, Chen H-Y, Lu Z-H. Amperometric hydrogen peroxide biosensor with sol-gel/chitosan network-like film as immobilization matrix. Biosensors and Bioelectronics 18(2003): 335 - 343.
- Wang H-S, Pan Q-X, Wang G-X. A Biosensor Based on Immobilization of Horseradish Peroxidase in Chitosan Matrix Cross-linked with Glyoxal for Amperometric Determination of Hydrogen Peroxide. Sensors 5(2005): 266-276.
- Wiles J.L., Vergano P.J., Barron F.H., Bunn J.M., Testin R.F. Water vapor transmission rates and sorption behavior of chitosan films. Journal of Food Science 65(2000): 1175–1179.

- Xua J-Z , Zhangb Y, Lia G-X , Zhub J-J . An electrochemical biosensor constructed by nanosized silver particles doped sol–gel film. Materials Science and Engineering 24(2004): 833–836.
- Xu J-Z, Zhang Y, Li G-X, Zhu J-J. An electrochemical biosensor constructed by nanosized silver particles doped sol–gel film. Materials Science and Engineering C 24(2004): 833–836.
- Xu Q ,Mao C , Liu N-N , Zhu J-J , Jian Shen . Immobilization of horseradish peroxidase on O-carboxymethylated chitosan/sol–gel matrix. Reactive &Functional Polymers 66(2006): 863–870.
- Xu Q, Mao C, Liu N-N , Zhu J-J , Sheng J . Direct electrochemistry of horseradish peroxidase based on biocompatible carboxymethyl chitosan–gold nanoparticle nanocomposite. Biosensors and Bioelectronics 22(2006): 768–773.
- Yan J, Wang A, Kim D-P. Preparation of Ordered Mesoporous SiC from Preceramic Polymer Templated by Nanoporous Silica. J. Phys. Chem. B 110(2006): 5429–5433.
- Yang Y, Yang H, Yang M, Liu Y, Shen G, Yu R . Amperometric glucose biosensor based on a surface treated nanoporous ZrO₂/Chitosan composite film as immobilization matrix. Analytica Chimica Acta 525(2004): 213–220.
- Zhao X-G, Shi J-L, Hu B, Zhang L-X, Hua Z-L. In situ formation of silver nanoparticles inside pore channels of ordered mesoporous silica. Materials Letters 58(2004): 2152– 2156.
- Zhao X, Mai Z, Kang X, Zou X. Direct electrochemistry and electrocatalysis of horseradish peroxidase based on clay–chitosan-gold nanoparticle nanocomposite. Biosensors and Bioelectronics 23(2008): 1032–1038.
- Zhou G-J, Wang G, Xu J-J, Chen H-Y. Reagentless chemiluminescence biosensor for determination of hydrogen peroxide based on the immobilization of horseradish peroxidase on biocompatible chitosan membrane. Sens Actuators B 81(2002): 334–339.
- Zhu S, Zhang D, Yang Na. Hydrophobic polymers modification of mesoporous silica with large pore size for drug release. J Nanopart Res (2007).

Ziani K., Oses J., Coma V., Mate J.I. Effect of the presence of glycerol and Tween 20 on the chemical and physical properties of films based on chitosan with different degree of deacetylation. LWT - Food Science and Technology 41(2008): 2159-2165.



ศูนย์วิทยทรัพยากร
จุฬาลงกรณ์มหาวิทยาลัย



APPENDICES

ศูนย์วิทยทรัพยากร
จุฬาลงกรณ์มหาวิทยาลัย

Appendix A

Raw data

Table A.1 Cyclic voltammogram of 0.1 M PBS pH 7 using bare electrode

V(volt)	I(μ A)
-0.499	0.152
-0.45	-1.155
-0.401	-0.357
-0.347	-0.039
-0.298	0.103
-0.245	0.176
-0.196	0.205
-0.147	0.225
-0.093	0.245
-0.044	0.25
0	0.245
0.054	0.254
0.103	0.269
0.157	0.279
0.205	0.254
0.254	0.259
0.308	0.284
0.357	0.308
0.411	0.303
0.46	0.333
0.489	0.308
0.435	0.176
0.386	0.137
0.333	0.113
0.284	0.093
0.235	0.093
0.181	0.073
0.132	0.059
0.078	0.083
0.029	0.064
-0.015	0.054
-0.068	0.029
-0.117	0.015
-0.171	0
-0.22	-0.034
-0.269	-0.083
-0.323	-0.196
-0.372	-0.416
-0.421	-0.788
-0.475	-1.433

Table A.2 Cyclic voltammogram of 0.1 mM H₂O₂ using bare electrode

V(volt)	I(μA)
-0.470	-2.505
-0.419	-0.643
-0.370	-0.161
-0.318	0.067
-0.267	0.171
-0.215	0.213
-0.166	0.248
-0.116	0.264
-0.064	0.277
-0.013	0.279
0.033	0.284
0.083	0.297
0.134	0.284
0.186	0.293
0.237	0.318
0.285	0.310
0.338	0.303
0.388	0.313
0.440	0.338
0.488	0.363
0.458	0.194
0.406	0.127
0.355	0.103
0.303	0.093
0.253	0.078
0.204	0.073
0.152	0.062
0.101	0.055
0.049	0.041
0.002	0.028
-0.046	0.005
-0.098	-0.010
-0.148	-0.036
-0.199	-0.057
-0.250	-0.095
-0.300	-0.150
-0.352	-0.297
-0.403	-0.584
-0.452	-1.130
-0.487	-1.903

Table A.3 Cyclic voltammogram of 0.1 mM Phenol using bare electrode

V(volt)	I(μA)
-0.489	-1.583
-0.437	-0.949
-0.386	-0.283
-0.336	0.000
-0.286	0.127
-0.235	0.197
-0.184	0.232
-0.134	0.259
-0.081	0.281
-0.031	0.279
0.015	0.289
0.065	0.289
0.116	0.297
0.168	0.294
0.218	0.293
0.269	0.297
0.320	0.305
0.370	0.325
0.423	0.346
0.473	0.380
0.475	0.277
0.424	0.149
0.374	0.109
0.323	0.090
0.271	0.072
0.220	0.070
0.169	0.049
0.119	0.050
0.068	0.036
0.018	0.028
-0.028	0.015
-0.080	0.000
-0.130	-0.026
-0.181	-0.041
-0.232	-0.070
-0.282	-0.121
-0.334	-0.235
-0.385	-0.463
-0.435	-0.851
-0.486	-1.556

Table A.4 Cyclic voltammograms of modified electrode with 0.5% w/v chitosan / HRP in presence of 0.1 mM of Phenol and 0.1 mM of H₂O₂

V(volt)	I(μA)
-0.481	-2.505
-0.429	-2.505
-0.378	-2.396
-0.328	-2.231
-0.277	-2.056
-0.227	-1.340
-0.175	-1.024
-0.124	-0.807
-0.073	-0.701
-0.023	-0.597
0.023	-0.507
0.075	-0.401
0.124	-0.292
0.176	-0.143
0.227	-0.011
0.277	0.122
0.329	0.249
0.378	0.352
0.431	0.414
0.481	0.498
0.466	0.271
0.416	0.097
0.365	0.015
0.315	-0.047
0.263	-0.163
0.212	-0.279
0.161	-0.417
0.111	-0.556
0.060	-0.696
0.010	-0.827
-0.038	-0.946
-0.088	-1.075
-0.139	-1.228
-0.189	-1.508
-0.241	-2.118
-0.290	-2.419
-0.342	-2.498
-0.393	-2.505
-0.444	-2.505
-0.486	-2.505

Table A.5 Cyclic voltammograms of modified electrode with 0.5% w/v chitosan / HRP / 0.1% w/v MCF in presence of 0.1 mM of Phenol and 0.1 mM of H₂O₂

V(volt)	I(μA)
-0.483	-2.456
-0.434	-2.505
-0.381	-2.505
-0.331	-2.397
-0.282	-1.216
-0.228	-0.806
-0.179	-0.597
-0.127	-0.553
-0.076	-0.555
-0.028	-0.628
0.021	-0.670
0.070	-0.613
0.120	-0.607
0.173	-0.545
0.222	-0.382
0.276	-0.140
0.325	0.121
0.375	0.274
0.427	0.388
0.476	0.458
0.468	0.260
0.419	0.093
0.369	-0.006
0.316	-0.155
0.267	-0.386
0.215	-0.685
0.165	-0.967
0.116	-1.204
0.062	-1.352
0.013	-1.425
-0.034	-1.513
-0.085	-1.565
-0.134	-1.649
-0.188	-1.869
-0.237	-2.166
-0.287	-2.423
-0.339	-2.505
-0.388	-2.505
-0.442	-2.505
-0.491	-2.505

Table A.6 Cyclic voltammograms of modified electrode with 0.5% w/v chitosan / HRP / 0.3% w/v MCF in presence of 0.1 mM of Phenol and 0.1 mM of H₂O₂

V(volt)	I(μA)
-0.487	-1.897
-0.436	-2.505
-0.385	-2.505
-0.336	-2.322
-0.282	-2.021
-0.233	-1.908
-0.181	-1.534
-0.130	-1.373
-0.081	-1.267
-0.028	-1.191
0.016	-1.142
0.068	-1.024
0.119	-0.859
0.168	-0.626
0.220	-0.368
0.271	-0.122
0.321	0.116
0.374	0.269
0.423	0.372
0.474	0.448
0.473	0.274
0.422	0.103
0.370	0.013
0.321	-0.112
0.269	-0.303
0.218	-0.564
0.169	-0.842
0.116	-1.115
0.067	-1.378
0.015	-1.579
-0.031	-1.727
-0.080	-1.857
-0.134	-1.973
-0.183	-2.253
-0.235	-2.505
-0.286	-2.505
-0.334	-2.505
-0.386	-2.505
-0.437	-2.505
-0.489	-2.505

Table A.7 Cyclic voltammograms of modified electrode with 0.5%w/v chitosan / HRP / 0.5% w/v MCF in presence of 0.1 mM of Phenol and 0.1 mM of H₂O₂

V(volt)	I(μA)
-0.469	-2.505
-0.421	-2.505
-0.370	-2.505
-0.318	-2.366
-0.269	-2.348
-0.215	-2.270
-0.166	-2.163
-0.116	-1.962
-0.063	-1.869
-0.016	-1.841
0.034	-1.814
0.083	-1.713
0.132	-1.592
0.186	-1.411
0.235	-1.068
0.289	-0.556
0.338	-0.077
0.387	0.210
0.441	0.365
0.482	0.423
0.458	0.167
0.406	0.038
0.357	-0.126
0.303	-0.463
0.254	-1.011
0.204	-1.628
0.151	-1.980
0.103	-2.084
0.049	-2.205
0.002	-2.285
-0.045	-2.293
-0.098	-2.379
-0.147	-2.490
-0.201	-2.505
-0.250	-2.505
-0.299	-2.505
-0.352	-2.505
-0.401	-2.505
-0.455	-2.505
-0.329	-1.670

Table A.8 Cyclic voltammograms of modified electrode with 0.5%w/v chitosan / HRP / 0.7% w/v MCF in presence of 0.1 mM of Phenol and 0.1 mM of H₂O₂

V(volt)	I(μA)
-0.455	-10.570
-0.401	-6.650
-0.352	-4.890
-0.303	-3.820
-0.250	-3.330
-0.201	-2.840
-0.147	-2.640
-0.098	-2.450
-0.049	-2.300
0.000	-2.350
0.049	-2.350
0.098	-2.100
0.152	-1.810
0.201	-1.220
0.254	-0.680
0.303	-0.240
0.352	0.050
0.406	0.340
0.455	0.490
0.489	0.440
0.440	0.050
0.391	0.050
0.338	-0.150
0.289	-0.390
0.235	-0.980
0.186	-1.610
0.137	-2.450
0.083	-2.690
0.034	-2.940
-0.015	-2.890
-0.064	-3.130
-0.113	-3.280
-0.166	-3.620
-0.215	-4.210
-0.264	-5.630
-0.318	-7.440
-0.367	-8.560
-0.421	-9.740
-0.470	-10.270
-0.479	-10.080

Table A.9 Cyclic voltammograms of modified electrode with 0.5%w/v chitosan / HRP / 0.9%w/v MCF in presence of 0.1 mM of Phenol and 0.1 mM of H₂O₂

V(volt)	I(μA)
-0.470	-6.680
-0.416	-6.600
-0.367	-4.450
-0.313	-3.030
-0.264	-2.250
-0.215	-1.910
-0.161	-1.520
-0.113	-1.470
-0.059	-1.420
-0.010	-1.370
0.034	-1.370
0.088	-1.170
0.137	-1.080
0.191	-0.730
0.240	-0.440
0.289	-0.340
0.342	0.200
0.391	0.240
0.445	0.340
0.494	0.390
0.455	0.150
0.401	0.000
0.352	-0.050
0.303	-0.340
0.250	-0.590
0.201	-0.980
0.147	-1.320
0.098	-1.710
0.049	-2.050
0.000	-2.010
-0.049	-2.250
-0.103	-2.300
-0.152	-2.500
-0.201	-2.790
-0.254	-3.720
-0.303	-4.940
-0.357	-6.210
-0.406	-7.090
-0.455	-7.930
-0.489	-8.370

Table A.10 Cyclic voltammograms of modified electrode with 0.1% w/v chitosan / HRP / 0.7% w/v MCF in presence of 0.1 mM of Phenol and 0.1 mM of H₂O₂

V(volt)	I(μA)
-0.489	-10.690
-0.440	-5.870
-0.386	-3.180
-0.338	-2.150
-0.284	-1.660
-0.235	-0.880
-0.186	-0.980
-0.132	-0.930
-0.083	-0.880
-0.034	-0.880
0.015	-0.780
0.064	-0.640
0.117	-0.490
0.166	-0.240
0.215	-0.150
0.269	-0.050
0.318	0.200
0.372	0.240
0.421	0.240
0.470	0.290
0.475	0.200
0.426	0.100
0.372	0.100
0.323	-0.100
0.274	-0.240
0.220	-0.340
0.171	-0.540
0.117	-0.640
0.068	-0.830
0.020	-0.980
-0.029	-1.170
-0.078	-1.080
-0.127	-1.270
-0.181	-1.370
-0.230	-1.960
-0.284	-2.790
-0.333	-3.620
-0.382	-4.110
-0.435	-4.700
-0.484	-5.430

Table A.11 Cyclic voltammograms of modified electrode with 0.3% w/v chitosan / HRP / 0.7% w/v MCF in presence of 0.1 mM of Phenol and 0.1 mM of H₂O₂

V(volt)	I(μA)
-0.465	-10.130
-0.411	-5.580
-0.362	-3.910
-0.313	-3.080
-0.259	-2.500
-0.210	-2.200
-0.157	-2.010
-0.108	-1.570
-0.059	-1.420
-0.005	-1.570
0.039	-1.710
0.088	-1.420
0.142	-1.270
0.191	-0.830
0.245	-0.490
0.294	-0.200
0.342	0.050
0.396	0.100
0.445	0.590
0.499	0.240
0.450	0.290
0.401	0.000
0.347	-0.200
0.298	-0.390
0.245	-0.490
0.196	-0.980
0.147	-1.170
0.093	-1.610
0.044	-1.810
-0.005	-1.910
-0.054	-2.200
-0.103	-1.960
-0.157	-2.540
-0.205	-2.590
-0.254	-3.130
-0.308	-4.700
-0.357	-5.280
-0.411	-6.070
-0.460	-6.850
-0.489	-7.190

Table A.12 Cyclic voltammograms of modified electrode with 0.7% w/v chitosan / HRP / 0.7% w/v MCF in presence of 0.1 mM of Phenol and 0.1 mM of H₂O₂

V(volt)	I(μA)
-0.494	-7.810
-0.440	-3.570
-0.391	-1.610
-0.342	-0.880
-0.289	-0.980
-0.240	-0.930
-0.186	-0.490
-0.137	-0.290
-0.088	-0.340
-0.034	-0.440
0.010	0.050
0.064	-0.150
0.113	-0.240
0.161	-0.240
0.215	0.050
0.264	0.150
0.318	0.290
0.367	0.340
0.416	0.390
0.470	0.440
0.479	0.290
0.426	0.150
0.377	0.000
0.328	0.050
0.274	-0.200
0.225	-0.290
0.176	-0.440
0.122	-0.490
0.073	-0.730
0.020	-0.880
-0.024	-0.880
-0.073	-1.170
-0.127	-1.370
-0.176	-1.420
-0.230	-1.730
-0.279	-2.690
-0.328	-2.930
-0.382	-3.720
-0.431	-1.030
-0.484	-0.730

Table A.13 Cyclic voltammograms of modified electrode with 0.5%w/v chitosan / HRP / 20 ppm Ag MCF 0.7%w/v in presence of 0.1 mM of Phenol and 0.1 mM of H₂O₂

V(volt)	I(μA)
-0.494	-6.7
-0.455	-4.75
-0.406	-2.98
-0.352	-1.91
-0.303	-1.13
-0.25	-0.44
-0.201	-0.29
-0.152	0
-0.098	0.2
-0.049	0.44
0	0.54
0.049	0.34
0.098	0.39
0.152	0.68
0.201	0.59
0.254	1.66
0.303	0.73
0.352	0.64
0.406	0.59
0.455	0.64
0.494	0.73
0.44	0.2
0.391	0.05
0.338	0
0.289	-0.1
0.24	-0.1
0.186	-0.1
0.137	-0.15
0.083	-0.2
0.034	-0.54
-0.01	-0.59
-0.064	-0.64
-0.113	-0.78
-0.166	-0.83
-0.215	-1.08
-0.264	-1.57
-0.318	-2.15
-0.367	-2.74
-0.421	-3.86
-0.47	-5.04
-0.479	-5.38

Table A.14 Cyclic voltammograms of modified electrode with 0.5%w/v chitosan / HRP / 100 ppm Ag MCF 0.7%w/v in presence of 0.1 mM of Phenol and 0.1 mM of H₂O₂

V(volt)	I(μA)
-0.47	-8.41
-0.421	-2.98
-0.367	-1.76
-0.318	-1.52
-0.264	-1.13
-0.215	-0.88
-0.166	-0.1
-0.113	-0.24
-0.064	0.1
-0.01	0.15
0.034	0.2
0.083	-0.05
0.137	0.15
0.186	0.15
0.235	0.34
0.289	2.25
0.338	1.08
0.391	0.73
0.44	0.44
0.489	0.59
0.455	0.15
0.406	0.1
0.352	-0.1
0.303	0.05
0.254	-0.15
0.201	-0.15
0.152	-0.1
0.098	-0.15
0.049	-0.44
0	-0.44
-0.049	-0.39
-0.098	-0.29
-0.152	-0.98
-0.201	-1.66
-0.25	-1.91
-0.303	-2.3
-0.352	-3.13
-0.401	-2.89
-0.455	-3.96
-0.494	-5.38

Table A.15 Cyclic voltammograms of modified electrode with 0.5%w/v chitosan / HRP / 500 ppm Ag MCF 0.7%w/v in presence of 0.1 mM of Phenol and 0.1 mM of H₂O₂

V(volt)	I(μA)
-0.484	-6.07
-0.431	-1.42
-0.382	-0.73
-0.328	-0.68
-0.279	-0.49
-0.23	-0.34
-0.176	-0.24
-0.127	-0.15
-0.078	0.15
-0.024	0.24
0.02	0.2
0.073	0.34
0.122	0.24
0.171	0.39
0.225	0.34
0.274	1.81
0.328	1.03
0.377	1.08
0.426	1.22
0.479	1.66
0.47	0.64
0.416	0.15
0.367	0
0.318	0
0.264	0
0.215	-0.1
0.161	-0.15
0.113	-0.15
0.064	-0.2
0.01	-0.44
-0.034	-0.54
-0.083	-0.73
-0.137	-1.13
-0.186	-1.66
-0.24	-2.01
-0.289	-2.15
-0.338	-2.69
-0.391	-3.38
-0.44	-5.19
-0.494	-5.23

Table A.16 Cyclic voltammograms of modified electrode with 0.5%w/v chitosan / HRP / 1000 ppm Ag MCF 0.7%w/v in presence of 0.1 mM of Phenol and 0.1 mM of H₂O₂

V(volt)	I(μA)
-0.499	-4.45
-0.45	-3.42
-0.401	-2.2
-0.347	-1.71
-0.298	-1.08
-0.25	-0.78
-0.196	-0.49
-0.147	-0.24
-0.093	0.05
-0.044	0.29
0	0.24
0.054	0.44
0.103	0.34
0.157	0.59
0.205	1.03
0.254	1.22
0.308	0.88
0.357	0.64
0.411	0.64
0.46	0.64
0.489	0.68
0.435	0.15
0.386	-0.05
0.333	-0.1
0.284	0.1
0.235	-0.34
0.181	-0.1
0.132	-0.24
0.083	-0.15
0.029	-0.44
-0.015	-0.34
-0.068	-0.49
-0.117	-0.64
-0.166	-0.93
-0.22	-1.22
-0.269	-1.52
-0.323	-1.66
-0.372	-2.15
-0.421	-3.28
-0.475	-3.86

Table A.17 Cyclic voltammograms of modified electrode with 0.5%w/v chitosan / HRP / 100 ppm Ag SiO₂ 0.7%w/v in presence of 0.1 mM of Phenol and 0.1 mM of H₂O₂

V(volt)	I(μA)
-0.499	-13.31
-0.445	-10.23
-0.396	-7.68
-0.347	-5.43
-0.294	-4.11
-0.245	-2.98
-0.191	-2.5
-0.142	-2.05
-0.093	-1.96
-0.039	-1.76
0.005	-1.61
0.059	-1.32
0.108	-0.88
0.157	0
0.21	1.66
0.259	5.04
0.313	6.75
0.362	4.21
0.411	3.52
0.465	3.28
0.484	2.69
0.431	1.22
0.382	0.83
0.333	0.49
0.279	0.05
0.23	-0.15
0.181	-0.59
0.127	-1.13
0.078	-1.91
0.024	-2.64
-0.02	-3.38
-0.068	-3.77
-0.122	-4.11
-0.171	-4.16
-0.225	-4.26
-0.274	-4.65
-0.323	-5.19
-0.377	-6.31
-0.426	-8.95
-0.479	-11.89

Table A.18 Cyclic voltammograms of modified electrode with 0.5%w/v chitosan / HRP / 500 ppm Ag SiO₂ 0.7%w/v in presence of 0.1 mM of Phenol and 0.1 mM of H₂O₂

V(volt)	I(μA)
-0.479	-20.4
-0.431	-15.41
-0.377	-11.55
-0.328	-8.41
-0.274	-5.72
-0.225	-3.82
-0.176	-2.74
-0.122	-1.76
-0.073	-1.37
-0.02	-1.22
0.024	-0.88
0.073	-0.64
0.127	0.15
0.176	1.76
0.225	6.21
0.279	17.66
0.328	5.14
0.382	3.33
0.431	2.74
0.479	2.15
0.465	1.22
0.416	0.49
0.362	0.29
0.313	0.15
0.264	0
0.21	-0.15
0.161	-0.34
0.108	-0.64
0.059	-1.42
0.01	-4.55
-0.039	-3.96
-0.088	-3.96
-0.142	-4.16
-0.191	-4.6
-0.24	-5.63
-0.294	-7.09
-0.342	-9.54
-0.391	-13.16
-0.445	-17.56
-0.494	-22.06

Table A.19 Cyclic voltammograms of modified electrode with 0.5%w/v chitosan / HRP / 1000 ppm Ag SiO₂ 0.7%w/v in presence of 0.1 mM of Phenol and 0.1 mM of H₂O₂

V(volt)	I(μA)
-0.484	-18.2
-0.435	-5.97
-0.382	-4.01
-0.333	-2.69
-0.284	-2.01
-0.23	-1.42
-0.181	-1.17
-0.127	-0.88
-0.078	-0.78
-0.029	-0.59
0.02	-0.49
0.068	-0.34
0.122	0.1
0.171	0.64
0.22	2.05
0.274	2.94
0.323	2.94
0.372	2.25
0.426	1.76
0.475	1.08
0.47	0.49
0.421	0.2
0.372	0.05
0.318	0.05
0.269	-0.05
0.215	-0.15
0.166	-0.24
0.117	-0.34
0.064	-0.49
0.015	-2.25
-0.034	-1.52
-0.083	-1.61
-0.132	-2.1
-0.186	-2.2
-0.235	-2.79
-0.289	-3.57
-0.338	-4.4
-0.386	-5.48
-0.44	-7.14
-0.489	-9.3

Table A.20 Cyclic voltammograms of modified electrode with 0.5%w/v chitosan / 20 ppm Ag / HRP / 0.7%w/v modified MCF in presence of 0.1 mM of Phenol and 0.1 mM of H₂O₂

V(volt)	I(μA)
-0.479	-23.75
-0.431	-23.21
-0.377	-15.26
-0.328	-12.24
-0.274	-10.41
-0.225	-9.43
-0.176	-8.56
-0.122	-8.16
-0.073	-7.65
-0.02	-7.38
0.024	-6.89
0.073	-5.96
0.127	-4.93
0.176	-3.56
0.225	-2.1
0.279	-0.78
0.328	0.18
0.382	0.64
0.431	0.98
0.479	1.08
0.465	0.94
0.416	0.4
0.362	-0.09
0.313	-0.29
0.264	-1.17
0.21	-1.71
0.161	-2.73
0.108	-3.81
0.059	-4.69
0.01	-5.47
-0.039	-5.91
-0.088	-6.11
-0.142	-6.4
-0.191	-6.94
-0.24	-8.16
-0.294	-10.12
-0.342	-12.08
-0.391	-13.2
-0.445	-14.13
-0.494	-14.82

Table A.21 Cyclic voltammograms of modified electrode with 0.5%w/v chitosan / 100 ppm Ag / HRP / 0.7%w/v modified MCF in presence of 0.1 mM of Phenol and 0.1 mM of H₂O₂

V(volt)	I(μA)
-0.455	-10.96
-0.406	-5.43
-0.357	-3.57
-0.303	-3.03
-0.254	-2.2
-0.201	-1.96
-0.152	-1.57
-0.103	-1.32
-0.049	-1.13
0	-1.03
0.044	-0.88
0.098	-0.59
0.147	-0.39
0.201	0.05
0.25	0.68
0.298	1.47
0.352	2.01
0.401	2.35
0.455	2.84
0.494	3.33
0.445	1.91
0.391	0.54
0.342	-0.1
0.289	-0.93
0.24	-1.42
0.191	-2.35
0.137	-3.33
0.088	-3.67
0.034	-3.47
-0.01	-2.98
-0.059	-2.15
-0.113	-2.3
-0.161	-2.54
-0.21	-3.13
-0.264	-4.11
-0.313	-5.04
-0.367	-5.38
-0.416	-5.92
-0.465	-6.7
-0.479	-6.7

Table A.22 Cyclic voltammograms of modified electrode with 0.5%w/v chitosan / 500 ppm Ag / HRP / 0.7%w/v modified MCF in presence of 0.1 mM of Phenol and 0.1 mM of H₂O₂

V(volt)	I(μA)
-0.484	-25.05
-0.431	-9
-0.382	-5.33
-0.333	-3.42
-0.279	-2.4
-0.23	-1.66
-0.176	-1.42
-0.127	-1.17
-0.078	-1.08
-0.024	-0.83
0.02	-0.78
0.068	-0.49
0.122	-0.44
0.171	-0.24
0.225	-0.2
0.274	0.05
0.323	0.29
0.377	0.29
0.426	0.44
0.479	0.88
0.47	0.64
0.421	0.15
0.367	0.05
0.318	-0.1
0.264	-0.29
0.215	-0.59
0.166	-1.08
0.113	-0.54
0.064	-0.93
0.01	-1.27
-0.034	-1.13
-0.083	-1.61
-0.137	-1.57
-0.186	-1.86
-0.235	-3.33
-0.289	-4.55
-0.338	-5.77
-0.391	-6.6
-0.44	-7.34
-0.489	-8.07

Table A.23 Cyclic voltammograms of modified electrode with 0.5%w/v chitosan / 1000 ppm Ag / HRP / 0.7%w/v modified MCF in presence of 0.1 mM of Phenol and 0.1 mM of H₂O₂

V(volt)	I(μA)
-0.484	-6.07
-0.431	-1.42
-0.382	-0.73
-0.328	-0.68
-0.279	-0.49
-0.23	-0.34
-0.176	-0.24
-0.127	-0.15
-0.078	0.15
-0.024	0.24
0.02	0.2
0.073	0.34
0.122	0.24
0.171	0.39
0.225	0.34
0.274	1.81
0.328	1.03
0.377	1.08
0.426	1.22
0.479	1.66
0.47	0.64
0.416	0.15
0.367	0
0.318	0
0.264	0
0.215	-0.1
0.161	-0.15
0.113	-0.15
0.064	-0.2
0.01	-0.44
-0.034	-0.54
-0.083	-0.73
-0.137	-1.13
-0.186	-1.66
-0.24	-2.01
-0.289	-2.15
-0.338	-2.69
-0.391	-3.38
-0.44	-5.19
-0.494	-5.23

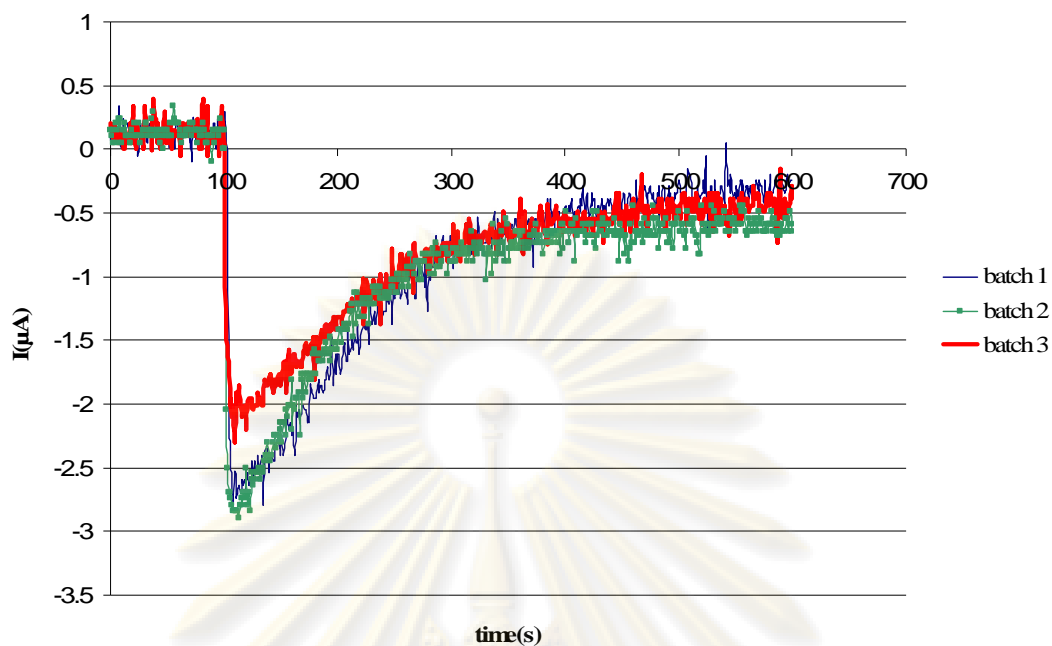


Figure A.1 Amperometric of modified electrode with 0.5%w/v chitosan mixed with 20 ppm Ag solution, HRP and 0.7%w/v modified MCF in presence of 0.1 mM of Phenol and 0.1 mM of H₂O₂ at 0 volt (first time)

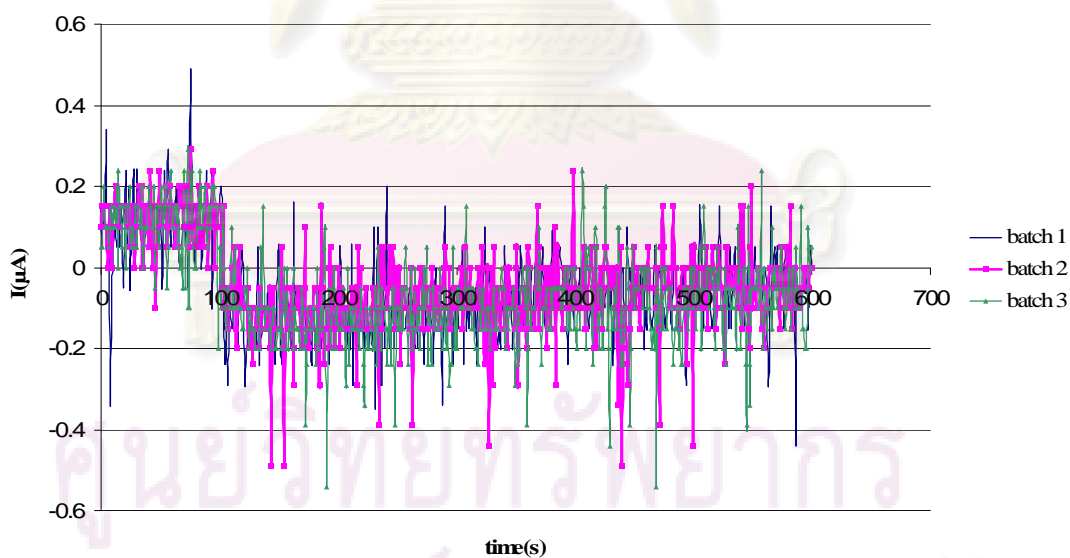


Figure A.2 Amperometric of modified electrode with 0.5%w/v chitosan mixed with 20 ppm Ag solution, HRP and 0.7%w/v modified MCF in presence of 0.1 mM of Phenol and 0.1 mM of H₂O₂ at 0 volt (second times)

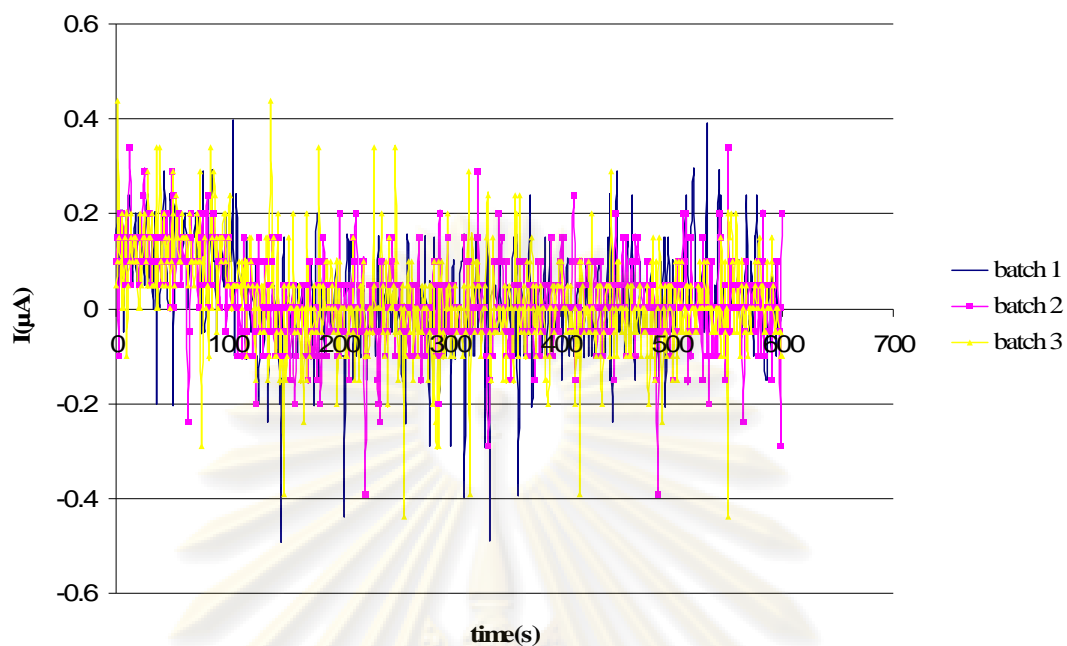


Figure A.3 Amperometric of modified electrode with 0.5%w/v chitosan mixed with 20 ppm Ag solution, HRP and 0.7%w/v modified MCF in presence of 0.1 mM of Phenol and 0.1 mM of H_2O_2 at 0 volt (third times)

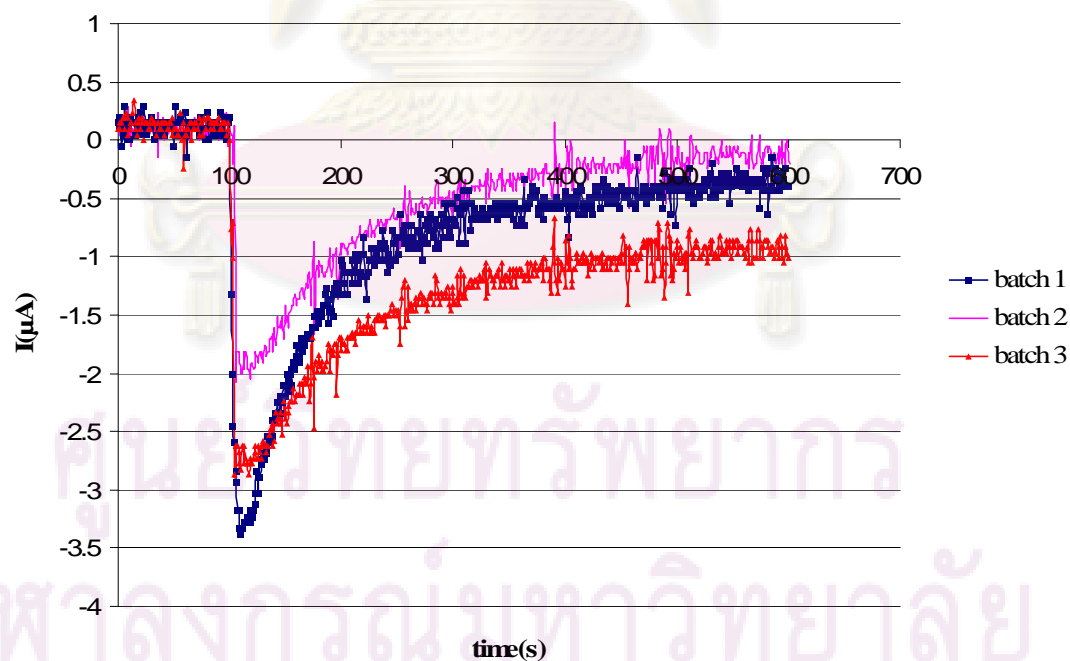


Figure A.4 Amperometric of modified electrode with 0.5%w/v chitosan, HRP and 0.7%w/v modified MCF in presence of 0.1 mM of Phenol and 0.1 mM of H_2O_2 at 0 volt (first time)

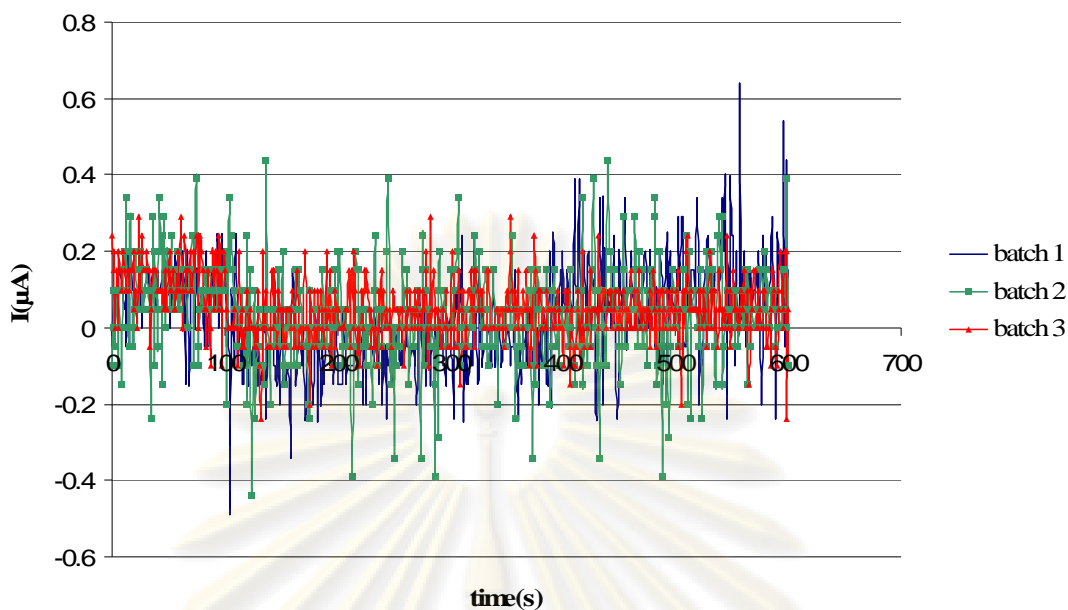


Figure A.5 Amperometric of modified electrode with 0.5% w/v chitosan, HRP and 0.7% w/v modified MCF in presence of 0.1 mM of Phenol and 0.1 mM of H_2O_2 at 0 volt (second times)

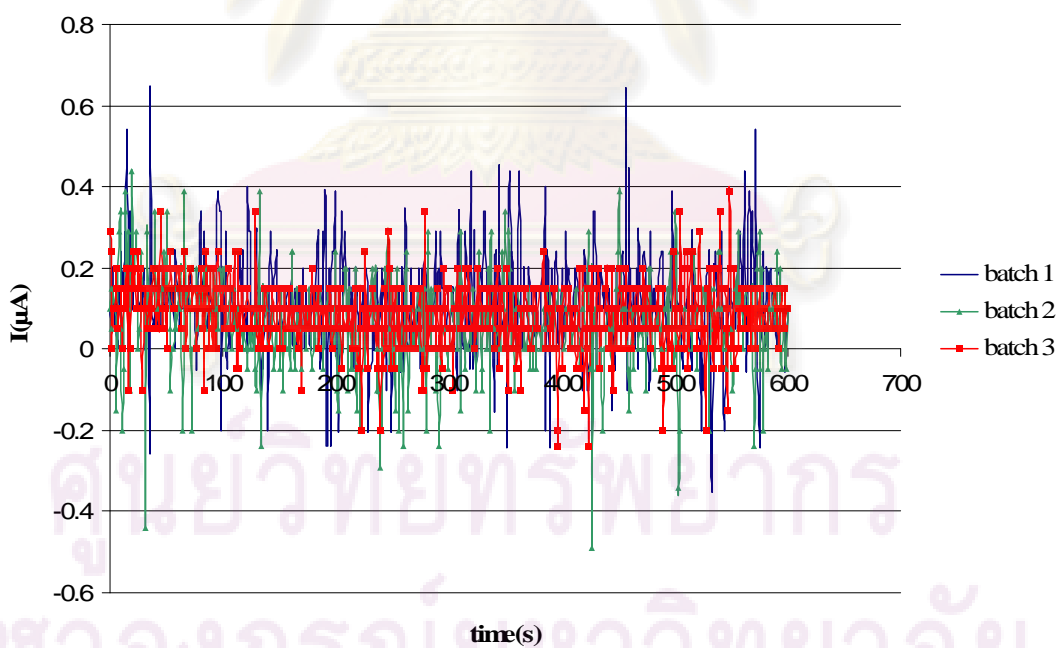


Figure A.6 Amperometric of modified electrode with 0.5% w/v chitosan, HRP and 0.7% w/v modified MCF in presence of 0.1 mM of Phenol and 0.1 mM of H_2O_2 at 0 volt (third times)

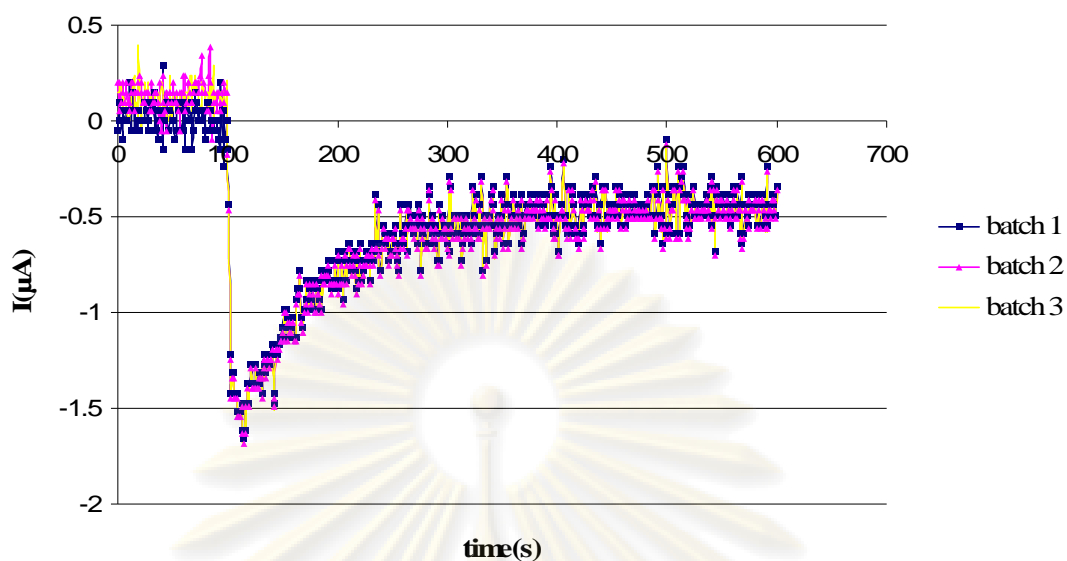


Figure A.7 Amperometric of modified electrode with 0.5% w/v chitosan, HRP and 20 ppm Ag solution in presence of 0.1 mM of Phenol and 0.1 mM of H_2O_2 at 0 volt (first time)

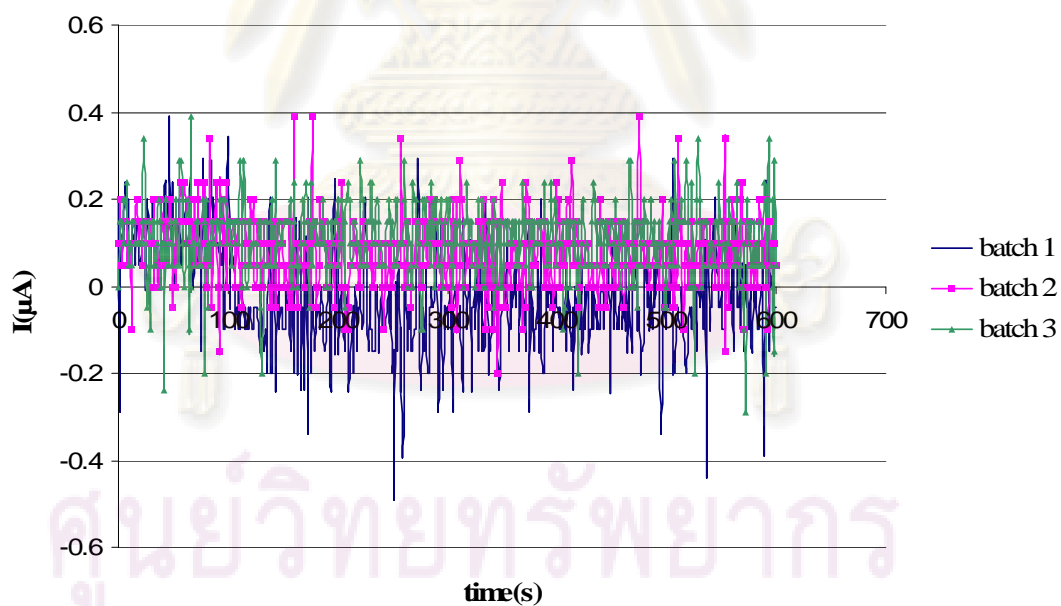


Figure A.8 Amperometric of modified electrode with chitosan 0.5% w/v, HRP and 20 ppm Ag solution in presence of 0.1 mM of Phenol and 0.1 mM of H_2O_2 at 0 volt (second times)

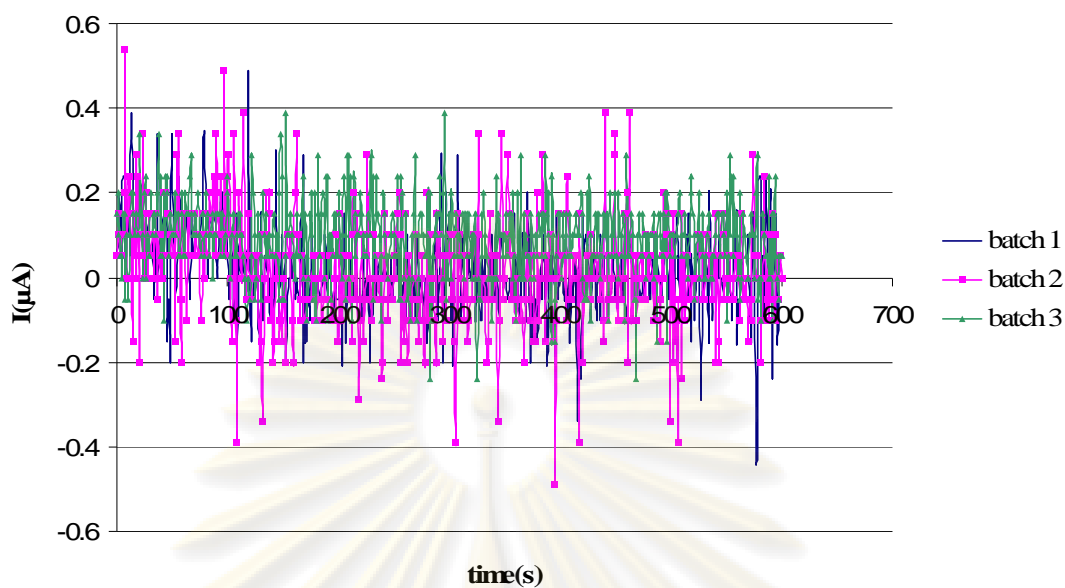


Figure A.9 Amperometric of modified electrode with 0.5% w/v chitosan, HRP and 20 ppm Ag solution in presence of 0.1 mM of Phenol and 0.1 mM of H₂O₂ at 0 volt (third times)

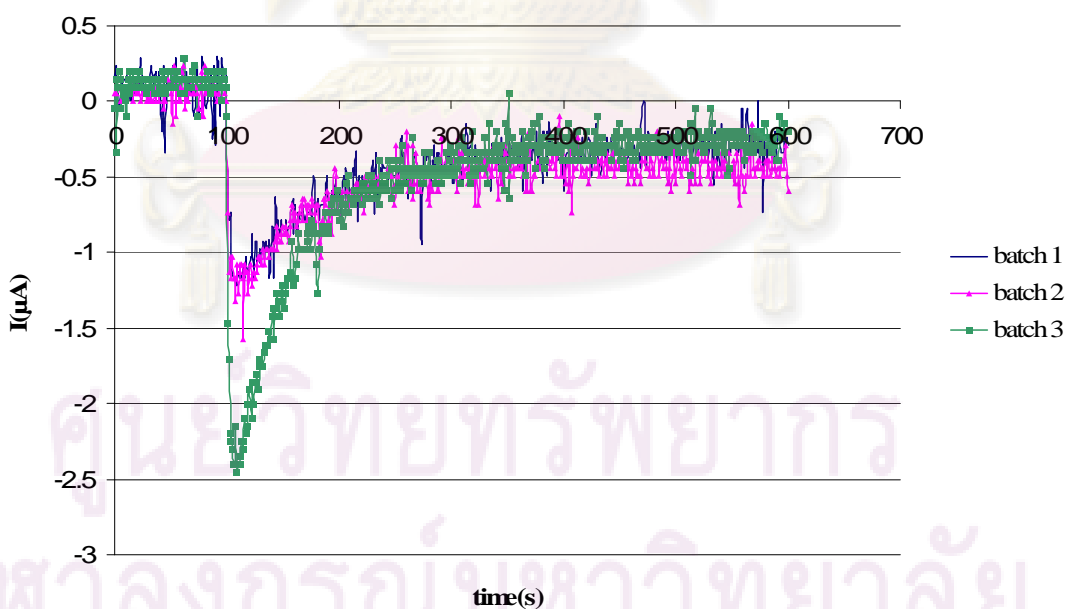


Figure A.10 Amperometric of modified electrode with 0.5% w/v chitosan and HRP in presence of 0.1 mM of Phenol and 0.1 mM of H₂O₂ at 0 volt (first time)

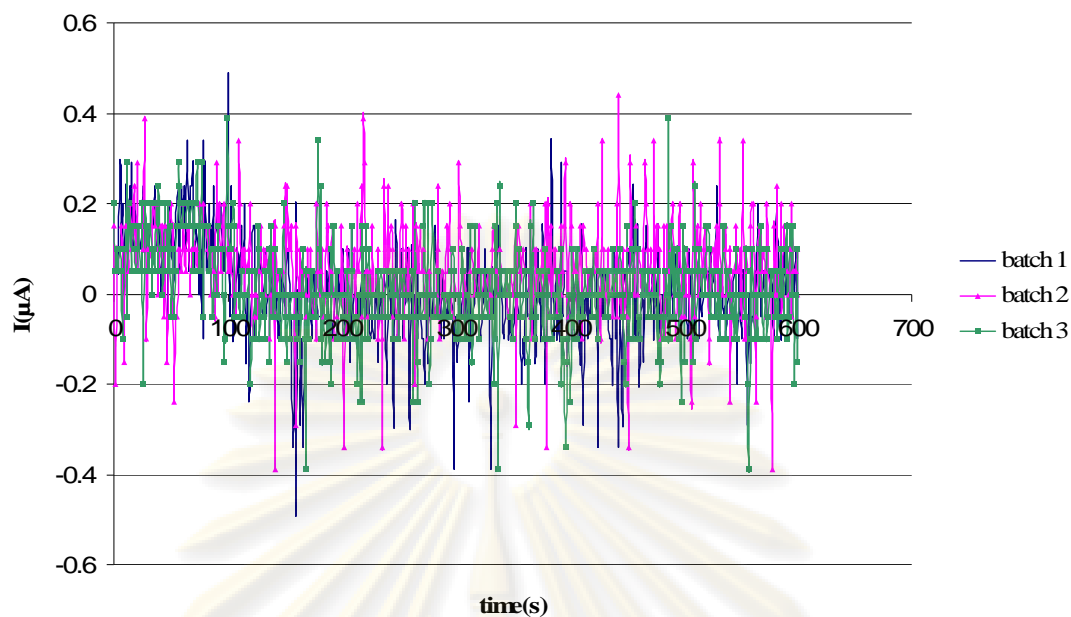


Figure A.11 Amperometric of modified electrode with 0.5% w/v chitosan and HRP in presence of 0.1 mM of Phenol and 0.1 mM of H_2O_2 at 0 volt (second times)

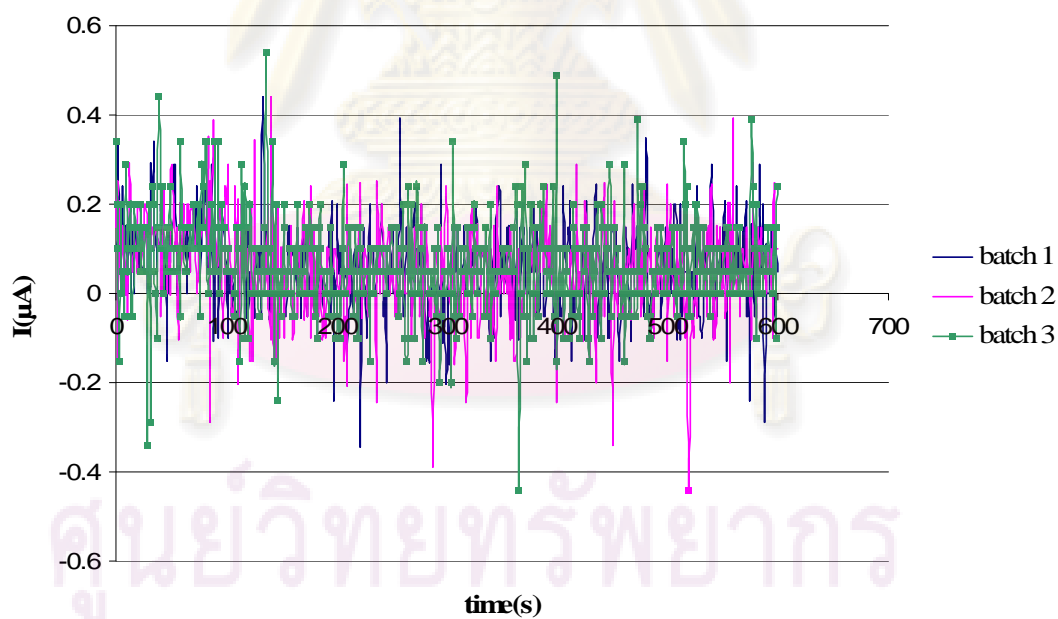


Figure A.12 Amperometric of modified electrode with 0.5% w/v chitosan and HRP in presence of 0.1 mM of Phenol and 0.1 mM of H_2O_2 at 0 volt (third times)

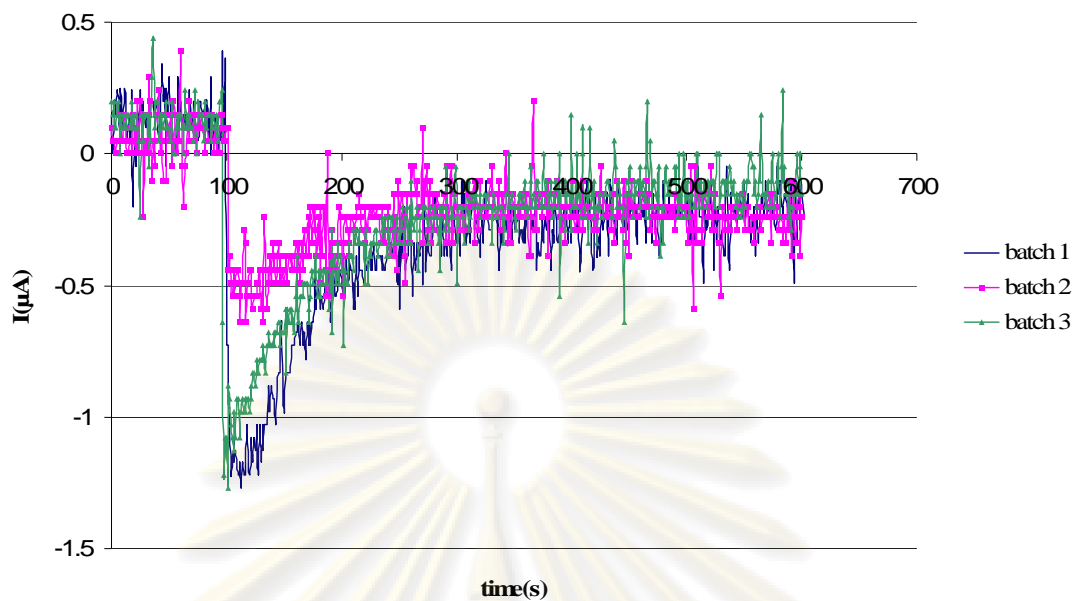


Figure A.13 Amperometric of modified electrode with 0.1% w/v chitosan and HRP in presence of 0.1 mM of Phenol and 0.1 mM of H_2O_2 at 0 volt

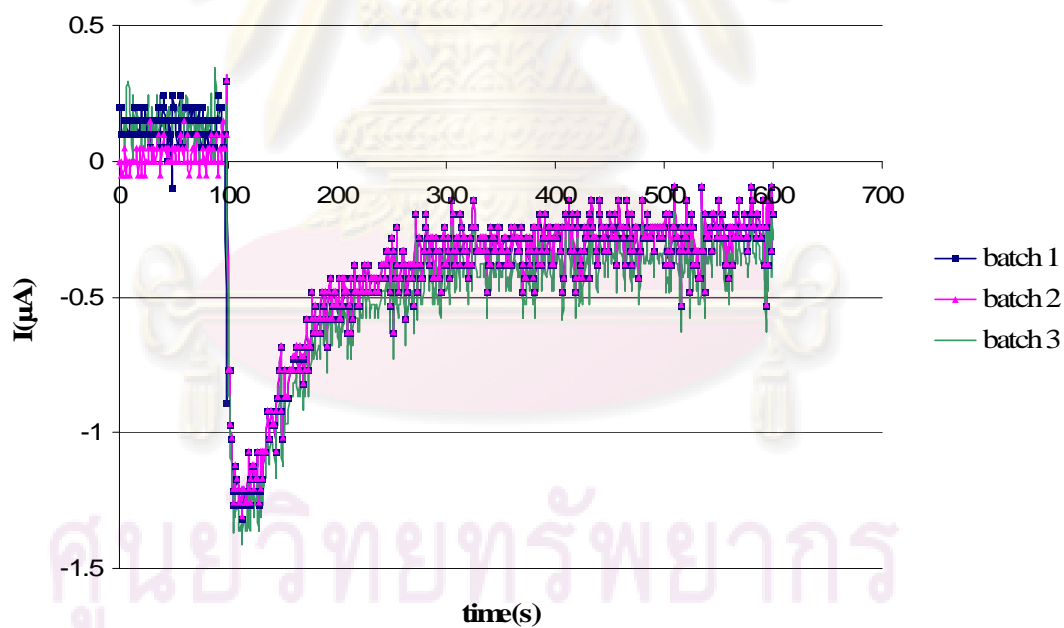


Figure A.14 Amperometric of modified electrode with 0.3% w/v chitosan and HRP in presence of 0.1 mM of Phenol and 0.1 mM of H_2O_2 at 0 volt

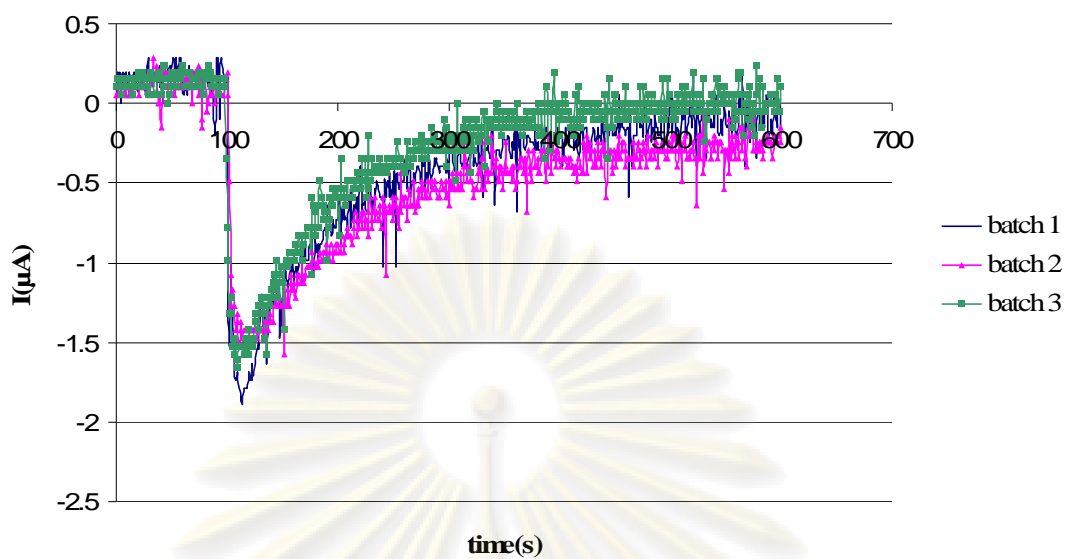


Figure A.15 Amperometric of modified electrode with 0.7% w/v chitosan and HRP in presence of 0.1 mM of Phenol and 0.1 mM of H_2O_2 at 0 volt

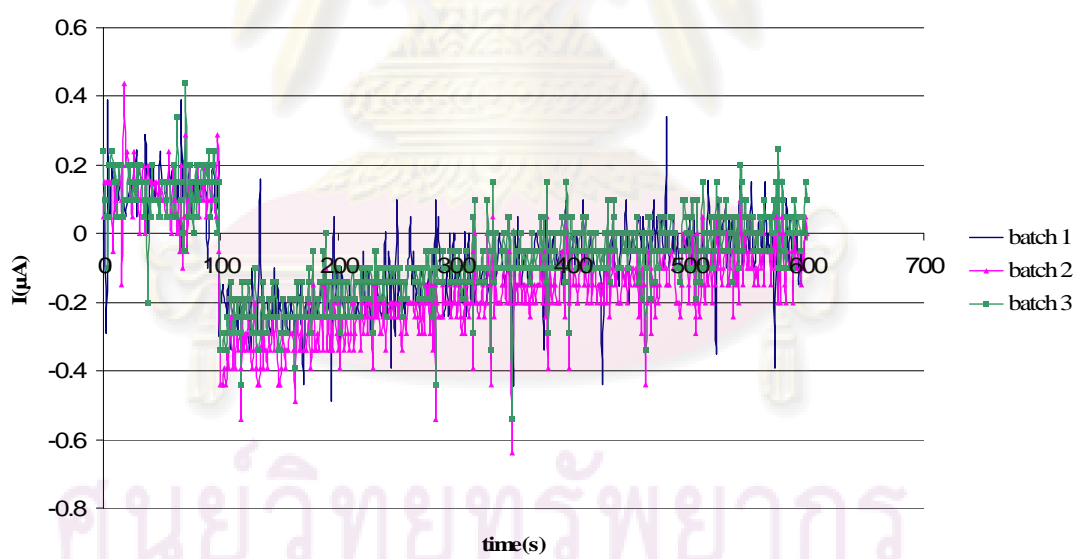


Figure A.16 Amperometric of modified electrode with 1.0% w/v chitosan and HRP in presence of 0.1 mM of Phenol and 0.1 mM of H_2O_2 at 0 volt

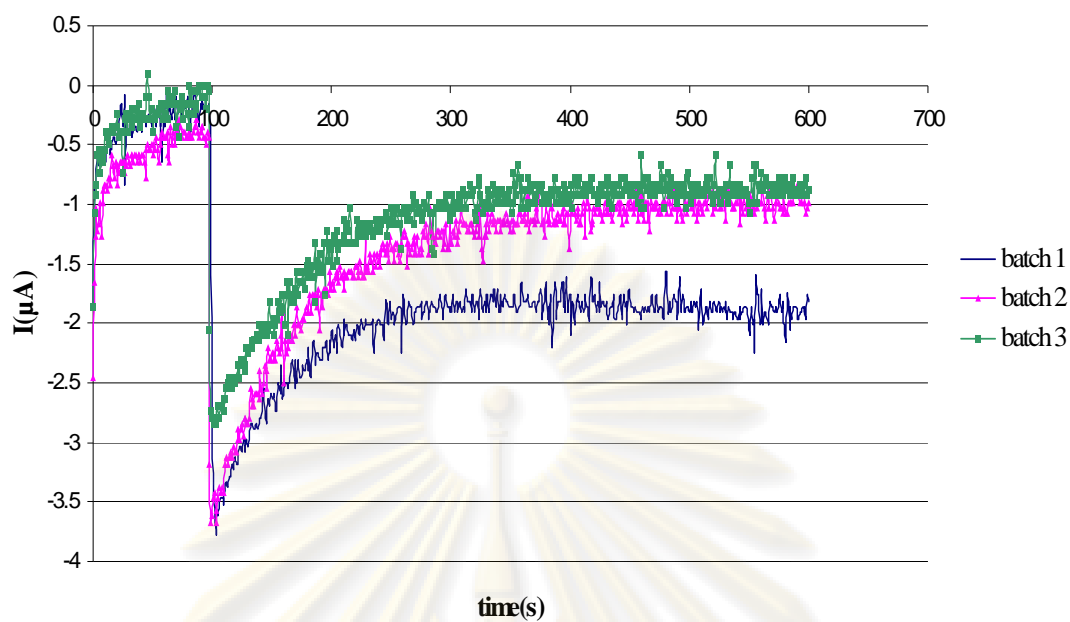


Figure A.17 Amperometric of modified electrode with 0.5% w/v chitosan and HRP in presence of 0.1 mM of Phenol and 0.1 mM of H_2O_2 at -0.2 volt

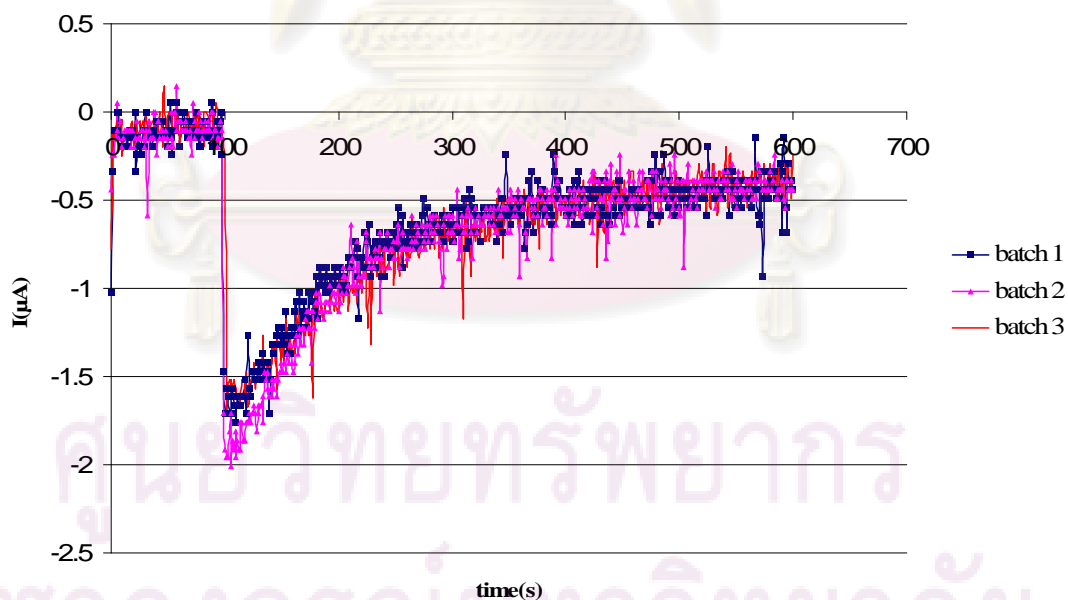


Figure A.18 Amperometric of modified electrode with 0.5% w/v chitosan and HRP in presence of 0.1 mM of Phenol and 0.1 mM of H_2O_2 at -0.1 volt

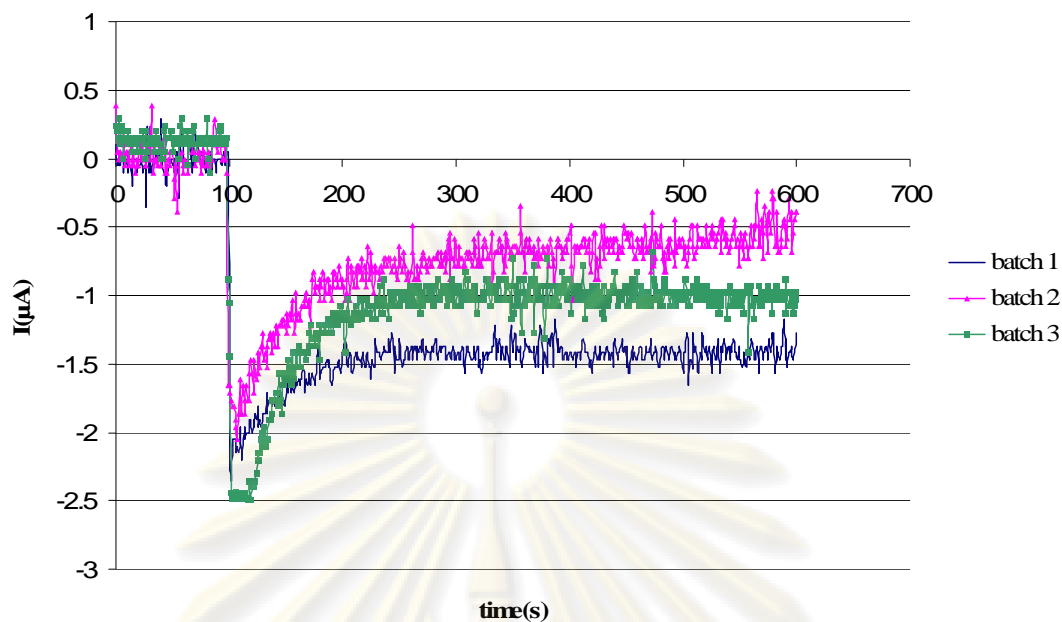


Figure A.19 Amperometric of modified electrode with 0.5% w/v chitosan and HRP in presence of 0.1 mM of Phenol and 0.1 mM of H_2O_2 at 0.1 volt

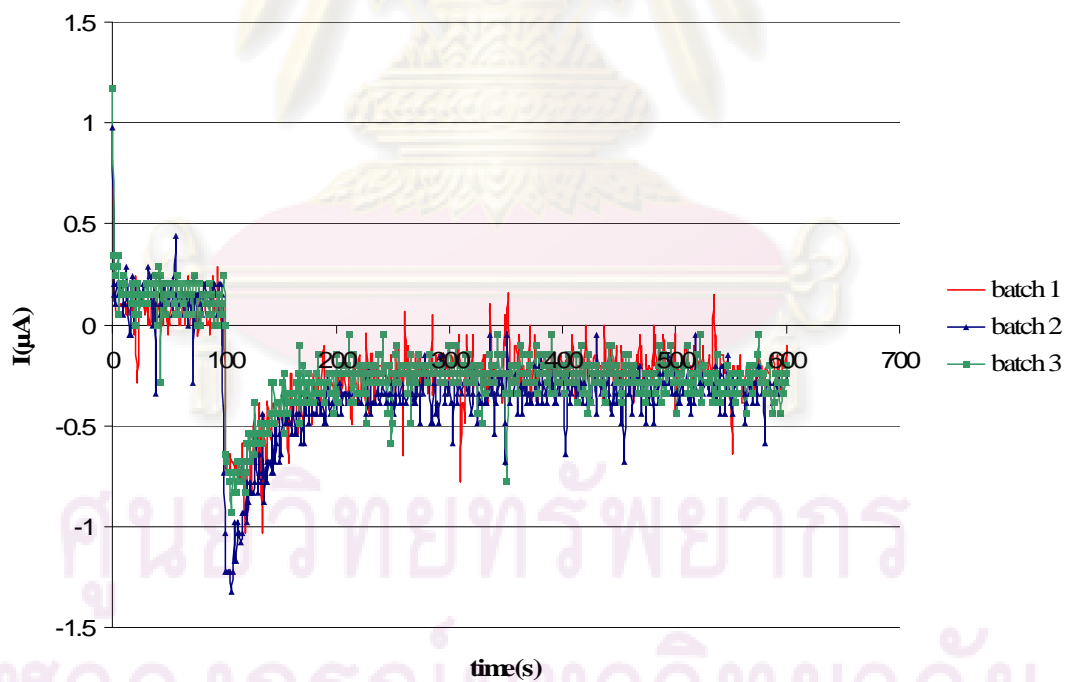
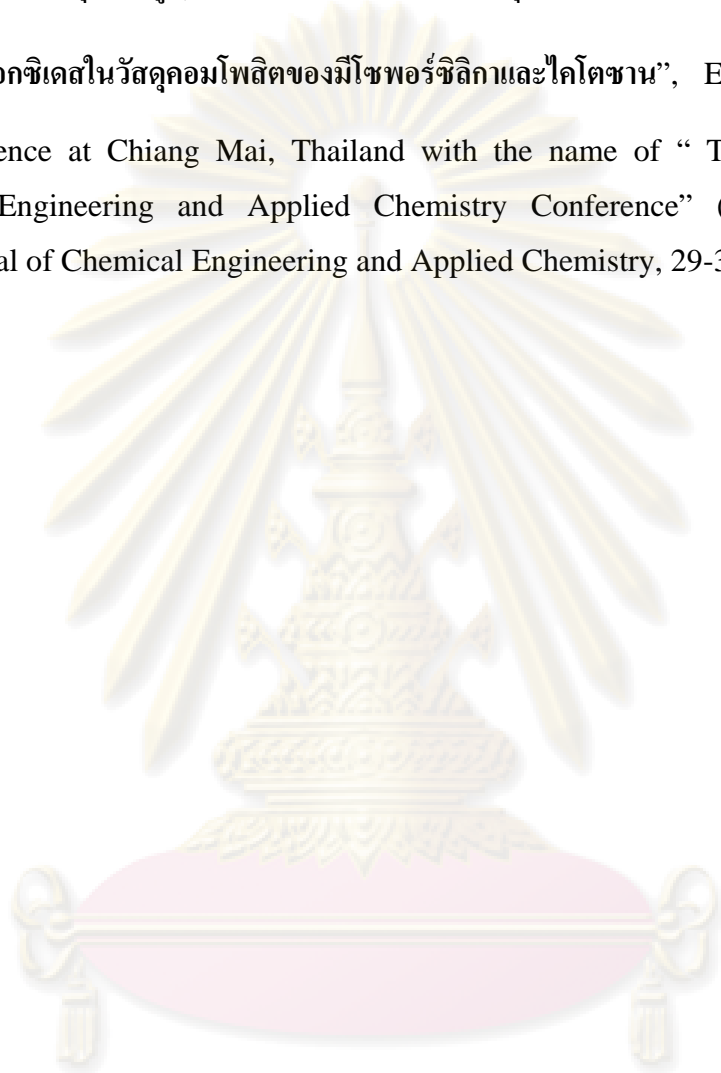


Figure A.20 Amperometric of modified electrode with 0.5% w/v chitosan and HRP in presence of 0.1 mM of Phenol and 0.1 mM of H_2O_2 at 0.2 volt

Appendix B

Conference

สกนธ์ พันธุ์วิทยกุล, วิไลวรรณ ช่วยยก และ สิริรุ่ง ปรีชานนท์, “การตรึงเอนไซม์ฮอร์ส แรดิซเปอร์ออกซิเดสในวัสดุคอมโพสิตของมีซพอร์ซิลิกาและไคโตซาน”, Extended Abstract for Conference at Chiang Mai, Thailand with the name of “ The 17th Thailand Chemical Engineering and Applied Chemistry Conference” (TICHE) 2007 – Fundamental of Chemical Engineering and Applied Chemistry, 29-30 October 2007.



ศูนย์วิทยทรัพยากร
จุฬาลงกรณ์มหาวิทยาลัย

การประชุมวิชาการวิศวกรรมเคมีและ เคมีประยุกต์แห่งประเทศไทย ครั้งที่ 17



29 – 30 ตุลาคม 2550
ณ โรงแรมดิเอ็มเพรส
จ.เชียงใหม่

จัดโดย

สมาคมวิศวกรรมเคมีและเคมีประยุกต์แห่งประเทศไทย

ร่วมกับ

ภาควิชาเคมีอุตสาหกรรม คณะวิทยาศาสตร์ มหาวิทยาลัยเชียงใหม่



การตรึงเอนไซม์ฮอร์สแรดิชเปอร์ออกซิเดสในวัสดุคอมโพสิตของมีโซพอร์ซิลิกาและไคโตซาน

สกนธ์ พันธุ์วิทยาภูล¹, วิไลวรรณ ช่วยยก¹ และ สิริรุ่ง ปริษานนท์*

1) ภาควิชาวิศวกรรมเคมี คณะวิศวกรรมศาสตร์ จุฬาลงกรณ์มหาวิทยาลัย เขตพญาไท กรุงเทพฯ 10330

บทคัดย่อ

การตรึงเอนไซม์ฮอร์สแรดิชเปอร์ออกซิเดสในมีโซพอร์ซิลิกาด้วยการดูดซับทางกายภาพ พบว่าปริมาณเอนไซม์ที่ดูดซับได้มีปริมาณสูงถึง 99% เนื่องจากมีโซพอร์ซิลิกาที่สังเคราะห์ได้ มีขนาดรูพรุน 24.1 nm ซึ่งใหญ่กว่าขนาดเฉลี่ยของโมเลกุลเอนไซม์ (48 Å) ประกอบด้วยมีพื้นที่ผิวสูง มีการหลุดออกของเอนไซม์ 2.5% และเมื่อห่อหุ้มเอนไซม์ที่ตรึงรูอยู่บนมีโซพอร์ซิลิกาด้วยไคโตซานแล้ว การหลุดออกของเอนไซม์ลดลงเหลือเพียง 0.4% อย่างไรก็ตามค่ากิจกรรมของเอนไซม์ลดลง ซึ่งอาจเกิดจากการถ่ายเทมวลสารผ่านแผ่นฟิล์มของไคโตซานถูกจำกัด

คำสำคัญ: ฮอร์สแรดิชเปอร์ออกซิเดส, มีโซพอร์ซิลิกา, ไคโตซาน, ค่ากิจกรรมของเอนไซม์

1. บทนำ

เอนไซม์ฮอร์สแรดิชเปอร์ออกซิเดสเป็นเอนไซม์ที่มีความสำคัญในปฏิกิริยาออกซิเดชัน ใช้สำหรับการตรวจวิเคราะห์สารต่างๆ ได้แก่ ตรวจวัดสารประกอบฟีนอล เช่น ไพโรแกลลอล (pyrogallol) ไฮโดรควิโนน (hydroquinone) คาเทคอล (catechol) ฯลฯ ซึ่งเป็นสารก่อมะเร็งเป็นอันตรายต่อร่างกายโดยพบว่ามีการปนเปื้อนอยู่ในอาหารและยา ปนเปื้อนอยู่ในน้ำที่จากโรงงานอุตสาหกรรมต่างๆ เพื่อความสะดวกในการใช้งาน จึงมีการศึกษาการตรึงรูบนเอนไซม์ชนิดนี้บนวัสดุต่างๆ [Caramori และคณะ, 2004; Rojas และคณะ, 2004] เพื่อให้เอนไซม์มีประสิทธิภาพและเสถียรภาพทั้งในด้านการทำงานและการเก็บรักษา โดยวัสดุที่มีความพรุนและพื้นที่ผิวสูง อย่างเช่น มีโซพอร์ซิลิกา กำลังได้รับความสนใจอย่างมากในปัจจุบัน เนื่องจากสามารถกักเก็บเอนไซม์ได้ในปริมาณมากด้วยการตรึงรูปแบบดูดซับ ซึ่งเป็นวิธีการตรึงรูอย่างง่าย อย่างไรก็ตามการหลุดออกของเอนไซม์ยังคงเป็นปัญหาสำหรับการตรึงรูบนเอนไซม์ด้วยวิธีนี้ [Yadav และคณะ, 2005] งานวิจัยนี้จึงศึกษาการนำวัสดุไคโตซาน ซึ่งมีความสามารถในการยึดจับขึ้นรูปได้ดีในการตรึงเอนไซม์ ไม่เป็นพิษ และมีราคาไม่แพง มาห่อหุ้มเอนไซม์ที่ตรึงรูอยู่บนวัสดุตรึง Mesocellular Foam (MCF) เพื่อป้องกันการหลุดออกของเอนไซม์ โดยศึกษาอิทธิพลของปริมาณซิลิกาที่ผ่านการตรึงรูแล้วในไคโตซาน ที่มีผลต่อการเร่งปฏิกิริยาของเอนไซม์ตรึงรูและการหลุดออกของเอนไซม์

2. อุปกรณ์และวิธีการทดลอง

2.1 สารเคมี

ไพโรแกลลอล (pyrogallol) ไฮโดรเจนเปอร์ออกไซด์ (H_2O_2) กรดอะซิติก (CH_3COOH) ไคโตซาน (chitosan) ฮอร์สแรดิชเปอร์ออกซิเดส (EC 1.11.1.7) กรดไฮโดรคลอริกเข้มข้น 36.5% โดยน้ำหนัก (HCL) พลูโรนิค พี 123 (Pluronic, P123) เตตระเอทิลอซิโกลิเกต ($C_8H_{20}O_4Si$) ไตรเมทิลเบนซีน (TMB)

2.2 การสังเคราะห์มีโซพอร์ซิลิกานชนิดMCF

MCF สังเคราะห์ตามวิธีของ Lettow และ คณะ [2000] ดังนี้ ผสมพลูโรนิค พี 123 ในสารละลายกรดไฮโดรคลอริกที่มีความเข้มข้น 1.6 โมลาร์ 75 มิลลิลิตร จากนั้นเติมไตรเมทิลเบนซีน 1 กรัมลงในสารละลายปั่นกวนอย่างน้อย 1 ชั่วโมง ใส่เตตระเอทิลอซิโกลิเกต 4.25 กรัมลงไปในปั่นกวนต่อเนื่อง 24 ชั่วโมง ที่ 35-40 องศาเซลเซียส เทใส่ขวดเพ็ลตอน และให้สารทำปฏิกิริยาต่อเนื่องที่ 100-120 องศาเซลเซียส เป็นเวลา 24 ชั่วโมง จากนั้นกรองและปล่อยให้แห้งที่อุณหภูมิห้อง นำไปเผาเพื่อเอาสารลดแรงตึงผิวออกที่ 500 องศาเซลเซียส เป็นเวลา 6 ชั่วโมง

2.4 การตรึงเอนไซม์ฮอร์สแรดิชเปอร์ออกซิเดสด้วยมีโซพอร์ซิลิกาจากนั้นห่อหุ้มด้วยไคโตซาน

มีโซพอร์ซิลิกา 0.4 กรัมเติมลงในสารละลายเอนไซม์ที่มี pH 8 ความเข้มข้น 0.1 มิลลิกรัม/ มิลลิลิตร ปริมาตร 8 มิลลิลิตร แล้วปั่นกวนที่อุณหภูมิ 4 องศาเซลเซียส เป็นเวลา 24 ชั่วโมง จากนั้นกรองและล้างด้วยสารละลายบัฟเฟอร์ที่มี pH เดียวกัน เพื่อล้างเอนไซม์ส่วนที่ไม่ถูกดูดซับออก จากนั้นนำมีโซพอร์ซิลิกาที่มีเอนไซม์ตรึงรูอยู่บนมีโซพอร์ซิลิกาที่เข้มข้น 0.5 % w/v ในกรดอะซิติก แล้วปรับค่า pH เท่ากับ 5 เทสารละลายลงในแบบพิมพ์ ที่ให้แห้งที่อุณหภูมิห้อง หลังจากนั้นจะได้เอนไซม์ตรึงรูบนแผ่นฟิล์มคอมโพสิตของมีโซพอร์ซิลิกาและไคโตซาน โดยสามารถตัดแบ่งเป็นชิ้น ขนาด 0.5 x 0.5 มิลลิเมตร ตัดแปลงวิธีมาจาก Rauf และคณะ [2006]

2.5 การวิเคราะห์ กิจกรรมของเอนไซม์

กิจกรรมของเอนไซม์อิสระและเอนไซม์ตรึงรูปในงานวิจัยนี้วิเคราะห์ตามวิธีการของ Fernandes และ คณะ [2004] มีวิธีการโดยย่อ ดังนี้ เติมเอนไซม์ลงในสารละลายบัฟเฟอร์ที่ประกอบด้วย ไพโรแกลลอล 2.4 มิลลิลิตร มีความเข้มข้น 0.013 mol/l ที่ pH 6 และไฮโดรเจนเปอร์ออกไซด์ 0.5 มิลลิลิตร มีความเข้มข้น 0.05 mol/l และให้ทำปฏิกิริยาที่อุณหภูมิ 30 องศาเซลเซียส เป็นเวลา 1 นาที นำสารละลายที่ได้ไปวัดผลค่าการดูดกลืนแสงของผลิตภัณฑ์ที่เกิดจากปฏิกิริยาออกซิเดชัน ที่ความยาวคลื่น 420 นาโนเมตร ด้วยเครื่องสเปกโตร-

* corresponding author; seeroong.p@chula.ac.th

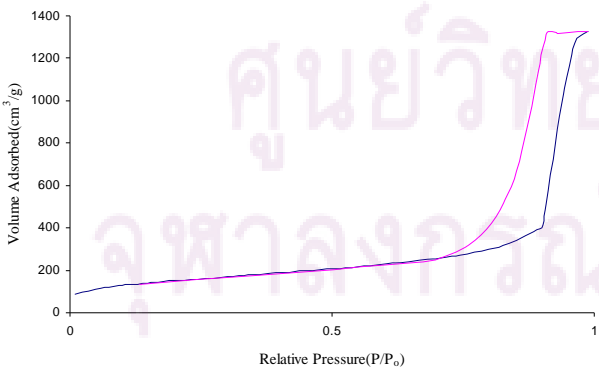
โฟโตมิเตอร์ โดยกิจกรรมเอนไซม์ฮอร์สแรดิชเปอร์ออกซิเดส 1 ยูนิต์ หมายถึง ปริมาณเอนไซม์ที่ทำให้ค่าการดูดกลืนแสงเปลี่ยนแปลงไป 0.1 หน่วย ในเวลา 1 นาที

3. ผลการทดลองและวิจารณ์ผล

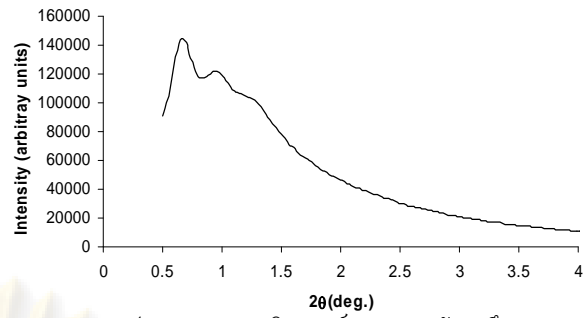
คุณสมบัติของวัสดุครึ่งเป็นข้อมูลที่สำคัญ ซึ่งสามารถใช้อธิบายการตรึงรูปของเอนไซม์ รวมทั้งการทำปฏิกิริยาของเอนไซม์ครึ่งรูป ซึ่งคุณสมบัติที่ควรพิจารณาของวัสดุครึ่งมีโซพอร์ซิลิกาชนิด MCF ได้แก่ พื้นที่ผิว ขนาดรูพรุน และปริมาตรรูพรุน ซึ่งได้จากการดูดซับและคายซับของก๊าซไนโตรเจน ซึ่งวิเคราะห์ด้วยเครื่อง BET ดังแสดงในกราฟรูปที่ 1 จากกราฟที่ได้มีลักษณะเป็น ชนิด IV isotherm ซึ่งเป็นการยืนยันว่าวัสดุครึ่งที่สังเคราะห์ให้มีขนาดระดับมีโซพอร์ (2-50 nm) และจากตารางที่ 1 ซึ่งพบว่า วัสดุ MCF มีขนาดรูพรุนขนาด 24.1 nm และใหญ่กว่าขนาดของเอนไซม์ (48 Å, Takahashi และ คณะ, 2001) เป็นการบ่งบอกว่า เอนไซม์สามารถแพร่เข้าไปภายในรูพรุนของวัสดุครึ่งได้ นอกจากนี้ ผลของการวิเคราะห์วัสดุครึ่งด้วย XRD ดังแสดงในรูปที่ 2 ทำให้ทราบว่าวัสดุครึ่งที่ได้มีรูปทรงกลมเช่นเดียวกับงานวิจัยของ Lettow และ คณะ [2000] ในขณะที่รูปที่ 3 แสดงหมู่ฟังก์ชันที่พบบนพื้นผิวของวัสดุครึ่งดังต่อไปนี้ ที่ตำแหน่งพิก 3700-3200 cm^{-1} แสดงถึงหมู่ฟังก์ชัน Si-O-H (silanol group) และที่ตำแหน่งพิก 1200-1000 แสดงถึงหมู่ฟังก์ชัน $-(Si-O)-$ (siloxane) โดยหมู่ silanol เป็นหมู่ที่มีความสำคัญต่อการตรึงรูปแบบดูดซับ เนื่องจากเป็นหมู่ที่เกิดพันธะไฮโดรเจนกับเอนไซม์

ตาราง 1 แสดงพื้นที่ผิว ขนาดเส้นผ่านศูนย์กลางรูพรุน และปริมาตรรูพรุนของวัสดุครึ่ง

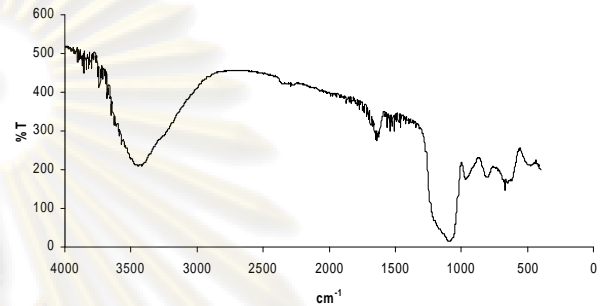
วัสดุครึ่ง	พื้นที่ผิว BET,(m ² /g)	เส้นผ่านศูนย์กลางรูพรุน (nm)	ปริมาตรรูพรุน (cm ³ /g)
MCF	549.3	24.1	2.03



รูป 1 แสดงการดูดซับและคายซับของก๊าซไนโตรเจน



รูป 2 แสดงผลการวิเคราะห์ XRD ของวัสดุครึ่ง



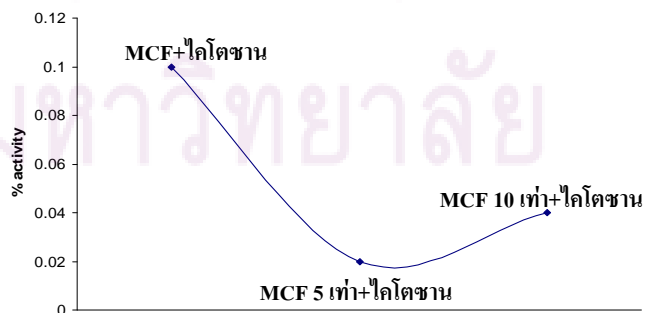
รูป 3 แสดงผลการวิเคราะห์ FTIR ของวัสดุครึ่ง

เอนไซม์ฮอร์สแรดิชเปอร์ออกซิเดสสามารถดูดซับบนมีโซพอร์ซิลิกาได้ในปริมาณสูงและเมื่อนำมาห่อหุ้มด้วยไคโตซานแล้วพบว่า ทำให้การหลุดออกของเอนไซม์ลดลงอย่างชัดเจน แต่ทำให้ค่ากิจกรรมเอนไซม์ลดลงเช่นเดียวกัน ดังแสดงในตารางที่ 2

ตาราง 2 แสดงค่ากิจกรรมเอนไซม์ ค่าการหลุดออกของเอนไซม์

วัสดุครึ่ง	ปริมาณการดูดซับเอนไซม์ (%)	ค่ากิจกรรมเอนไซม์ (%)	ค่าการหลุดออกของเอนไซม์ (%)
MCF	99	0.5	2.5
MCF+ไคโตซาน	-	0.1	0.4

เมื่อเพิ่มปริมาณมีโซพอร์ซิลิกาที่ครึ่งรูปเอนไซม์แล้วเป็น 5 เท่า และ 10 เท่า พบว่าค่ากิจกรรมเอนไซม์ไม่เพิ่มขึ้น อาจเกิดจากแผ่นฟิล์มมีความหนาแน่นของมีโซพอร์ซิลิกามากเกินไป ส่งผลให้อัตราการถ่ายเทมวลสารเกิดขึ้นอย่างจำกัด แสดงในรูปที่ 4



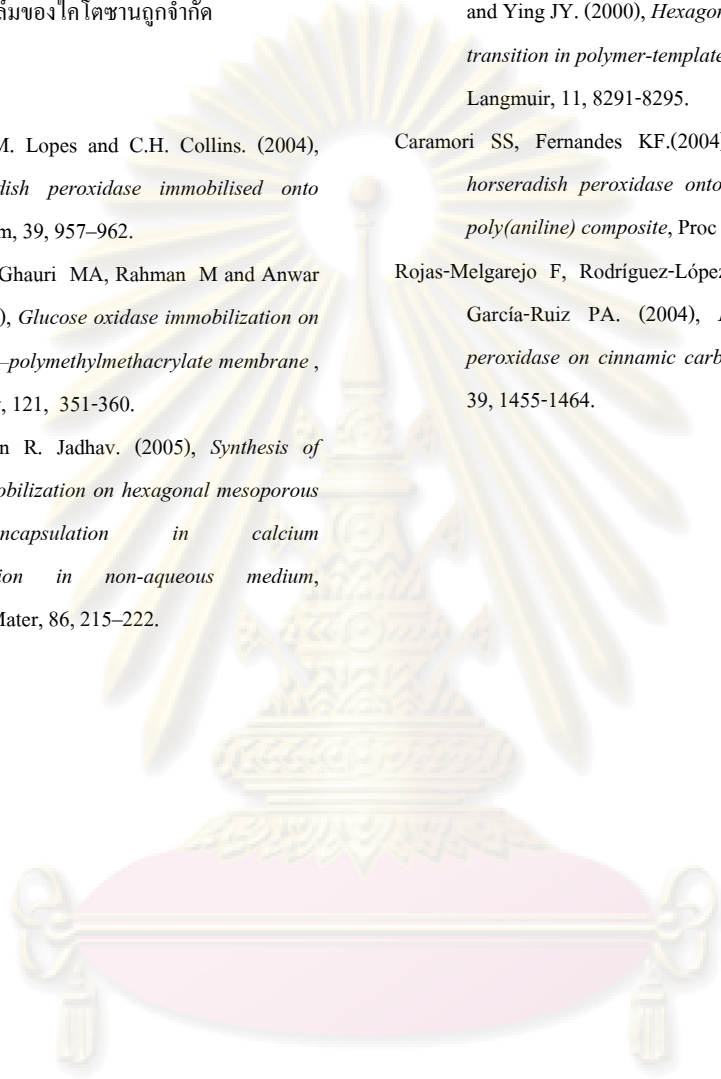
รูป 4 แสดงค่ากิจกรรมของเอนไซม์ที่ปริมาณต่างๆของมีโซพอร์ซิลิกาที่ครึ่งรูปเอนไซม์แล้วห่อหุ้มด้วยไคโตซาน

4. สรุปผลการทดลอง

มีโซพอร์ซิลิกาชนิด MCF เป็นวัสดุที่มีพื้นที่ผิวมาก ขนาดรูพรุนใหญ่และปริมาตรรูพรุนสูง ซึ่งมีความเหมาะสมต่อการตรึงรูปเอนไซม์ จึงทำให้ดูดซับเอนไซม์ได้ดี และเมื่อห่อหุ้มเอนไซม์ที่ผ่านการตรึงรูปในมีโซพอร์ซิลิกาด้วยไคโตซานแล้วสามารถลดการหลุดออกของเอนไซม์ได้ อย่างไรก็ตามค่ากิจกรรมของเอนไซม์ลดลง ซึ่งอาจเกิดจากการถ่ายเทมวลสารผ่านแผ่นฟิล์มของไคโตซานถูกจำกัด

5. เอกสารอ้างอิง

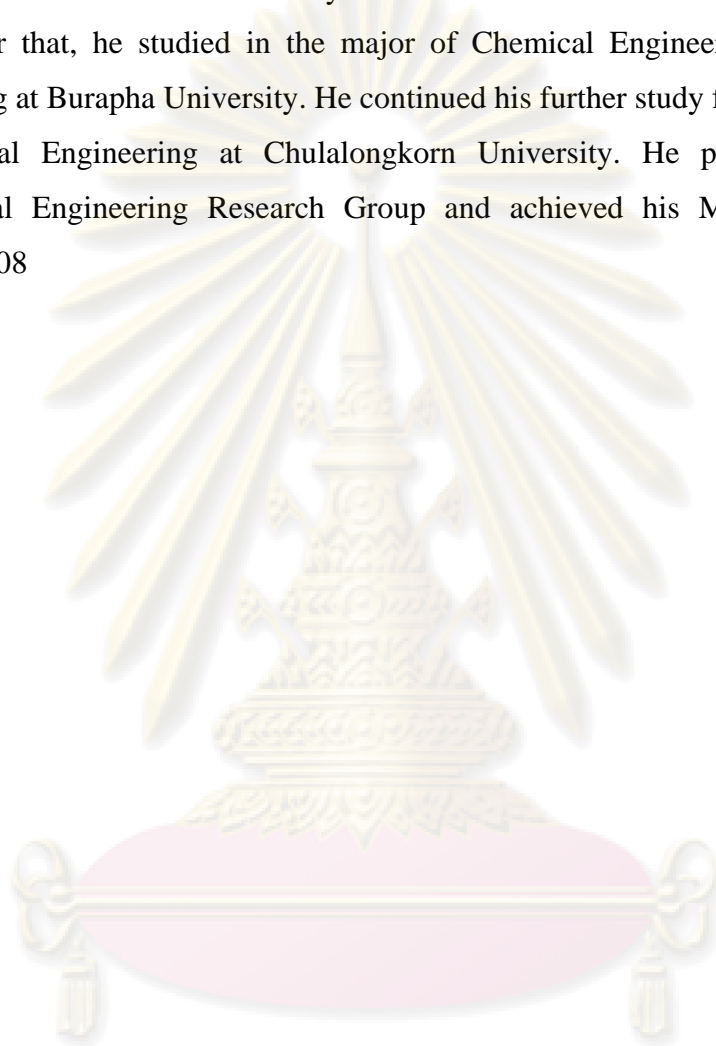
- K.F. Fernandes, C.S. Lima, F.M. Lopes and C.H. Collins. (2004), *Properties of horseradish peroxidase immobilised onto polyaniline*, Proc Biochem, 39, 957-962.
- Rauf S, Ihsan A , Akhtar K , Ghauri MA, Rahman M and Anwar MA Khalid AM. (2006), *Glucose oxidase immobilization on a novel cellulose acetate-polyethylmethacrylate membrane* , Journal of Biotechnology, 121, 351-360.
- Ganapati D. Yadav and Sachin R. Jadhav. (2005), *Synthesis of reusable lipases by immobilization on hexagonal mesoporous silica and encapsulation in calcium alginate:Transesterification in non-aqueous medium*, Micropor and Mesopor Mater, 86, 215-222.
- Takahashi H, Li B, Sasaki T, Miyazaki C, Kajino T and Inagaki S. (2001), *Immobilized enzymes in ordered mesoporous silica materials and improvement of their stability and catalytic activity in an organic solvent*, Micropor and Mesopor Mater, 44-45, 755-762.
- Lettow JS, Han YJ, Schmidt-Winkel P, Yang P, Zhao D, Stucky GD and Ying JY. (2000), *Hexagonal to mesocellular foam phase transition in polymer-templated mesoporous silicas*, Langmuir, 11, 8291-8295.
- Caramori SS, Fernandes KF.(2004), *Covalent immobilization of horseradish peroxidase onto poly (ethylene terephthalate)-poly(aniline) composite*, Proc Biochem, 39, 883-888.
- Rojas-Melgarejo F, Rodríguez-López JN, Carcía-Cánovas FG and García-Ruiz PA. (2004), *Immobilization of horseradish peroxidase on cinnamic carbohydrate esters*, Proc Biochem, 39, 1455-1464.



ศูนย์วิทยทรัพยากร
จุฬาลงกรณ์มหาวิทยาลัย

VITA

Mr. Sakon Punwittayakool was born in Kamphaengphet, Thailand on August 10, 1984. He finished his secondary course from Nakhonsawan School in March, 2002. After that, he studied in the major of Chemical Engineering in Faculty of Engineering at Burapha University. He continued his further study for master's degree in Chemical Engineering at Chulalongkorn University. He participated in the Biochemical Engineering Research Group and achieved his Master's degree in October, 2008



ศุภชัยวิทย์ทรัพย์ากร
จุฬาลงกรณ์มหาวิทยาลัย